CALIFORNIA STATE UNIVERSITY, NORTHRIDGE

SEDIMENTOLOGY, PALEONTOLOGY, C AND O ISOTOPE CHEMISTRY, AND GEOCHRONOLOGY OF HOLOCENE SEDIMENT FROM LAKE THETIS, CERVANTES, WESTERN AUSTRALIA

A thesis submitted in partial fulfillment of the

requirements for the degree of Master of Science in

Geology

By Franky Telles

December 2005

The thesis of Franky Telles is approved:

Dr. Jorge Vazquez	Date
Dr. Jon Sloan	Date
Dr. Vicki Pedone, Chair	Date

California State University, Northridge

DEDICATION

To my Father and to my Mentor.

ACKNOWLEDGEMENTS

My Advisor, Dr. Vicki Pedone
I would like to give my deep thanks to my thesis advisor, Dr. Vicki Pedone. She gave me the opportunity to travel to Western Australia to help core the samples in this thesis. Even though she was busy with her new career as Interim Dean of the College of Science and Math, she sacrificed a lot of her time to help me develop my research thesis, read and critique my work, and advise me on my career path for the past couple of years.

Supporting Cast of the University of Western Australia
I would like to thank Dr. Annette George for helping us decide which lake to core. I would also like to thank Bill Wilson and Linda Sprigg of the University of Western Australia for helping core and take GPS readings of the lake. I would also like to thank Dr. Kendrick for identifying the gastropod *Coxiella exposita*; Dr. John Backhouse for identifying and quantifying the pollen in this study; Dr. Sandie McHugh for identifying diatoms.

Supporting Cast of the California State University, Northridge
I would like to thank my undergraduate supporter, Nathan Guzman. He helped around the laboratory that saved time like sieving core samples, picking out ostracodes, and washing beakers. I would like to thank the faculty of the National Science Foundation Catalyst program that helped fund my tuition, research in the laboratory, and travel to Western Australia. Dr. Kathie Marsaglia helped me hone in my petrographic skills and helped me get involved in geology activities. Dr. Gerry Simila discovered my talent for geology while working at the Jet Propulsion Laboratory in Pasadena and helped me enroll in the Catalyst program. Dr. Doug Yule helped develop my writing skills for proposals and critical and effective reading of scientific journals. I would also like to thank all the people from the Department of Geological Sciences like Terry, Mari, and Susan. Thanks to Dr. George Dunne for making me a better reader and communicator when it comes to presenting research. Thanks to Dr. Ali Tabidian for revealing polluted areas (e.g. SuperFund Sites).

My Thesis Committee
I would like to thank my thesis committee for reading and critiquing my report. Dr. Jon Sloan helped me identify microfossils. His classes are a lot of fun filled with energy, enthusiasm, and entertainment; the way that classes ought to be taught. I have known Dr. Jorge Vazquez as an undergraduate at the University of California, Los Angeles. He was a teaching assistant for a few of my introductory courses in the geosciences. I would like to not only thank him for helping me as an undergraduate in geology, but also for participating in my committee.

Peripheral supporting cast
I would like to thank the world famous ostracode* micropaleontologist Dr. Patrick De Deckker of the National Australian University for identifying the ostracode species in my core samples. I would like to thank Miguel Rincon of the University of Southern California for analyzing my ostracodes and endogenic carbonate in the mass

spectrometer. I would like to thank Dr. Craig Manning and his student Codi Lazar for helping me analyze samples at the University of California, Los Angeles X-ray Diffractometer. I would also like to thank David Carson of the Getty Center for doing further X-ray diffractometer tests on my samples.

I would like to acknowledge my father because he not only encouraged science and politics and introduced the outdoors to me, but also spent his final years trying to raise me. One day we shall meet again.

Finally, I would like to give my deepest gratitude to my old mentor, Al Diamond, who saved my life from the streets of Los Angeles. I would not be in this position without his help in middle school and high school. He helped me realize my love for science, my passion for film and television, and traveling to remote places, and learning new languages and cultures.

Funding for the study was provided by a grant from the National Science Foundation Program Opportunity for Enhancing Diversity in Geosciences, award number 0119936: Mentor though Research: Catalyst for Success in the Geosciences.

* "ostracode" is spelled "ostracod" in Australia

TABLE OF CONTENTS

LIST OF ILLUSTRATIONS

LIST OF TABLES

ABSTRACT

SEDIMENTOLOGY, PALEONTOLOGY, C AND O ISOTOPE CHEMISTRY, AND GEOCHRONOLOGY OF HOLOCENE SEDIMENT FROM LAKE THETIS, CERVANTES, WESTERN AUSTRALIA

By

Franky Telles

Master of Science in Geology

Lake Thetis is a small, hydrologically closed coastal lake located ~240 km north of Perth, Western Australia (30°30'S). The sediment record of Lake Thetis obtained in two cores spans the past ~4100 y and shows changes in sediment type, sedimentation rate, biota, and C and O isotopes that are related to climate change and the evolving nature of the lake. The oldest sediment is dominated by organic-rich sand and accumulated at rates of >20 cm/100 y. During this phase of sedimentation, the control on $\delta^{13}C$ of the lake changed from photosynthesis to addition of isotopically light carbon derived from organic decomposition, shown by the significant decrease in $\delta^{13}C$ in endogenic micrite. The $\delta^{18}O$ of endogenic micrite during this phase has an average value of +1.0 ‰, indicating that it formed from water that had a $\delta^{18}O$ value higher than seawater and meteoric water of the region. Therefore during this period of time, evaporation must have slightly exceeded precipitation and inflow. However, the sediment of this interval contains abundant, well preserved diatoms and ostracode species *Mytilocypris ambiguosa.* These observations constrain the salinity of the lake to be only brackish (<10 g/L). This period likely represents the lowest salinity and largest lake size of the time represented in the cores.

Between ~4000 y and 3650 y, sand deposition increased and organic-rich sand deposition decreased. Since this time, sand and organic-rich sand (and uncompacted organic-rich sand, i.e., sludge) have accumulated at rates between 3 and 6 cm/100y. The increase in eolian sand brought to the lake suggests that the vegetation in the area surrounding Lake Thetis decreased owing to increasing aridity. Concomitant with the change in sedimentation is the disappearance of *Mytilocypris ambiguosa* from the sediment record, which signals that the lake reached a salinity level above the biological tolerance of this species. The average size and salinity of the lake have probably similar to those of today for the past ~3800 y, particularly after ~2770 y when the average $\delta^{18}O$ of the micrite increased from +1 ‰ to its modern value of +2 ‰. Today, evaporation greatly exceeds precipitation. The lake water is hypersaline, generally>40 g/L, exceeding the documented tolerance level of *Cyprideis australiensis*, the only ostracode extant in the lake. Biodiversity is low, indicating that the lake is inhospitable to many species.

Superposed on the overall history of increasing salinity and decreasing lake size are small excursions that mark short-term increases and decreases in salinity and lake size. These excursions are recorded in small (~1 ‰) changes in $\delta^{18}O$ of micrite and in changes in the abundance of *Cyprideis australiensis*. The excursions are likely associated with drought/wet cycles in the area of Lake Thetis. Definition of the magnitude and frequency of drought/wet cycles require additional high-resolution temporal and spatial studies.

CHAPTER 1 – OVERVIEW OF THE STUDY

INTRODUCTION

This chapter provides an overview of the study, including the geologic setting, physical and biological features of Lake Thetis, hypotheses that were tested, and methodology of the study. The goal of this study is to determine if the sediment record from two short cores from the center of Lake Thetis, a small, hydrologically-closed, coastal lake about 240 km north of Perth, Western Australia, contain a high-resolution archive of climate proxies related to drought-wet cycles during the middle to late Holocene for the southwestern margin of Australia. This study documents changes in parameters, such as are sensitive to lake-volume changes, and hence, are potential recorders of drought-wet cycles: sedimentology, biota, and carbon and oxygen isotopic composition in lacustrine carbonate minerals. Accelerator-mass-spectrometry (AMS) radiocarbon dating of organic matter from one core provides a geochronologic framework for deposition of the sediment. The impact of the study is twofold. First, the results augment the relatively sparse record of Holocene climate changes from terrestrial archives. In particular, there are no published detailed records from this part of Australia. An expanded record will contribute to understanding the global correlation of frequency and magnitude of drought-wet cycles during the latter Holocene. Second, because most of the population of Western Australia lives along the southwestern coast (Fig. 1.1), a study of the magnitude and effects precipitation/storm frequency on coastal systems is important. Historic climate records for the southwestern margin of Australia extend back less than 200 years. Therefore, climate proxies must supply data on the magnitude, timing, and frequency of Holocene climate change in this region.

Well preserved sediment records in lakes are among the best high-temporal-resolution archives of terrestrial climate change (Duplessy and Overpeck, 1996). There are no studies of this kind for this area of Australia. This study of the sediment record of Lake Thetis will provide the first data and insight into the Holocene climate record for the region.

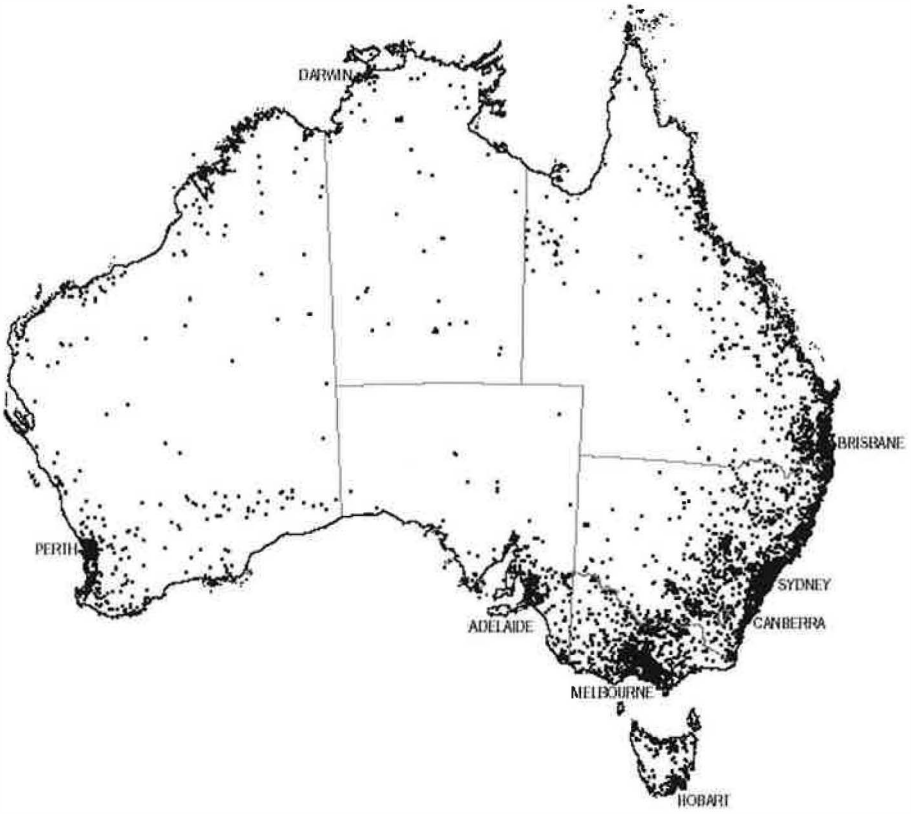

Figure 1.1. Population distribution of Australia in 2000 (Australian Bureau of Statistics, 2002).

GEOLOGIC SETTING

The coastal region of Western Australia is one of the least tectonically active areas in the world. The Mesozoic and Cenozoic sedimentary rocks of the southwestern margin of Western Australia are separated from the Archean rocks of the Yilgarn Craton by the Darling fault (Fig. 1.2). This fault has been episodically active since ~2.57 Ga, but

significant displacement has not occurred since the Late Jurassic (~150 Ma) (Moss and others, 1998). The southwestern coastal region has experienced no uplift or subsidence during the Holocene (Hallam, 1992).

Lake Thetis is located 12 km southeast of the town of Cervantes within the Swan Coastal Plain about 30°30'S (Figs. 1.2 and 1.3). The low-lying Swan Coastal Plain is separated from elevated plateaus of the Perth Basin by the Gingin Scarp, located about 20 km east of the lake. The scarp was formed by marine erosion (Kern, 1993). The coastal plain is a gently undulating area covered by Holocene and Pleistocene coastal dunes and shoreline deposits. The Swan Coastal Plain is subdivided into two geomorphic units: the Coastal Belt and the Bassendean Dunes (Fig. 1.3). The 15 km-wide Bassendean Dunes zone contains older Pleistocene and Triassic rocks overlain unconformably by a thin veneer of Pleistocene and Holocene eolianite. The underlying rocks are the Middle-Upper Triassic Lesueur Sandstone and the Pleistocene Guildford Formation, which contains both siliciclastic sand and mud facies. The overlying Bassendean Sand forms a series of low sand hills derived from reworking the underlying siliciclastic units. The Bassendean Sand is unlithified to poorly lithified and was deposited at various periods from the Late Pleistocene to Holocene. The dune field also contains inter-dune lake and swamp deposits.

The Coastal Belt consists of Holocene eolianite, the Safety Bay Sand, unconformably overlying the upper Pleistocene to lower Holocene Tamala Limestone. The Tamala Limestone was deposited as coastal sand, primarily as eolian facies. It is a calcarenite, consisting mainly of sand-sized, abraded fragments of mollusks with variable amounts of quartz, up to a maximum of 50%, but generally less than 20% (Playford,

1997). The formation weathers to quartz-rich sandy soil, which can produce sheets of

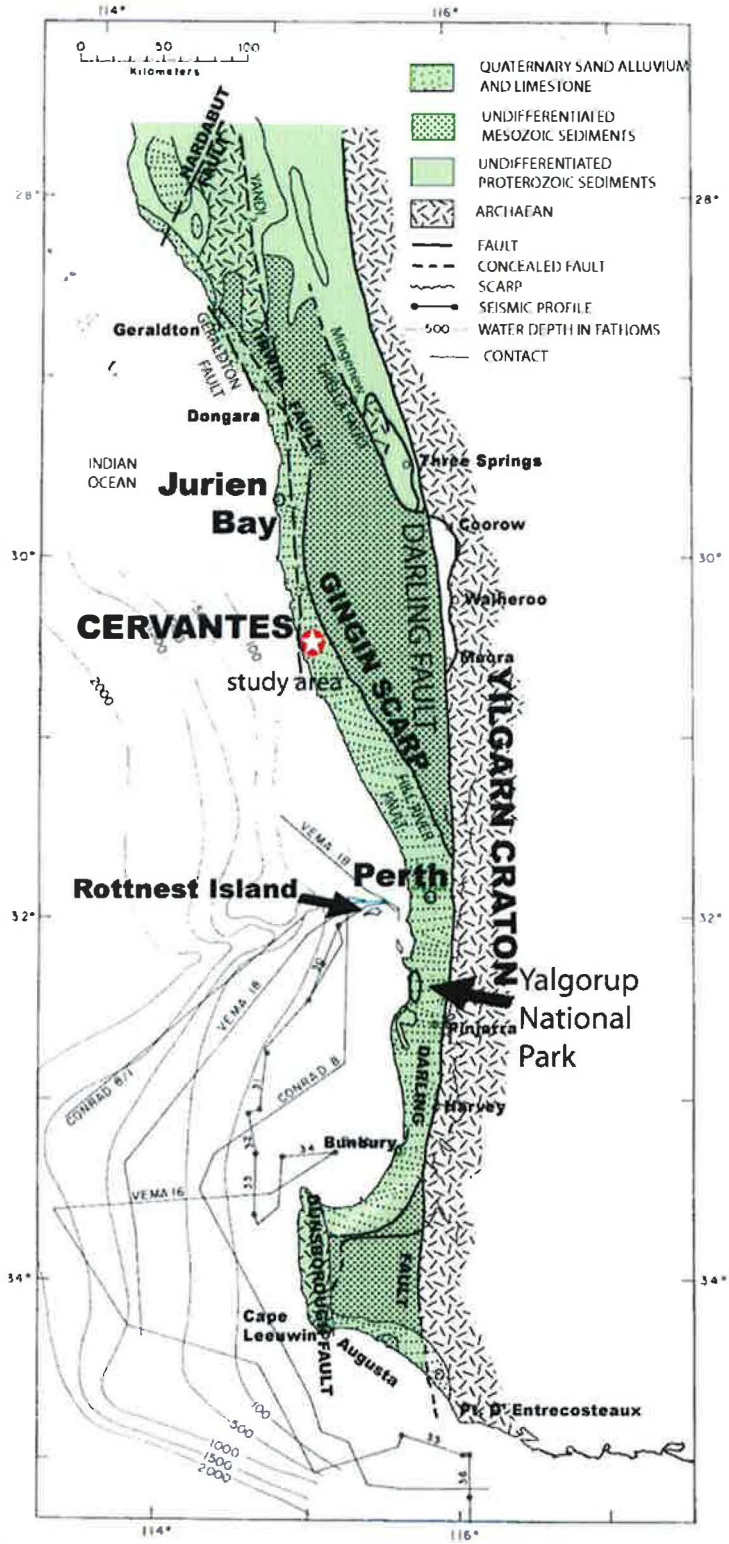

Figure 1.2. Geology of the southwestern Australia. Modified from Hawkins, 1965.

sand (Tamala Limestone sand) in some areas (Fig. 1.3). Some beds of the Tamala Limestone contain a diverse and abundant assemblage of bivalves, gastropods, and other marine fauna (Moss and others, 1998).

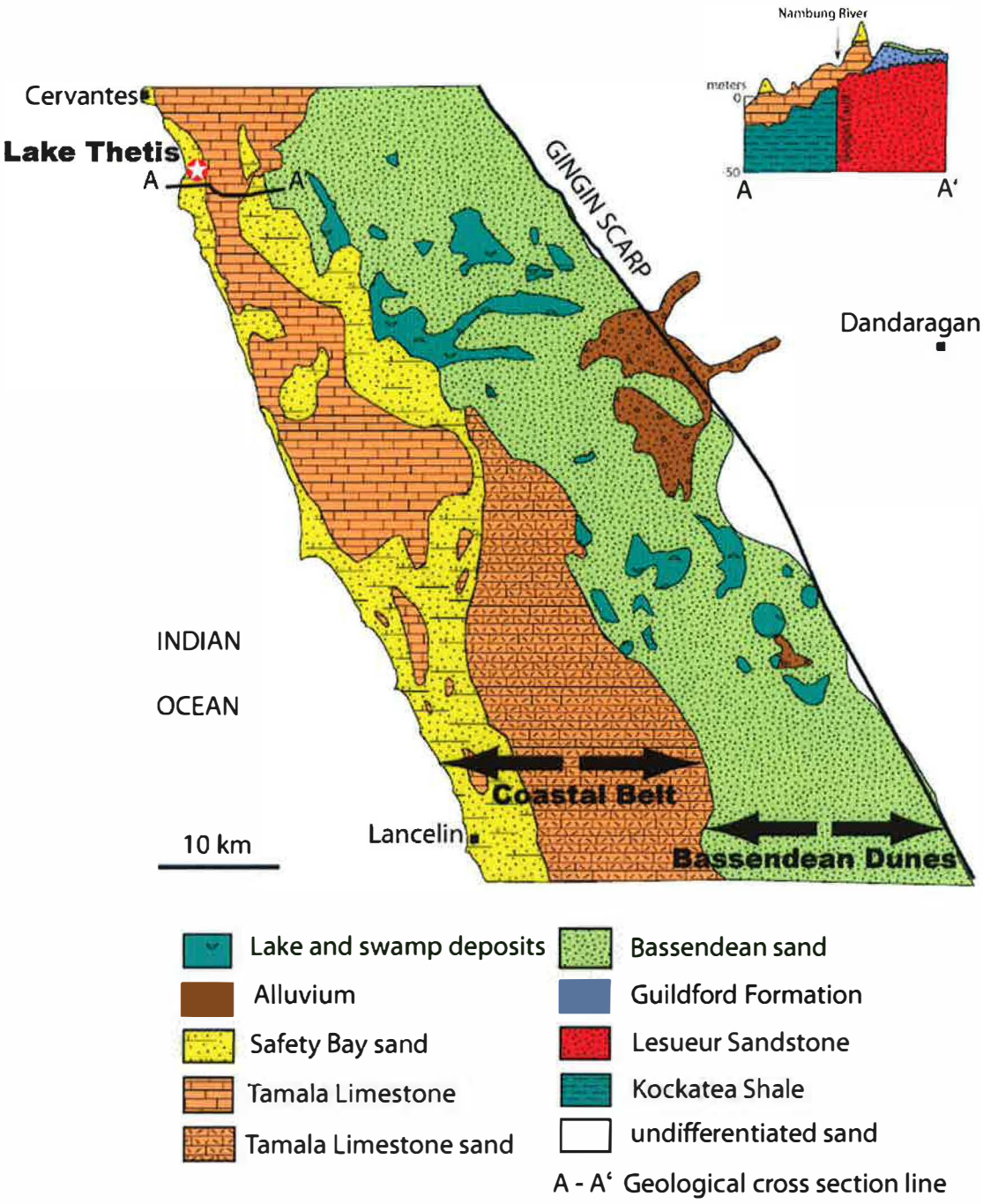

Figure 1.3. Geologic map and cross section of the Swan Coastal Plain in the study area. Modified from Kern, 1993.

Eolianite of the Tamala Limestone forms the Spearwood Dune system, which is younger than the Bassendean Sand dune system (Moss and others, 1998). Linear ridges of the Spearwood Dunes rise 164 m above the Australian height datum (AHD), which is based on the determination of mean sea level of zero at thirty gauges around the coastline of the continent coastline (Luton and Johnston, 2001). The youngest geologic unit in the study area is the Holocene to modern Safety Bay Sand. The Safety Bay Sand consists of unlithified to poorly lithified nearshore, beach, and dune sand (Shepherd and Eliot, 1995). The sand is similar in composition to the Tamala Limestone, consisting sand-sized fragments of mollusks and forams, with a significant component of detrital quartz (Kern, 1993). In places, it forms large mobile and stabilized dunes up to 150 m high.

Lake Thetis, named for a sailing ship that performed a coastal survey between 1847 and 1848, is separated from the Indian Ocean by a sandy foredune plain, that is 1.25 to 2.5 km wide. It is situated in a deflation basin between sparsely vegetated parabolic dunes (Fig. 1.4), equivalents of the calcareous Holocene Safety Bay Sand (Grey and others, 1990). Underlying the dunes, at least north of the lake, is a friable, highly fossiliferous limestone (coquinite), which presumably is nearshore to beach deposit of the Safety Bay Sand. This limestone contains a bivalve index fossil, *Katelysia rhytiphora*, which is restricted to the Vincent Member of the middle Holocene Herschell Limestone of Rottnest Island (Fig. 1.2). Radiocarbon dating of shells in the Vincent Member on Rottnest indicates that the member was deposited between 5900 and 4800 y B.P. (Playford, 1988). Assuming that the coquinite north of Lake Thetis is equivalent to the Vincent Member, the maximum age of formation of the Lake Thetis basin is ~4800.

PHYSICAL ENVIRONMENT OF LAKE THETIS

Lake Thetis is triangular in shape (Fig. 1.4). The northern shoreline has the maximum length of about 400 m. A low dune (<3 m high) parallel to the northern margin separates the lake from an abandoned limestone coquinite quarry (Figs. 1.4 and 1.5). The east and west margins are bounded by vegetated dunes, and the southern margin is part of

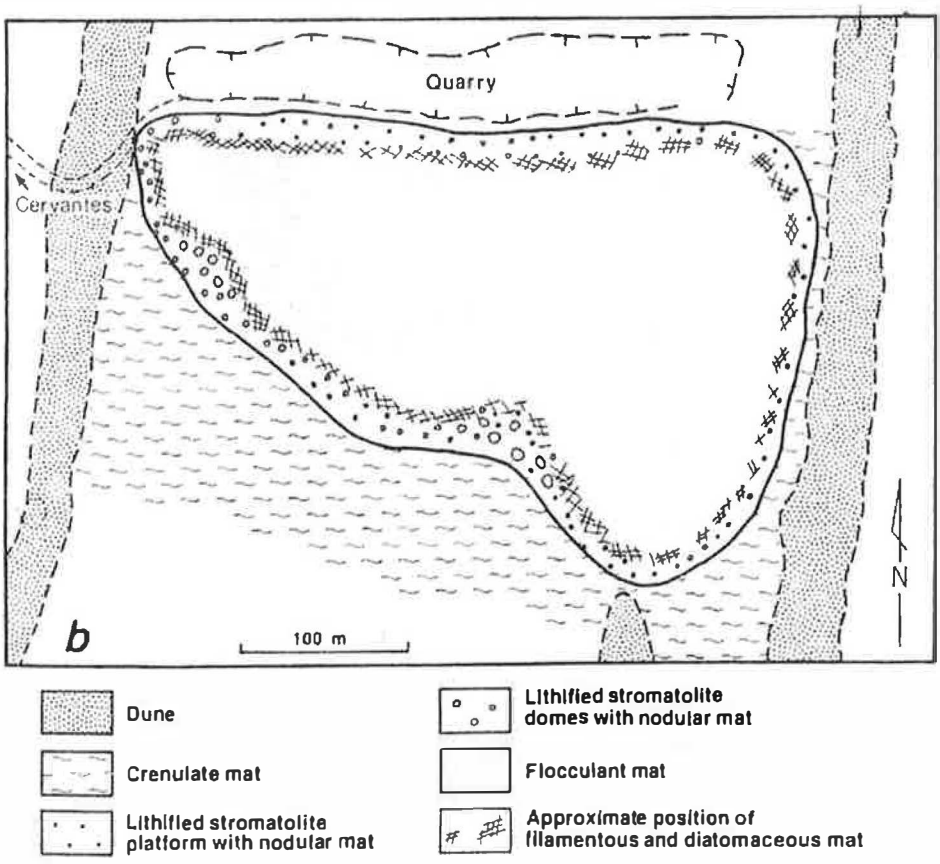

Figure 1.4. Depositional environments and distribution of microbial mats and stromatolites in Lake Thetis. The lakeward margin of the filamentous and diatomaceous mat is the platform edge (slope break). The landward edge of this mat is the approximate position of the typical summer water level. The solid bounding line is the upper limit of the foreshore, winter level high water. The crenulate mat marks the position of marshes formed in winter months. From Grey and others (1990).

Figure 1.5. View of Lake Thetis, June 2004, looking towards the west. The lake is bounded by low dunes on all sides, except the south.

the gently sloping deflation basin that forms a marsh in winter months (Grey and others, 1990). The lake is steep sided, with narrow, rimming carbonate terraces (Fig. 1.6). The shape and topography of the lake suggest that it fills a karst sinkhole. Similar saline lakes on Rottnest Island (Fig. 1.2) are interpreted to fill sinkholes developed in reef platforms during Pleistocene sea-level lowstands (Playford, 1997).

Lake-level elevation is similar to sea level. Variations in lake level of up to 0.5 m were measured by Grey and others (1990) during the period between 1986 and 1989. Maximum lake level was measured in October 1986 at +0.29 m AHD, and minimum was measured in April 1987 at -0.23 m AHD. This difference in elevation alternately floods and exposes a strip of foreshore about 5 m wide. In summer (low water), the lake is about 2 m deep, except along the northern shore where the depth is about 2.25 m. The entire bottom of the lake is covered by a thick (~0.5 m) flocculent microbial mat.

Narrow carbonate terraces, or benches, of the foreshore environment define shoreline positions of the lake (Grey and others, 1990) (Figs. 1.6, 1.7, and 1.8). They are formed by coalesed stromatolite domes. Bench 1 is topographically the lowest and is continuous around the lake. It is the only bench that is continuously submerged, lying below lowest seasonal lake level. In the aerial image in Figure 1.8, it is the pale green rim between the shoreline and the deep-green lake center. Bench 2 is exposed during summer

months and submerged during winter months. In Figure 1.8, it is the whitish band surrounding the modern lake. The third bench is discontinuous and only patchily preserved. The best exposure is along the north shore. The relict stromatolites that form the carbonate platform at this level are karstified, indicating that this shoreline position has long been abandoned. The maximum extent of the lake is traced by the patchy exposures of bench 3 (Fig. 1.8).

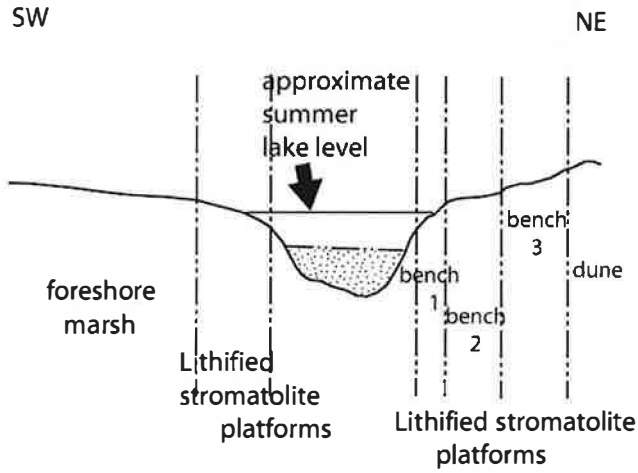

Figure 1.6. Diagrammatic profile of Lake Thetis from Grey and others (1990).

MODERN CLIMATE

The nearest rainfall and temperature measurements to Lake Thetis are from the Jurien area (rainfall from Badgingarra Research Station, 30.30°S, 115.60°E, and temperature from Jurien Bay, 30.30°S, 115.05°E (Figs. 1.2 and 1.9). The climate is Mediterranean, with cool, wet winters and warm, dry summers. Maximum rainfall of about 140 mm occurs in June and minimum of about 9 mm occurs in January. Total annual rainfall averages 608 mm. Average winter temperatures are about 15°C, whereas

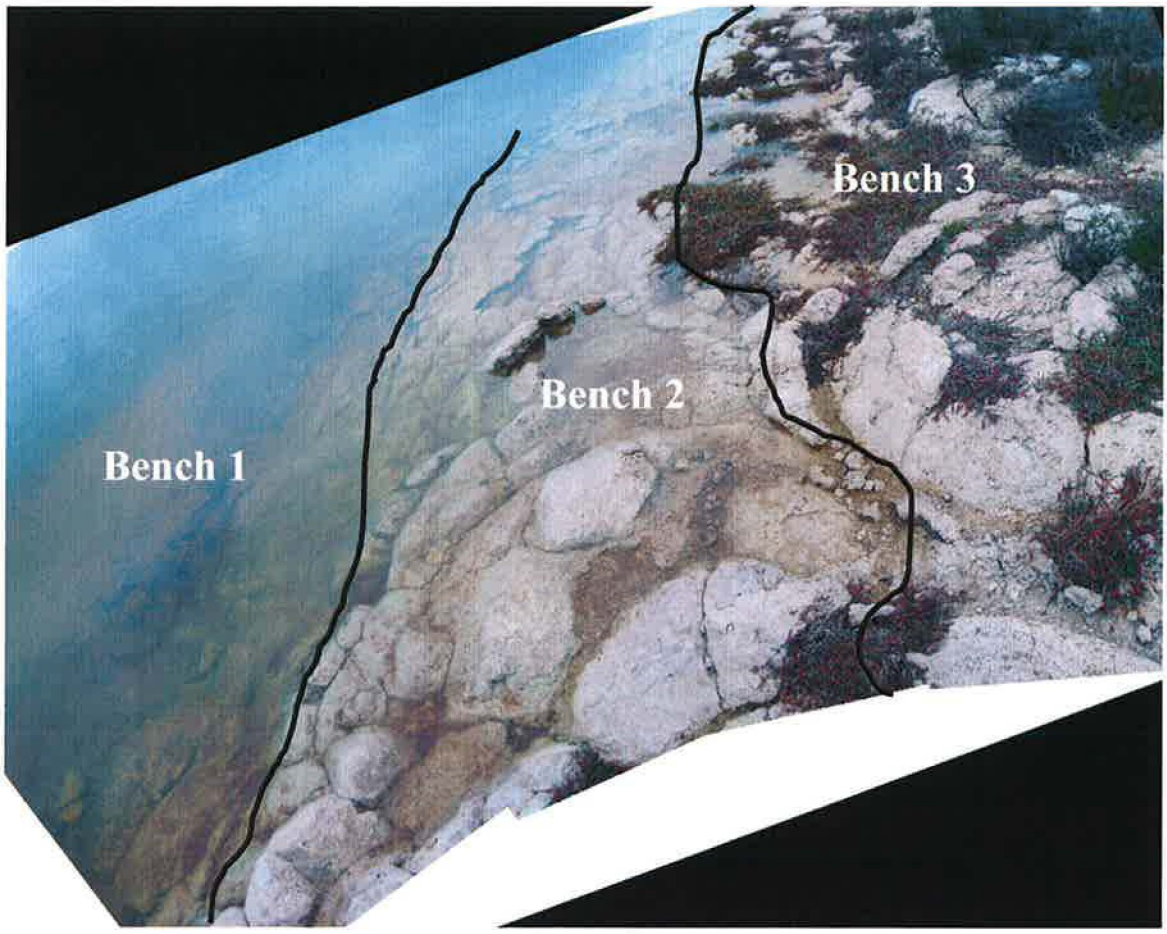

Figure 1.7. Carbonate benches on the north shore of Lake Thetis, June 2004

summer temperatures are about 23°C. Average annual evaporation is placed at 1700 mm (Grey and others, 1990) to 2000 mm (Kern, 1993), and rainfall exceeds evaporation only in the winter months. Southwesterly winds prevail in the summer, and northwesterly gales in the winter (Grey and others, 1990). The southerly component is enhanced through funneling between dunes that run longitudinally parallel to the lake, which results in strong wave activity on the northern shore of Lake Thetis. In historic times, tropical cyclones from the north cross the region on average every 10 to 12 years (Shepherd and Eliot, 1995).

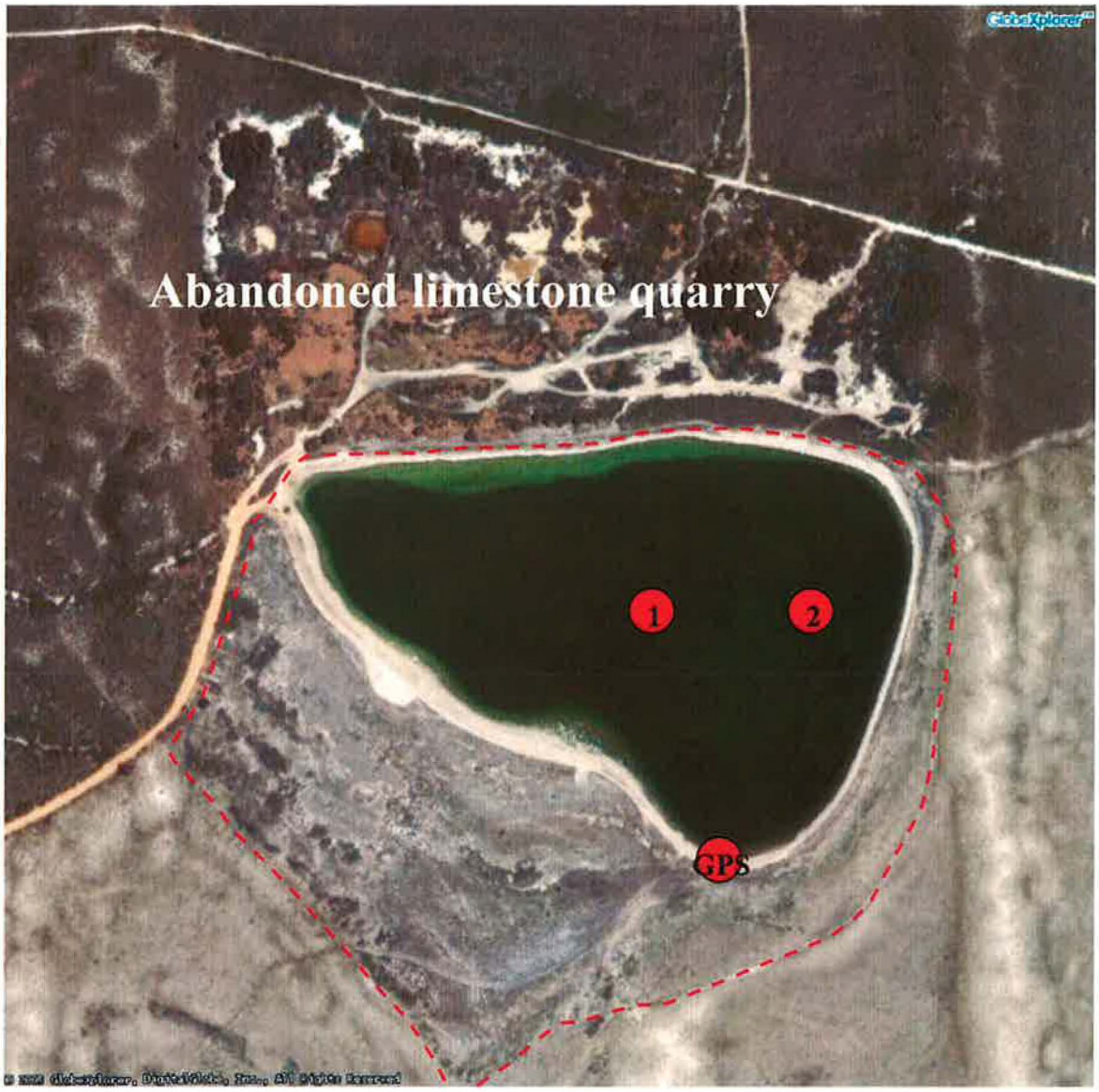

Figure 1.8. Aerial image of Lake Thetis. The maximum extent of the paleolake, which is defined by patchily preserved relict shoreline features, is shown by the dashed red line. Red dots 1 and 2 indicate approximate locations of cores 1 and 2. A GPS measurement of 30° 30' 29'' S, 115° 04' 53'' at the position of core 2 plots at the red dot GPS, which is physically incorrect. No GPS reading was taken for Core 1. The image and GPS plotting are from http://globexplorer.com GlobeXplorer, LLC.

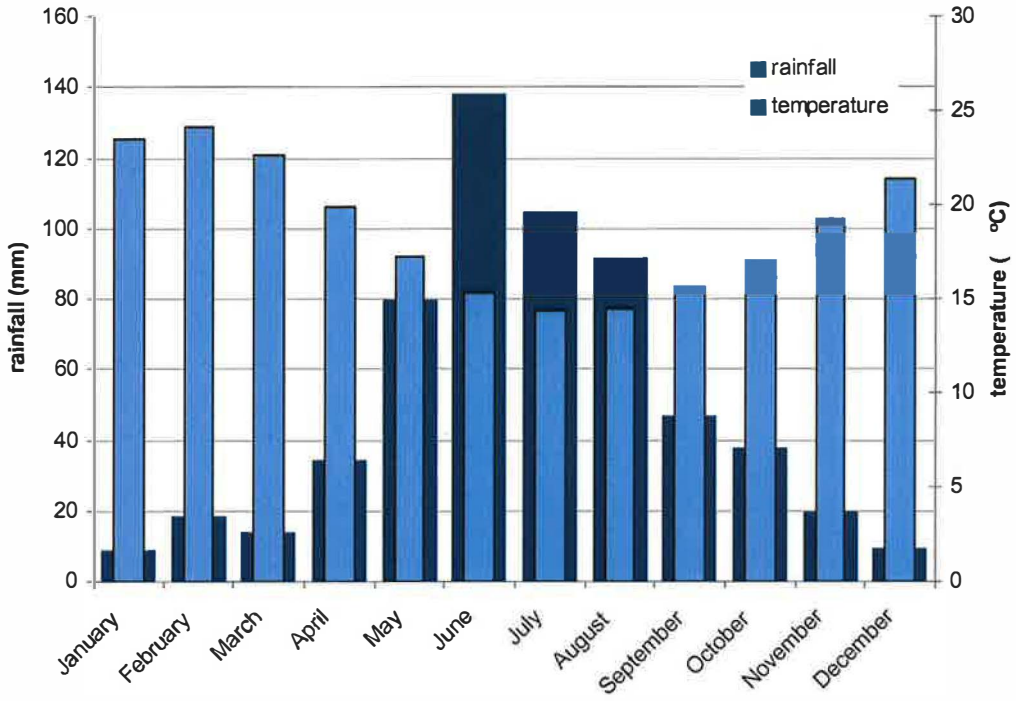

Figure 1.9. Temperature and rainfall data from stations near Lake Thetis. Average rainfall data between 1962 and 1982. Average temperature data between 1969 and 1992. Data from http://www.worldclimate.com WorldClimate.

FLORA AND FAUNA

Vegetation near the lake consists of low scrub, with abundant *Salicornia* and reeds in low-lying areas, and coastal acacia (*Acacia rostellifera*) and grasses on the dunes. The lake lacks macrophytes, but is rich in microbial communities, described below. Lake fauna include small telost fish, nematodes, amphipods, trichopteran larvae, ostracodes, and diatoms. The gastropod *Coxiella* inhabits the carbonate terraces. Numerous bird species, such as sea gulls, ducks, emus, and many species of migrants, feed on the lake fauna.

MICROBIAL COMMUNITIES OF LAKE THETIS

Lake Thetis is one of only three known lakes where living stromatolites occur in Western Australia. Therefore, the microbial communities in Lake Thetis were the focus of a study by Grey and others (1990). The surface sediment at Lake Thetis is covered by mucilaginous microbial communities dominated by cyanobacteria. Mats of different morphology and biology form concentric zones around the lake (Fig. 1.4). From the outermost margin to the lake center, mat types include: crenulate, nodular, filamentous, diatomaceous, and flocculent. Grey and others (1990) described the flocculent mat because it is the most extensive and is a possible analog for petroleum sources in ancient rocks (Burne and Bauld, 1985).

The crenulate mat on the outer edges of Lake Thetis is black to olive-green and has a reticulate pattern of centimeter-scale ridges and blisters. During the summertime, the mat becomes desiccated and very friable. During the wintertime, the mat becomes moist and leathery. The crenulate mat consists of organic matter, with lenses and thin layers of calcareous mud and coarse-grained calcareous sand. Filamentous cyanobacteria *Calothrix* and *Scythonema* and the coccoid cyanobacterium *Gloeocapsa* are the principal species in this mat.

The nodular mat forms in the splash zone surrounding and coating stromatolite domes in the calm waters located on the southwestern shoreline. This knobby, nodular mat is black to gray green. The mucilaginous coating formed by the coccoid cyanobacterium *Gloeocapsa* on the lithified nodules acts as the locus for the accumulation of sediment and precipitation of carbonate.

The filamentous mat is found in areas of reduced light penetration, on the undersurfaces and in cracks of the submerged carbonate bench 1 and as a thin, fragile film on top of flocculent mat. This mat is dominated by oscillatorian, filamentous, and coccoid cyanobacteria and diatoms.

The diatomaceous mat occurs in the continually submerged shallow margin of the lake. This orange-brown mat occurs just lakeward of and sometimes coating the nodular mat. Grey and others (1990) found that diatom frustules compose a significant portion of the lithified surfaces of stromatolites, and they conclude that diatoms might play a significant role in the stromatolite development at Lake Thetis.

The flocculent mat is extensive and thick, covering the entire bottom of the lake, where the water depth is about >2 m (Grey and others, 1990). It has a thickness between 50 and 60 cm, a gently undulating surface, fragile cohesion, and a texture that resembles gelatinous, gooey cottage cheese. The top few millimeters are blue green, but the rest of the mat is pinkish red to pinkish purple and structureless. The surface of the mat approximates the interface between oxic and anoxic environments during the day, as seen by the occurrence of healthy diatoms and nematodes on the mat surface.

Spectroradiometry of intact cores of the flocculent mat show that all photosynthetically utilizable light energy is absorbed within 3 to 4 mm below the mat-water interface. The microbial community of the surface consists of two or three species of oscillatoriacean cyanobacteria, pennate and naviculoid diatoms, a coccoid cyanobacterium (cf. *Synechocystis*). The surface community also includes two genera of non-phototrophic filamentous bacteria, *Beggiatoa* sp. and *Oscillatoria* spp. *Beggiatoa,* requires both H_2S and O_2 for growth, and *Oscillatoria* tolerates and/or utilizes H_2S. Their

presence in the surface community suggests that the H_2S-O_2 interface shifts on a diural basis such that H_2S diffuses into the water column at night. Bacteria within the pinkish-red to pinkish-purple mat below the surface layer consist only of anoxygenic, H_2S-utilizing species. Degraded cells of the surface community occur in progressively decreasing quantities downward in the flocculent mat. They are essentially absent at the mat-sediment interface, where large accumulations of partly decomposed organic matter are present, derived from the anaerobic decomposition of cells in the mat.

HYDROLOGY OF THE STUDY AREA

Surface drainage is absent in the Coastal Belt (Fig. 1.3). The seasonal Nambung River, located about 13 km south of Lake Thetis, is the only river in the area, active during the winter months. However, the surface flow does not reach the ocean. Instead, it enters a well developed cave system in the Tamala Limestone and flows in the subsurface to the sea (Kern, 1993). The salinity of the river ranges between fresh and brackish, with the highest salinities in the early winter before the heavy rainfall. Unlike most rivers, the salinity decreases downstream as a result of dilution by less saline tributaries. The lowest salinities occur where the river goes underground into the cave system.

Lake Thetis lacks major surface-water drainage and is separated from the ocean by a series of longitudinal dunes, which also form divides for shallow groundwater. Grey and others (1990) concluded that the only sources of water in the lake are shallow groundwater and direct precipitation. Generally, the salinity of the groundwater in the Coastal Belt is less than 1 g/L (Kern, 1993). Grey and others (1990) discount a permanent subterranean connection with the open sea. Even though the lake level is similar to sea

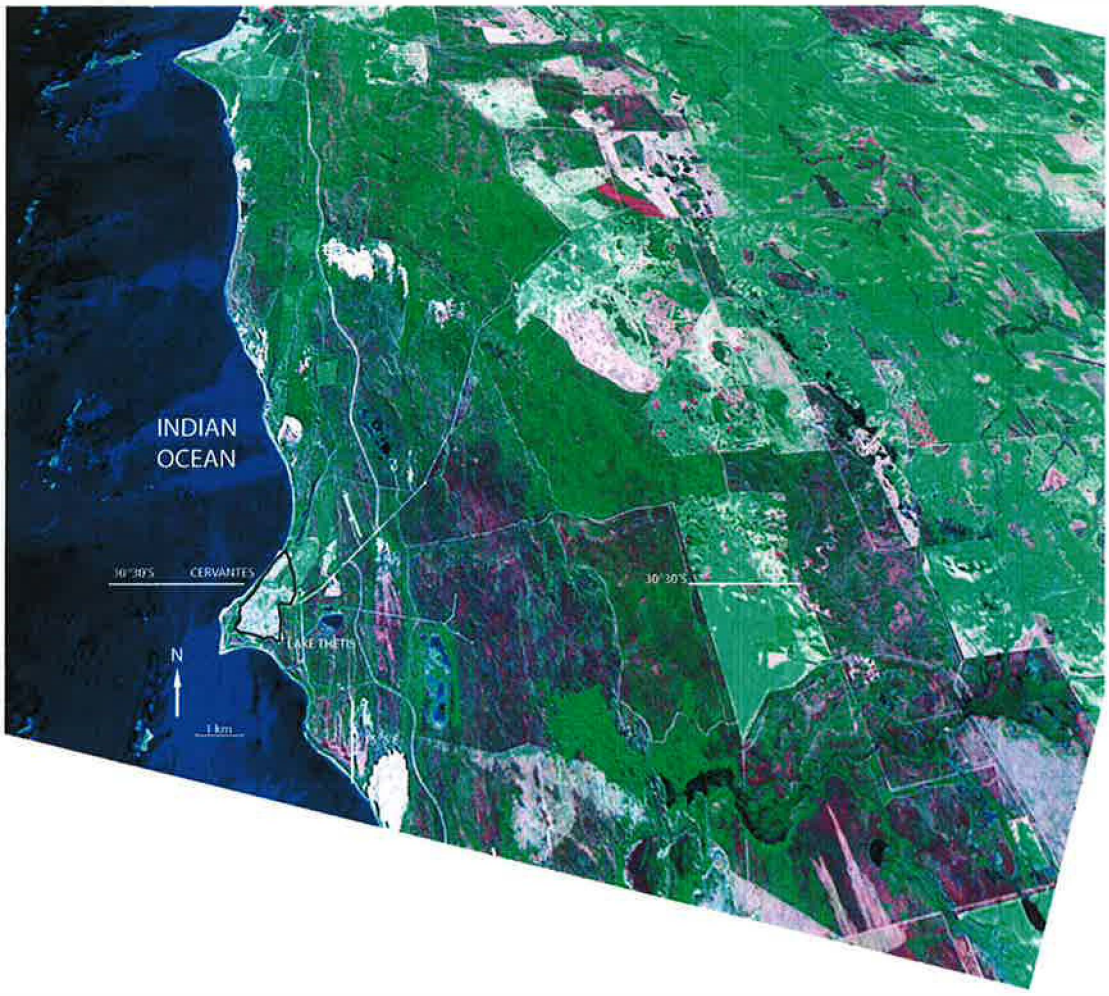

Figure 1.10. LANDSAT-7 image of the Swan Coastal Plain, showing Lake Thetis.

level, they observe that the ~0.5-m changes in lake level follow seasonal trends related to rainfall and evaporation and that the lake lacks observable tidal influences. Playford (1997) noted similar hydrology in the saline lakes on Rottnest Island, analogous to Lake Thetis in shape, topography, and the presence of a thick BMC. These lakes rise to more than 1 m above sea level in the winter as a result of rainfall intake and fall to more than 1 m below sea level in the summer as a result of evaporation. Playford (1997) postulates that impervious microbial mats and muddy sediment act as seals on the floor of the lake, which prevent the inflow of groundwater from below.

The idea, however, that Lake Thetis has a deeper groundwater connection to the ocean persists. Tourist information sheets (undated) in the Visitors Center in Cervantes state that water level in the lake rises and falls with the tides, indicating a possible underground connection to the sea. Ms. Rebecca Carter, a staff member in the Moora District Office of the Department of Conservation and Land Management in Jurien Bay, was considering writing a small grant proposal in June 2004 to investigate whether the lake level exhibited any tidal influence (personal communication). The question remains whether or not the lake currently has, or has had in the past, a subterranean connection to the sea.

WATER CHEMISTRY OF LAKE THETIS

Lake Thetis is hypersaline, with measured salinity between 39 g/L (1.1 times the salinity of seawater) and 53 g/L (1.5 times the salinity of seawater) (Tables 1.1 and 1.2). The water is a Na-Cl brine, with ionic ratios similar to those of seawater (Table 1.1). The pH is also similar to that of the surface seawater in the Indian Ocean, which varies from 8 and 8.4 (World Ocean Atlas, 2001). Grey and others (1990) measured a pH range of 8.3 to 8.6 during their study between 1985 and 1989. The pH measured by this study on 16 June 2004 was 8.0 (Table 1.2). In addition, measurements to date indicate that the lake water is vertically and laterally well mixed. Samples collected at different surface sites and from surface and bottom by Grey and others on 25 May 1985 showed no variation in chemistry. Bottom and surface salinity, pH, and temperature measurements by this study at one site were identical (Table 1.2). The temperature of the lake water in June 2004 was similar to the average annual air temperature in June (Fig. 1.9), suggesting that the

Table 1.1. Chemistry of water from Lake Thetis, ephemeral pools in the abandoned quarry, and nearby groundwater, with standard seawater for comparison. Concentrations are in g/L. Data from Grey and others (1990) for 1985-1987 from lake samples from surface at shelf break on south shore.

date	sample	Na	K	Ca	Mg	Cl	SO_4^{2-}	Total alk	Na/Cl	K/Cl	Ca/Mg	Ca/SO_4	Mg/SO_4	Salinity	Lake level
25 May 85	lake water	15.69	0.559	0.445	1.88	26.90	4.15	0.247	0.58	0.021	0.267	0.107	0.453	47	low
26 July 85	lake water	14.17	0.520	0.409	1.77	24.18	5.24	0.241	0.59	0.022	0.231	0.078	0.338	--	
16 Nov 85	lake water	15.49	0.559	0.451	1.96	28.40	4.05	0.232	0.55	0.020	0.230	0.111	0.484	48	low
09 July 86	lake water	Not measured							--	--	--	--	--	39	max high
1 April 87	lake water	Not measured							--	--	--	--	--	53	very low
26 May 87	lake water	15.00	0.575	0.571	1.85	25.99	3.83	0.287	0.58	0.022	0.309	0.149	0.483	--	
3 March 89	lake water	14.90	0.534	0.433	1.87	26.41	3.39	0.201	0.56	0.021	0.232	0.128	0.488	48	low
16 June 04	lake water	Not measured							--	--	--	--	--	42	high
25 May 85	quarry pool	2.76	0.098	0.148	0.377	5.03	0.591	0.452	0.55	0.019	0.393	0.250	0.638	--	
26 July 85	quarry pool	0.860	0.031	0.600	0.136	1.68	0.038	0.262	0.51	0.018	4.412	15.789	3.579	4	
26 July 85	quarry piezometer	1.85	0.059	0.150	0.194	3.47	0.024	0.445	0.53	0.017	0.773	6.25	8.083	7	
26 July 85	s. shore piezometer	22.91	0.833	0.533	2.89	38.54	9.09	0.391	0.59	0.022	0.184	0.059	0.318	76	
	standard seawater	10.76	0.399	0.411	1.29	19.35	2.71	0.142	0.56	0.021	0.319	0.152	0.476	35	

Table 1.2. Properties of water measured by this study, 16 June 2004 near the center of Lake Thetis

Depth (m)	Salinity (g/l)	Temperature (° C)	PH	Turbidity (NTU)	dissolved oxygen (mg/l)
0	42	16.5	7.9	20.6	104.6
1.9	42	16.4	8.0	19.5	103.7

shallow lake equilibrates relatively quickly to the ambient air temperature.

This study also measured turbidity and dissolved oxygen of the lake water. Turbidity is a measurement of the cloudiness of water and it is measured in nephelometric turbidity units (NTU). The World Health Organization recommends a maximum of 5 NTU (MDBMC, 1987) for drinking water; although it is typically much less. For example, the turbidity of Los Angles drinking water ranges between 0.10 and 0.25 NTU (Los Angeles Department of Water and Power Water Quality Report 2004). Turbidity of seawater is variable, depending on productivity and proximity to stream inflow. For example, turbidity in Corpus Christi Bay off the coast of Texas ranges from 2 to over 100 NTU. High turbidity is caused by inflow of sediment-laden stream water during flooding (Duranceau and Henthorne, 2004). The ~20 NTU turbidity of Lake Thetis is high enough so that the bottom of the 2-m-deep lake cannot be seen from the surface. It results from high organic productivity because there is no stream flow into the lake.

Dissolved oxygen (DO), the measurement of the amount of oxygen dissolved in a unit volume of water, is typically no more than 2 mg/L in drinking water (Lenntech, 2005). DO is not an important characteristic of drinking water, except in improving its taste. DO in lake water, however, is important in influencing biological productivity. An average monthly concentration of 8 mg/L DO is needed for the survival of eukaryotic,

heterotrophic aquatic life (British Columbia Water Quality Report, 1997). Annual dissolved oxygen in the Indian Ocean off the coast from Jurien to Cape Leeuwin ranges between 5 and 5.25 mg/L (World Ocean Atlas, 2001). Thus, the extremely high ~104 mg/L daytime DO of Lake Thetis (Table 1.2) reflects the photosynthetic activity of the active benthic microbial community and is important in maintaining fauna in the lake.

The quarry water was sampled from standing pools. Groundwater samples were taken from piezometers placed north of the lake in the quarry and south of the lake, just past the foreshore zone. Grey and others (1990) did not give the depths of the piezometers. These authors interpret the low salinities of the surface and shallow subsurface waters of the quarry (Table 1.1) to represent meteoric water that has interacted to varying degrees with the surrounding carbonate aquifer of the Holocene limestone. They interpret the high salinity of the water from the piezometer south of the lake to represent an internal groundwater system with a body of hypersaline water underlying the lake.

PREVIOUS WORK ON SEDIMENTOLOGY OF LAKE THETIS

In 1990, Grey and others published the only journal article yet devoted to the limnology of Lake Thetis. The article addressed the geology and geomorphology of the area, the hydrology and water chemistry, the diverse benthic microbial community, the stromatolite petrology, and the sedimentology of a 96-cm-long core. Their data also included limited stable isotope analyses on stromatolites and radiocarbon ages on core sediment, stromatolites, and lake water.

Grey and others (1990) divided the sediment of the core into three zones, but provide only a general description of each interval. The top 0 to 50 cm consist of purple mud, composed of carbonate mud and organic detritus with irregular sandy laminae. Fauna include ostracodes indicative of a permanent saline lake (species not identified). The middle 50 to 73 cm consist of alternating brown, purple and white varves of muddy sand. Grains include brown-stained rounded quartz grains and carbonate sand and ostracodes similar to those in the top of the core, indicative of saline conditions and, possibly, episodic stratification. The bottom 73 to 96 cm consist of alternating brown and buff fine-grained carbonate sand. The top of this zone at 73 cm is marked by a micro-breccia horizon of white chips of fine-grained, lightly indurated carbonate. Within this zone, a solitary charophyte oogonium was recognized, in addition to ostracodes identical to those in the middle zone.

PREVIOUS WORK ON GEOCHRONOLOGY OF LAKE THETIS

Radiocarbon ages were determined on water, sediment, and stromatolites using the beta-counting technique on dissolved bicarbonate in water and on carbonate minerals in the solid matter. This technique requires a large sample volume, and therefore, has low spatial resolution in the rock and sediment samples (Faure, 1986). Furthermore, carbonate minerals formed in lakes in carbonate-rich drainage basins are not ideal materials for radiocarbon dating techniques because they incorporate dissolved bicarbonate derived from dissolution of older materials and in turn, give anomalously old ages (the "hardwater effect") (Wagner, 1998). Radiocarbon analyses of bulk samples of carbonate sediment can also include wind- or water-deposited sediment from older terrains, which

results in anomalously old ages. In addition, porous material like stromatolites may incorporate younger carbonate cement, which resulting in anomalously young ages. Therefore, the ages determined by Grey and others (1990) provide only a very general geochronological framework.

Grey and others (1990) measured the age of the lake water as 670±180 y B.P., indicating that it contains bicarbonate derived from older material that has not equilibrated with carbon reservoir of the atmosphere. The radiocarbon age obtained from carbonate material concentrated from the 0-50 cm interval of the sediment core is modern, the age from the 50-73 cm interval is 3100±80 y B.P., and the age from the 73-96 cm interval is 3920±90 y B.P. The papillate crust of submerged bench 1 yields an age of 630±260 y B.P. The core, or oldest part, of a stromatolite on bench 2, the seasonally exposed terrace, has a radiocarbon age of 1720±70 y B.P. As described below in Methods, samples were taken from core 2 of this study for radiocarbon dating of organic matter using the Accelerated Mass Spectrometry (AMS) technique (Dickin, 1995). These samples provide a geochronological framework with a higher spatial resolution than that of Grey and others (1990). Measurements on organic matter avoids the error introduced by incorporation of older dissolved bicarbonate into carbonate minerals.

PREVIOUS WORK ON HOLOCENE CLIMATE IN WESTERN AUSTRALIA

Tropical cyclones, storm surges, and droughts have influenced the geomorphology and ecosystems along the Western Australian coast throughout the Holocene. An understanding of the timing and magnitude of drought-wet cycles is important in interpreting the impact of climate change on the region and in correlating

these events to global changes. However, prehistoric climate records for this area based on detailed study of climate proxies are lacking. In fact, no high-resolution climate records have been published for the region of southwestern Australia.

Zheng and others (2002) show that rainfall and temperature increased to a maximum during the Holocene between 8000 and 5000 y BP. Their climate study was based on observations of high shoreline deposits of Lake Cowan and Lake Lefroy of southwestern Australia (Fig. 1.10). Shepherd and Eliot (1995) described an increase in marine erosion of coastal dunes and marine cliffs in the Cervantes area between 2000 and 3000 y BP that they attribute to an increase in the occurrence and/or frequency of either tropical cyclones or winter cyclonic storms.

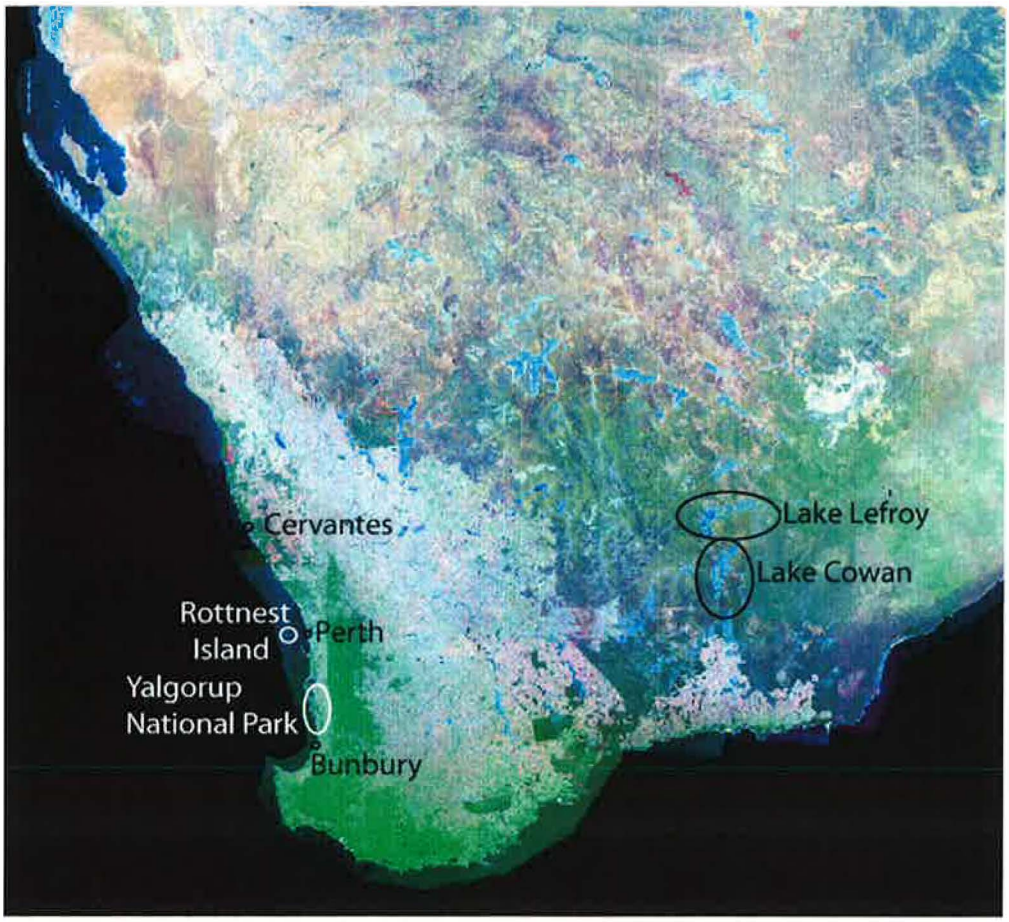

Figure 1.10. LANDSAT-7 image of Western Australia showing the locations mentioned in the text.

Playford (1980) studied shoreline deposits of saline lakes on Rottnest Island, 18 km west of Perth, Western Australia (Fig. 1.10). He interpreted these to be marine shorelines, formed when the lakes were joined to the sea at times of higher sea level. He published an apparent sea-level curve for the southwestern coast of Australia for the past 8000 y (Fig. 1.11). However, he noted that the sea-level highs between 5000 and 6000 y and 2000 and 3000 y do not have global correlations and cannot represent global eustacy. He offers several possibilities related to tectonism, geoid deformation, and changes in water circulation and temperature in the Indian Ocean. The cause of apparent sea-level rise in this area is yet unexplained, but it is interesting to note that these intervals in the Holocene coincide with periods of increased storm intensity and periods of increased rainfall documented by Shephard and Eliot (1995) and Zheng and others (2002).

In addition, Backhouse (1993) used radiocarbon ages of charcoal to calculate sedimentation rates in different intervals of a core from Barker Swamp on Rottnest Island. A high sedimentation rate of 10 cm/100 y occurred between 5645 and 5300 y, coincide with the high sea-level stand documented by Playford (1980). A decrease in pollen abundance and sedimentation rate at ~4500 y represents a prolonged drought interval, which coincides with reduced winter water flow in the Swan River system in the mid Holocene (Kendrick, 1977).

Rosen and others (1995) measured the seasonal isotopic composition of the water in Lake Hayward in the Yalgorup National Park (Fig. 1.10), as well as the isotopic composition of carbonate precipitated in the lake. They found that the highest $\delta^{18}O$ of the water occurs during the dry season in the late summer/early autumn. Precipitation of the bulk of carbonates coincides with this time of warmest water. These findings show that

summer data could dominate the stable isotope record of carbonates formed in Lake Thetis so that the record could show long-term trends in summer conditions only.

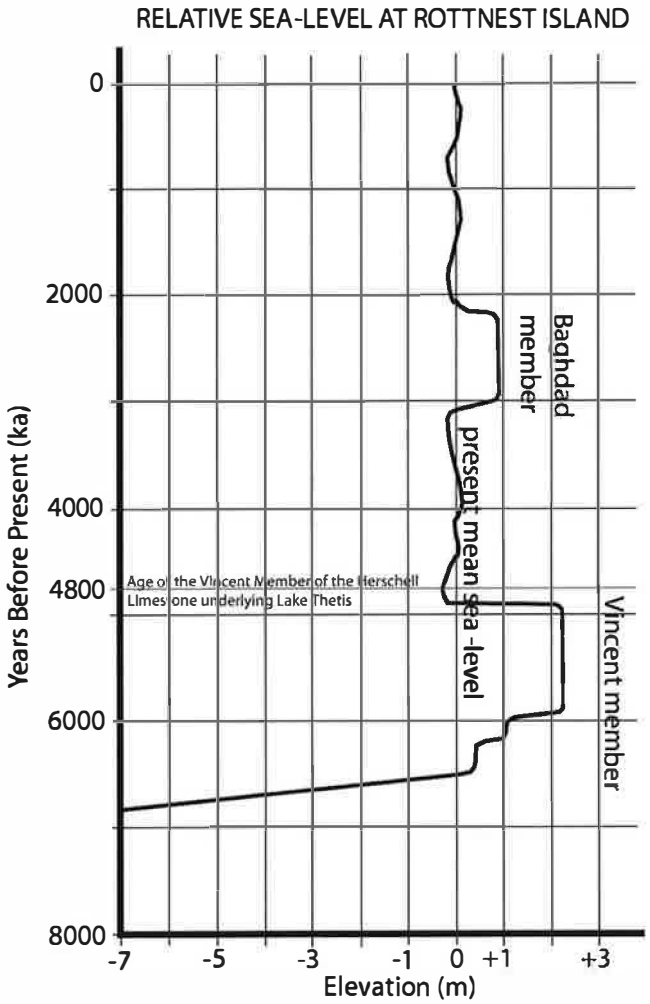

Figure 1.11. Holocene sea-level curve based upon elevations and radiocarbon ages of serpulid terrace deposits along lake margins on Rottnest Island (modifed from Playford, 1988).

PREVIOUS WORK ON HOLOCENE CLIMATE IN WESTERN AUSTRALIA

Lake Thetis is located near the boundary between the northern and southern storm tracks (Shepherd and Elliott, 1995) and therefore is in a critical location to contain excellent archives for studies of short-term climate changes. In addition to the post-5000 y major trends in Holocene climate described above (assuming the bottom of the lake is

bounded by the ~4800 y equivalent of the Vincent Member of the Herschell Limestone), the sediment record of Lake Thetis has the potential to define a high temporal resolution record of small magnitude variations in rainfall and/or temperature.

The primary focus of this study was directed at documenting parameters directly affected by changes in lake volume associated with drought-wet cycles. During times of drought when evaporation exceeds precipitation, lake volume and lake area will decrease, which will promote the following: 1) deposition of coarser-grained sediment in the lake center, 2) shift of species to those tolerant of high salinity, and 3) increase in $\delta^{18}O$ values in both endogenic micrite and ostracodes. In contrast, during times of frequent and intense precipitation, precipitation will exceed evaporation and lake volume will increase. Under these conditions, 1) finer-grained sediment will be deposited in the lake center, 2) species will shift to those tolerant of brackish to fresh water, and 3) $\delta^{18}O$ values in both endogenic micrite and ostracodes will decrease.

The magnitude of the change in these parameters will be influenced by the source(s) of water that enter the lake. As noted above in the section on Hydrology of the Study Area, it is not certain whether or not the lake has a strong groundwater connection to the Indian Ocean. If so, then the lake will contain a major component of seawater-derived groundwater. Inflow of a significant seawater component throughout the lake history will have acted to moderate the changes in lake volume, salinity, and O-isotope composition caused by drought-wet climate cycles. Therefore, the shifts in sediment, biota, and O-isotope values in carbonates are predicted to be less intense if Lake Thetis has a strong oceanic groundwater connection than if it is solely fed by meteoric sources.

Alternatively, Lake Thetis could be an evolved saline lake, where the water in the

lake is solely derived from meteoric precipitation and meteorically derived groundwater in a region where evaporation generally exceeds precipitation. The $\delta^{18}O$ of precipitation in the Perth area, which should be similar to that in Cervantes, is -4.2‰ (VSMOW) in July and -0.8‰ (VSMOW) in January. Because the largest volume of rainfall is in the winter months of June and July, the average annual $\delta^{18}O$ is -2.9‰. Rainfall on the porous limestone of the drainage basin of Lake Thetis will infiltrate and undergo some water-rock interaction with the marine limestone, which has a $\delta^{18}O$ of +0.3 (measurements from quarry limestone in Grey and others, 1990). This interaction will cause the $\delta^{18}O$ of the rainwater to increase. There are no measurements of $\delta^{18}O$ of Lake Thetis, but because the direct rainfall and groundwater inflow would have a minimum value of ~-3‰ (VSMOW), only very large volumes of meteoric water would show significant changes to the overall $\delta^{18}O$ of the lake. For example, if the lake had a $\delta^{18}O$ similar to slightly evaporated seawater of ~+2 ‰ (VSMOW), an increase in volume of 5% from addition of meteoric water with a $\delta^{18}O$ = -3‰ (VSMOW) would result in a lake with a $\delta^{18}O$ = +1.75 ‰ (VSMOW). An increase of 10% would change the $\delta^{18}O$ of the lake to −1.5 ‰ (VSMOW).

Because the $\delta^{18}O$ of the meteoric water in the area of Lake Thetis is only slightly negative relative to seawater (0 ‰ (VSMOW)) and because water-rock interaction in the shallow groundwater system will act to further increase the $\delta^{18}O$ of the meteoric water, only large volumes of meteoric inflow will be easily detected in the lake. In order to be detected in the sediment record, such isotopic conditions must persist for a period of time long enough to form endogenic sediment and/or ostracode carapaces. Moreover, the sampling interval must also be of sufficient resolution to sample the changes.

APPROACHES AND METHODOLOGY

Field Study

In June 2004, a field party from California State University Northridge (CSUN) and University of Western Australia (UWA) conducted a three-day reconnaissance of the lake. Members of the party were Dr. Vicki Pedone and the author from CSUN, and Dr. Annette George, Mr. William Wilson, and Ms. Linda Sprigg from UWA. The group examined and photographed features of the lake perimeter (particularly the stromatolite benches) and abandoned quarry. Operations in the lake center were conducted from a 4-m-long, flat-bottomed aluminum punt. Measurements of water properties (salinity, temperature, pH, turbidity, and dissolved oxygen) from a position in the lake center were made using a Hydrolab Multimeter 4a.

Two ~2-m-long cores from the lake center (Fig. 1.8) were taken by driving 6-m-long, 5-cm-diameter PVC pipe into the sediment with a 5-kg weight above a slip-collar around the pipe until ~1.5 m of pipe remained above water. The top of the pipe was filled with lake water and was tightly capped. The pipe was pulled by hand using tongs fitted to the pipe diameter. The core was laid horizontally in the punt, and the bottom of the pipe was tightly capped. A maximum length of ~2 m of sediment could be cored in water 2 to 2.5 m deep because ~1.5 m of pipe above the water surface was needed in order to lift the core. The pipe was easily driven into the lake bottom, indicating that lithified rock of the basement was not encountered. The total thickness of the sediment record in Lake Thetis is therefore unknown. The water-filled tops of the PVC pipe were cut off and the cores re-capped. The cores were transported in a vertical position back to UWA to minimize disturbance of the layers.

Laboratory Work at the University of Western Australia

The cores were set in a frame, and the PVC on opposite sides of the pipe was cut with a radial saw set exactly to the depth of the pipe thickness. A taut steel wire was pulled quickly through the split core, making a clean longitudinal separation of the core halves. Dr. Pedone made initial millimeter-scale descriptions using a handlens of 151-cm-long core 1 and 184-cm-long core 2. The author made digital-image records of the fresh surfaces. The core halves were cut in sections, tightly wrapped in plastic wrap, covered by cardboard cut to fit, and shipped by air to CSUN.

Core halves that remained in Perth were sampled for different analyses. Dr. Pedone sampled ten organic-rich layers over the extent of core 2 for AMS-radiocarbon dating. A thin horizontal slice was taken from the layer and all margins were trimmed with an Exacto knife to minimize the potential of contamination that might have occurred during coring and/or core processing. The ~1 to 2 g samples were placed in small ziplock bags and sent by air to CSUN in late June 2004, where they were kept frozen until they were sent to the NSF-University of Arizona Accelerator Mass Spectrometry (AMS) Laboratory in March 2005. These dates provide timing of deposition and the means to calculate sedimentation rates. Dr. Sandie McHugh, a research fellow and diatom expert at UWA, processed eight samples to isolate diatoms from eight of the layers in core 2 sampled for AMS dating. Results of her findings are presented in Chapter 2.

Laboratory Work at California State University Northridge

Core Description

Millimeter-scale descriptions of cores 1 and 2 were made using a handlens. Lithology, color, texture, composition, and fossil type and abundance were noted. Color was recorded using the Geological Society of America Mussell Color Chart, and texture was quantified by comparison to an Amstrat card. To augment data from handlens inspection, smear slides were made every 5 cm to further describe and quantify the composition, to examine the relationship between the organic and mineral components, and to identify microfossils. Smear slides were made as follows. A small quantity of sample was scraped off with a toothpick and mixed with a few drops of Norland Optical Adhesive 60 on a 45-X-27-mm glass slide. The mixture was cover slipped and placed under 366-nm UV light for five minutes to harden the adhesive. The slides were examined with reflected, transmitted-plane, and polarized light.

X-ray Diffraction Analyses

X-ray diffraction (XRD) analyses were conducted at the University of California, Los Angeles on a Philips XRD (patent #253798) and at the Getty Conservation Institute on a Siemens D5005 to determine the mineralogy of the sand and <20-micron fractions. Each sample was powdered and homogenized using an agate mortar and pestle and made into a slurry with alcohol and dried onto glass slides.

The position of the (104) peak was used to determine Mg content of calcite (Goldsmith and others, 1961; Lumsden, 1979). Calcite with >5 mole% $MgCO_3$ is considered as Mg calcite (Burton and Walter, 1987). Semi-quantitative estimates of the proportions of aragonite and calcite were made by comparing peak areas of the Lake

Thetis samples to peak areas of different mixtures of known proportions of aragonite and calcite that were previously measured on the now-defunct Diano Z80 at California State University Northridge.

C and O Isotopic Analyses

Sediment layers from the core contain varying amounts of organic matter, which had to be removed to prepare samples for C and O isotopic analyses. A razor blade was used to sample a 1-mm-thickness (about 0.4 g) from each layer to be analyzed. Samples were placed in small beakers with ~25 mL of Ultra Clorox Germicidal bleach and placed into a 50°C oven at for 48 hours to complete the oxidation reaction. Samples of the carbonate standards, Ultiss and NBS-19, used by the Stable Isotope Laboratory of the University of Southern California were subjected to the identical treatment to ensure that the oxidation by bleach did not affect the isotopic values of the carbonate. Analyses of the treated standards showed no deviation from the accepted values.

After oxidation of organic matter, each sample was wet sieved with de-ionized water through 1ϕ, 2 ϕ, and 3 ϕ metal meshes, and 4 ϕ (63 μm), 4.5 ϕ (45 μm), 5 ϕ (32 μm), and 5.5 ϕ (20 μm) nylon meshes into 1000-mL Pyrex glass beakers. Two components were selected for isotopic analyses: ostracodes and the <20-μm fraction, which consists dominantly of carbonate mud. Ostracodes were handpicked from the 2-ϕ mesh under reflected light at low magnification (~10X). Only those carapaces that were completely translucent and had no trace of chalky, white micrite were selected. The ostracode carapaces were washed five times using deionized water and once using methanol.

The fraction that passed through the 20-μm mesh settled completely, leaving the

overlying water completely clear. This indicates that the samples contained little or no clay particles. Much of the large volume of water in the 1000-mL beakers was decanted, and the remaining water and <20- μm sediment were washed into 15-mL HDPE-plastic test tubes. Samples were washed five times using deionized water and once using methanol. Samples were dried in a 50°C oven for 24 hours, then powdered and homogenized using an agate mortar and pestle.

The samples were taken to the Stable Isotope Laboratory at the University of Southern California and analyzed with a VG Isotech mass spectrometer under the supervision of Dr. Miguel Rincon. Approximately 20 μg of sample was used for analyses of ostracodes. This required five *Cyprideis australiensis* carapaces and one *Mytilocypris ambiguosa* carapace. Because the <20-μm fraction was not certain to be 100% carbonate, 40 μg of endogenic carbonate sediment was used for isotopic analyses. Duplicates to quintuplicates were run on nearly all samples, both endogenic and ostracodes, to assess intra-sample variation. The analytical precision was 0.1 ‰, based on the analyses of laboratory standards run with the samples.

AMS-Radiocarbon Analyses

Samples were sent to the NSF Arizona Accelerator Mass Spectrometer (AMS) Facility at the University of Arizona for age determination of the bulk organic matter in ten samples. The laboratory did all the sample preparation, which included drying, removal of carbonate, and combustion of the organic matter. Ages are reported as calibrated ages and are calibrated to the dendrochronology of Taylor (1987).

CHAPTER 2 -- RESULTS

INTRODUCTION

This chapter presents the results of sedimentology, paleontology, stable-isotope composition of carbonate mud and ostracodes, and radiocarbon dating. The majority of the data come from core 2 because it has the longest sediment record, but observations from core 1 are also included where appropriate.

As noted in Chapter 1, organic matter was oxidized by bleach in order to separate and clean carbonate components for isotopic analyses. The mineral residue was sieved to concentrate ostracodes in the sand fractions and concentrate the micrite in the <20-μm fraction. The weight fractions collected by sieving allowed construction of frequency weight percent plots of 37 selected samples. In addition, the sum of the dry mineral weights was compared to the starting wet sample weight, allowing the percent weight loss of water and organic matter to be calculated.

SEDIMENTOLOGY OF CORE 2

Overview

Three sediment types were identified in core 2, distinguished by differences in texture: sludge, sand and organic-rich sand. Table 2.1 shows the compositional and textural characteristics used to define each type of sediment. Each sediment type is further subdivided based on color into two sludges, three sands, and four organic-rich sands. Table 2.2 provides a description of sediment types, including their faunal content and stratigraphic distribution, and Figures 2.1 and 2.2 show images of the sediment types. Appendix A includes detailed descriptions of cores 1 and 2, and Appendix B shows the

full image records of the cores 1 and 2. Appendix C shows the observations that were made from the smear slides.

Table 2.1. Characteristics used to define sediment types in Lake Thetis cores

sediment type	organic matter	sand	compaction
Sludge	>30%	15-65%	uncompacted
Sand	5-35%	>60%	uncompacted in top 64 cm, compacted below them
Organic-rich sand	40-90%	5-55%	compacted

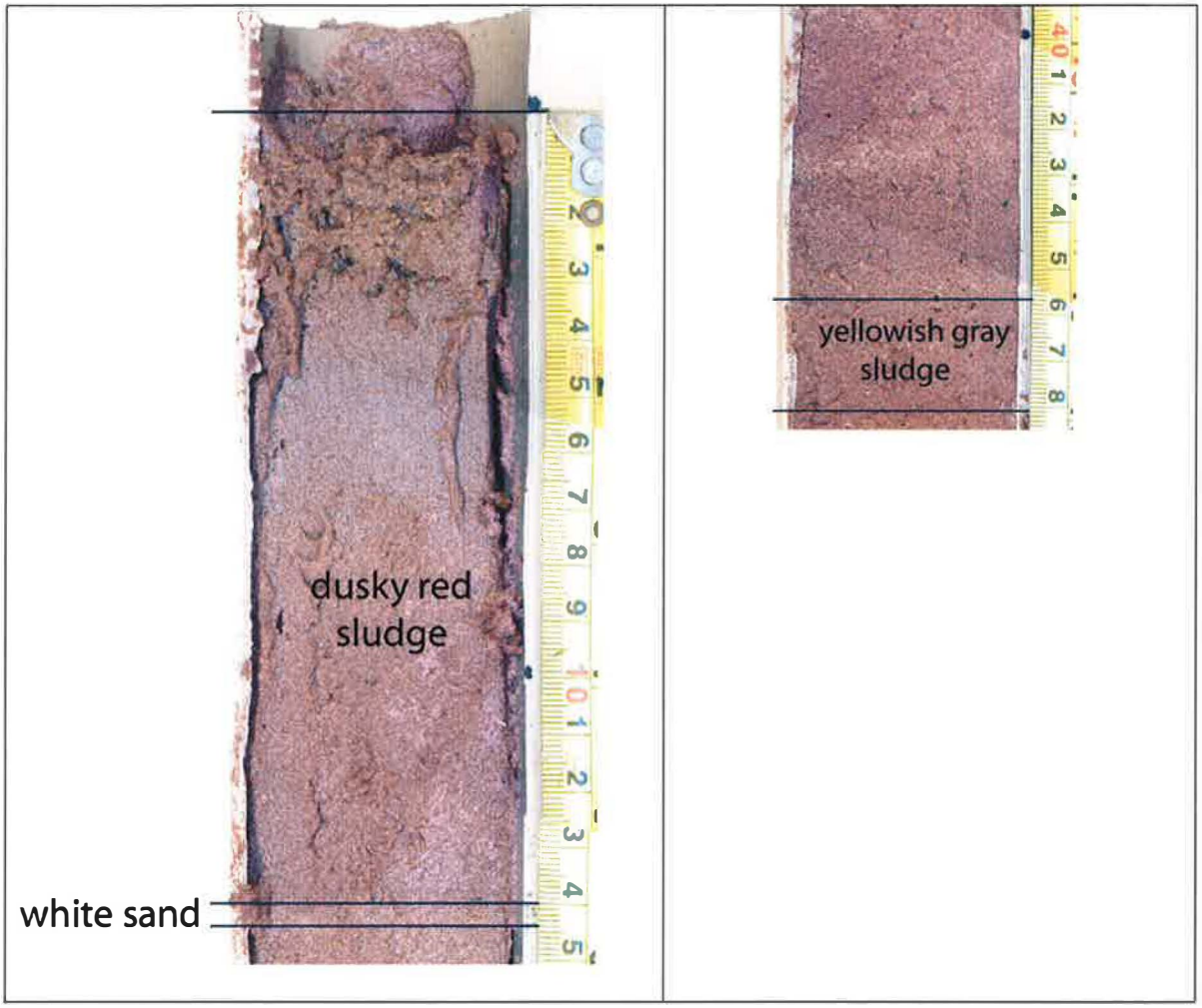

Figure 2.1. Images of the two types of sludge in Core #2. Scale is in centimeters.

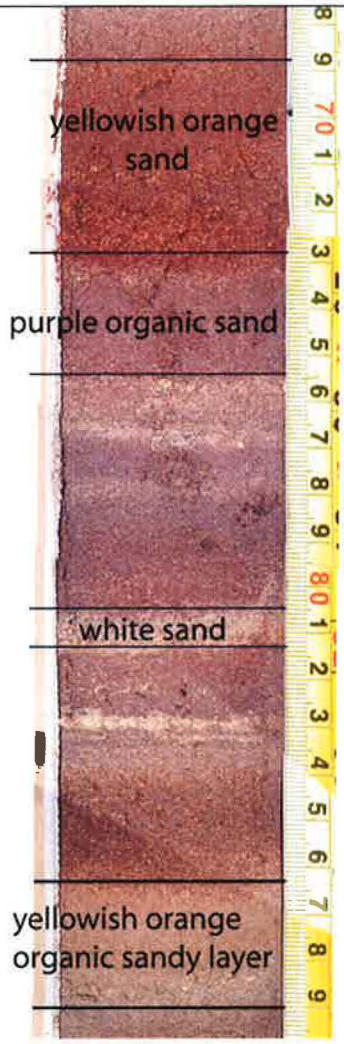

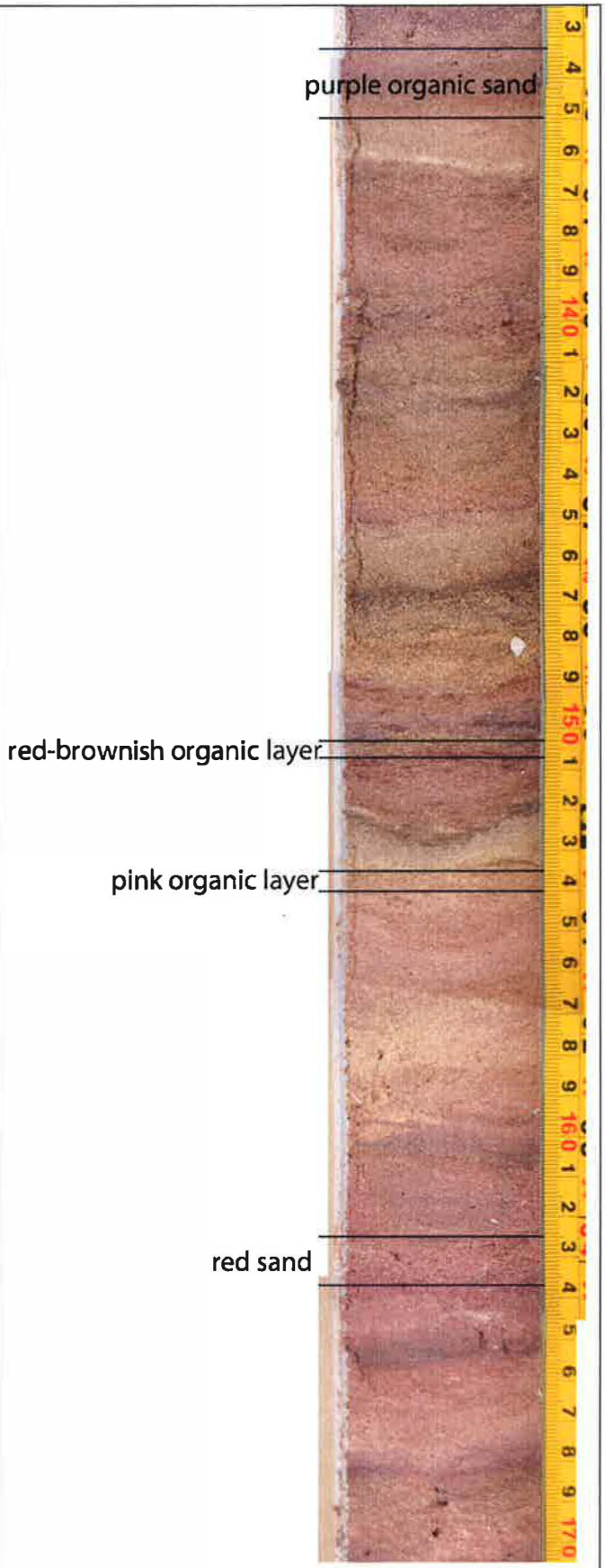

Figure 2.2. Images of sand and organic-rich sand in Core #2. Scale is in centimeters

Table 2.2. Lake Thetis Sediment Types. Average thickness values and mode values of composition are shown in parentheses.

SEDIMENT TYPE	COLOR(S)	THICKNESS (cm) range and average	COMPOSITION Range and mode	SAND SIZE	SKELETAL GRAINS	DISTRIBUTION IN CORE (cm)
Dusky red sludge	Dusky red (5R 3/4)	0.3-14 (3.1)	Organic: 45-80% (45%) Mud: 5% Sand: 15-50% (50%)	Very fine to fine	*Cyprideis australiensis*, *Coxiella exposita* (61 cm)	0-64.0
Yellowish gray sludge	Yellowish gray (5Y 8/1)	2.4	Organic: 45% Mud: 5% Sand: 50%	Very fine to fine	*Cyprideis australiensis*	45.7-48.1
Yellowish orange organic-rich sand	Dark yellowish orange (10YR 6/6)	0.7-8.1 (2.9)	Organic: 45-80% Mud: 5% Sand: 15-50%	Very fine to medium	*Cyprideis australiensis*	86.3-143.1
Purple organic-rich sand	Grayish red purple (5RP 4/2), very dusky purple (5RP 2/2, 5P 2/2), grayish purple (5P 4/2), pale yellowish brown (10YR 6/2)	0.1-2.7 (1.6)	Organic: 40-90% (85%) Mud: 5% Sand: 5-55% (10%)	Fine to medium	*Cyprideis australiensis*, *Mytilocypris ambiguosa*	114.4-143.2
Red Brownish organic-rich sand	Grayish red (10R 4/2), blackish red (5R 2/2)	0.1-1.8 (0.8)	Organic: 65-90% (90%) Mud: 5% Sand: 5-30% (5%)	Very fine	*Mytilocypris ambiguosa*	150.7-184.2
Pink organic-rich sand	Pink (5YR 8/1)	0.1-1.7 (0.8)	Organic: 75-90% Mud: 5% Sand: 5-20% (5%)	Very fine		153.5-179

Table 2.2 continued.

Purple organic-rich sand	Very dusky purple (5RP 2/2), Pale brown (5YR 5/2)	0.1-2.7 (1.6)	Organic: 40-90% (85%) Mud: 5% Sand: 5-55% (10%)	Very fine	*Cyprideis australiensis, Mytilocypris ambiguosa*	84.1-143.2
Yellowish orange sand	Pale yellowish brown (10YR 8/6), dark yellowish orange (10YR 6/6), yellowish gray, grayish orange	0.3-8.3 (2.3)	Organic: 5-25% (25%) Mud: 5% Sand: 70-90% (70%)	Fine to medium	*Cyprideis australiensis*	27.1-119
White sand	White, Dusky red (5R 3/4)	0.1-4.3 (1.1)	Organic: 5-35% (25%) Mud: 5% Sand: 60-90% (70%)	Fine to medium	Charophyte oogonia (107 cm). *Cyprideis australiensis, Coxiella exposita* (108 cm)	14.0-172.6
Red sand	Red-pink (5YR 8/1), Brownish gray (5YR 4/1), light gray (5YR 6/1), light brownish (5Y 3/2) gray, dark gray, olive gray	0.1-5.0 (1.0)	Organic: 5-35% (25%) Mud: 5% Sand: 60-90% (70%)	Very fine to fine	*Mytilocypris ambiguosa, Coxiella exposita* (76 cm)	120.6-185.9

Sand in the Lake Thetis cores ranges from 63 μm (boundary between silt and very-fine grained sand) to 500 μm (boundary between medium- and coarse-grained sand). With a given layer, sand is very well sorted to well sorted. Grain composition is dominantly carbonate, with angular quartz forming <5% of the fine- to very fine-grained sand fraction. Carbonate grains range from angular to well rounded, generally with roundness increasing with grain size. Most layers contain a percentage of carbonate grains that are partly to completely coated with submicron-size crystals of a yellowish-orange mineral, which, based on color, is interpreted to be an iron oxide mineral or mixture of iron oxide and hydroxide minerals. All shapes and sizes are coated, but the larger and more rounded grains especially tend to be coated (Fig. 2.3). Sediment layers in which >70% of the sand grains are coated are yellow gray to yellow orange in color. The core contains little silt and only ~5% carbonate mud in the 2-5 μm size range in all sediment types.

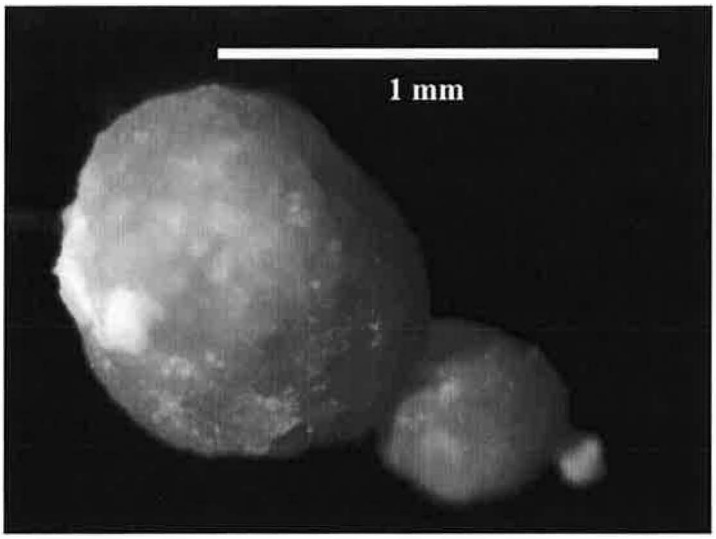

Figure 2.3. Carbonate grain coated with submicron-size iron oxide and/or hydroxide

Core 2 is divided into three intervals based on changes in sedimentology (Fig. 2.4). The top 64.5 cm consist of 57% sludge and 43% sand. Two sands occur in this interval: white sand and yellowish-orange sand. Sand grains in both sludge and sand layers in the top 64.5 cm are very fine to fine grained. The middle of the core (64.5-131

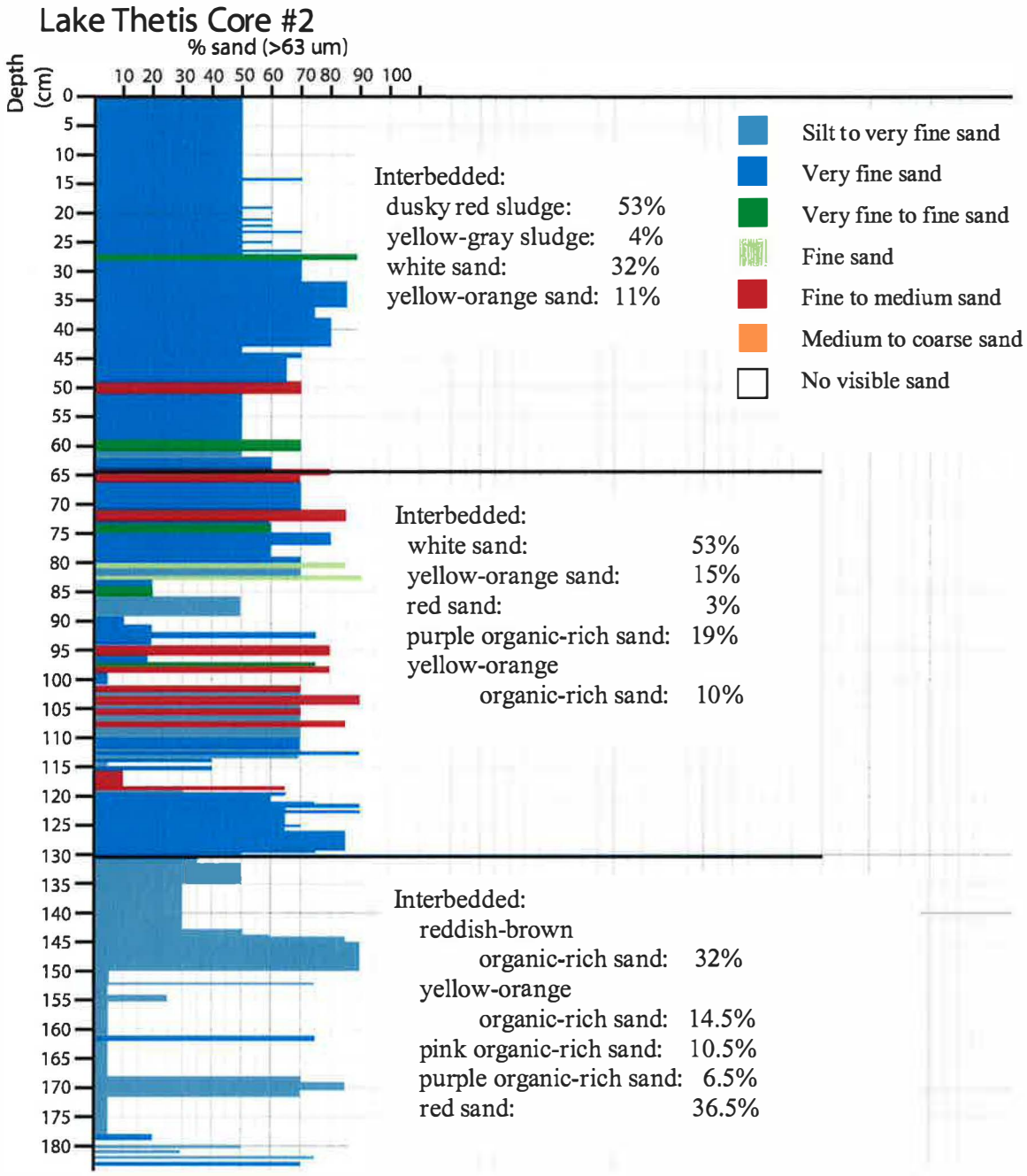

Figure 2.4. Stratigraphy of Lake Thetis core 2.

cm) consists of 71% sand and 29% organic-rich sand. Three sands occur in this interval: white, yellowish-orange and red. Grains are mostly fine- to medium-grained. White sand dominates, forming 53% of the middle interval. Because sand defined by this study can contain up to 35% organic matter, these "white" sand layers are commonly pale purple.

The bottom 54 cm of the core (131-183 cm) consists of 64% organic-rich sand and 36% sand. Except for one 0.2-cm-thick white sand, all sand in the lower interval is red. This interval contains all four organic-rich sands. However, the purple and yellowish orange organic-rich sands occur only between 131 and 143 cm, and the reddish brown and pink organic-rich sands occur only between 150 and 183 cm. The boundary with the overlying sand-dominated interval is gradational over a short interval and is characterized by a change to sediment dominated by partly decayed organic matter rather than sand and by the end of deposition of white and yellowish-orange sand layers.

Comparison with Core 1

The sedimentology of core 1 is generally similar that of core 2 (Figs. 2.4 and 2.5 and Appendix B), except that there is no lower interval dominated by organic-rich sand. There is, however, a change in core 1 at about the same stratigraphy level where the boundary occurs in core 2 to much finer-grained sands than in the interval above. In addition, white sand and yellow-orange sand are absent below 135 cm. Another distinct difference between the two cores is that core 1 contains coarser grain sizes than core 2. The sludge interval between 0 and 56 cm is dominated by fine- to medium-grained sand. The middle interval between 56 and 135 cm is predominantly fine- to medium-grained sand, but contains several layers of medium- to coarse-grained sand. The lower interval from 135 to 151 cm contains fine to very fine sand.

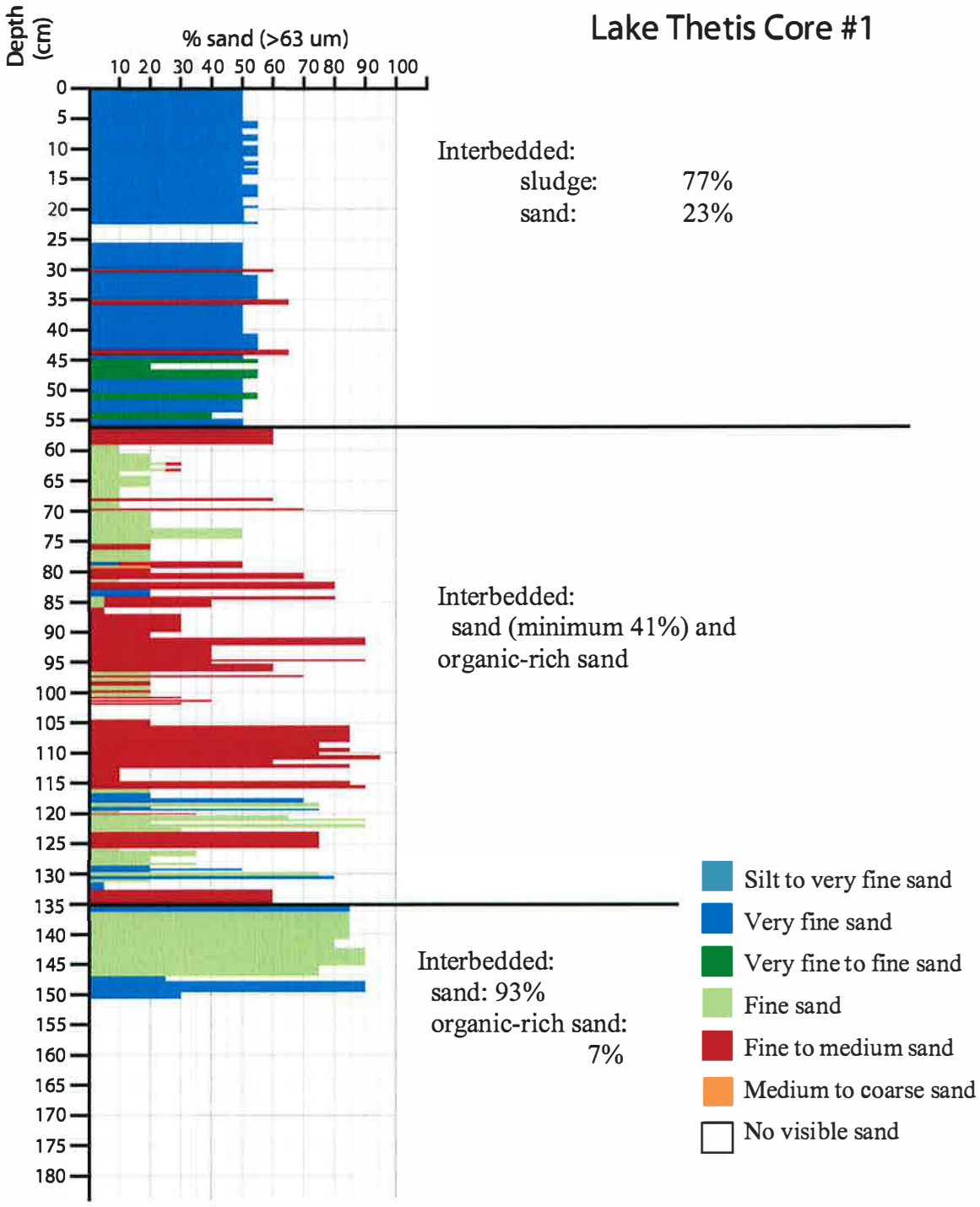

Figure 2.5. Stratigraphy of Lake Thetis core 1.

The detailed lithology of core 1 is not known as well as that of core 2 because percentages of organic matter, sand, and mud were not quantified for core 1 in smear

slides, which provide the most accurate way to quantify composition. Comparison of handlens examination and smear-slide study of core 2 shows that handlens examination tends to underestimate sand content, especially of very fine- to fine-grained sand, owing to the dense and opaque nature of compacted partly decomposed organic matter. Therefore, the estimate of the percentage of sand layers in core 1 in the middle interval is regarded as a minimum value.

Sludge

The two sludges were identified based on color and composition (Table 2.2 and Fig. 2.1). The dusky-red sludge forms 53% and the yellowish-gray sludge forms 4% of the top 64 cm. The only difference between the two sludges is color, which is the result of a high percentage of orange-coated sand grains in the yellowish-gray sludge. The unique characteristic of sludge is that it is uncompacted, containing abundant water-porosity. The sludge consists of >45% partly decomposed organic matter, 5% mud, and 15-50% scattered fine to very fine, well sorted sand. Smear slides show that sand grains are stuck to and embedded within the gelatinous organic matter. Furthermore, clay-sized crystals (<5 μm) with high birefringence form common clusters within the organic matter, often with a radial pattern around a central nucleus (Fig. 2.6). These crystals readily dissolve in cold HCl and are therefore identified as calcium carbonate (micrite).

Four samples of dusky-red sludge and one sample of yellowish-gray sludge were bleach treated and sieved. The frequency weight percent plot of the sludge samples shows a unimodal distribution with a mode of 3 ϕ (fine sand) (Fig. 2.7). The percentage weight loss of water and organic matter ranges from 35 to 79%, with an average of 65% (Appendix D).

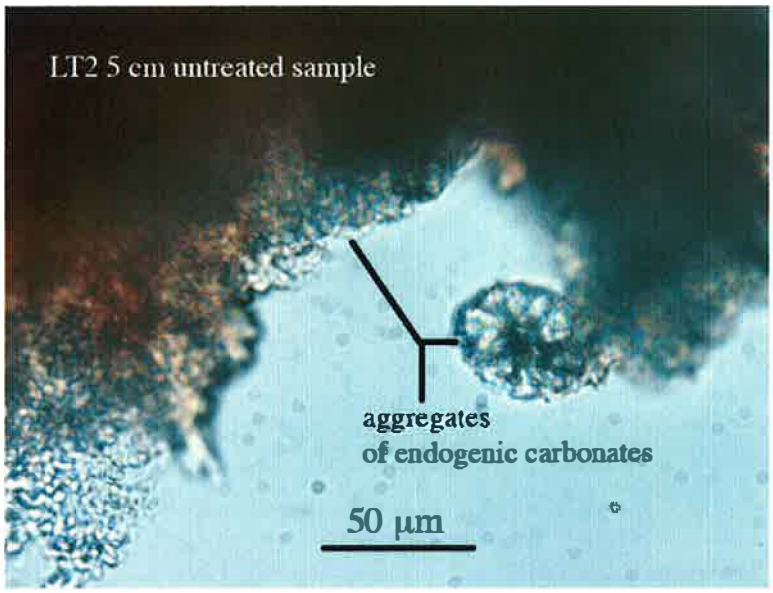

Figure 2.6. Photomicrograph of sludge showing an aggregate of micrite crystals with a radial pattern around a central nucleus and gelatinous organic matter.

Organic-rich sand

Four organic-rich sands are distinguished by color: purple, reddish-brown, pink, and yellowish-orange. Organic-rich sand differs from sludge in being dense (compacted) and cohesive (Table 2.1 and Fig. 2.2). This sediment type consists of 5 to 55% sand, 5% mud, and 40 to 90% organic matter. The purple and yellowish-orange organic-rich sands occur in the middle, sand-dominated interval (64 to 131 cm) and the top of the basal organic-rich sand interval (131 to 143 cm) (Fig. 2.4). The reddish-brown and pink organic-rich sand occur only in the basal interval below 157 cm.

Eight organic-rich sands were bleach treated and sieved: two purple, three reddish brown, and three yellow orange. The purple and yellowish-orange organic-rich sands are generally coarser grained than the reddish-brown organic-rich sand (Fig. 2.8). Both purple organic-rich sands have a unimodal distribution with a mode of 3 ϕ. The sample that occurs higher in the stratigraphic sequence in the sand-dominated interval at 85.5 cm

is less well sorted and has a significantly higher percentages of grains coarser than 3 ϕ than the sample that occurs at 129 cm near the boundary with the organic-rich sand-

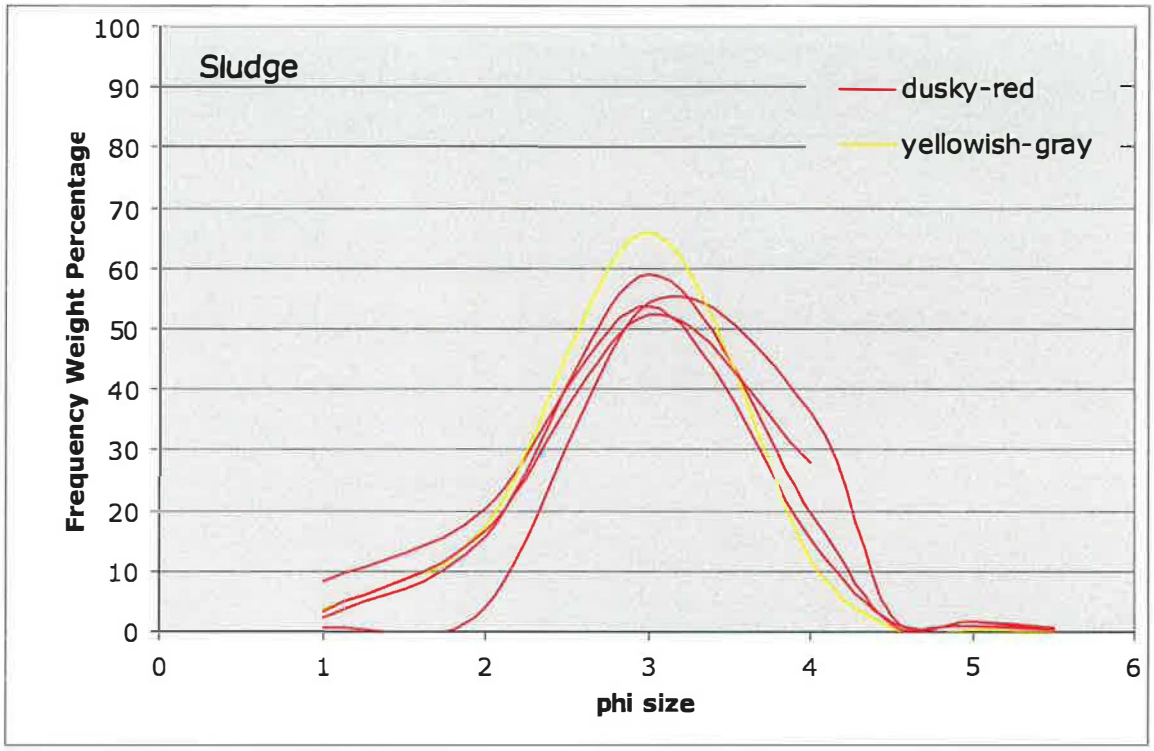

Figure 2.7. Grain size distribution of sludge.

dominated interval. Two of the yellowish-orange organic-rich sands have unimodal distribution with a mode of 3 ϕ, whereas the other two are coarser grained. One has a bimodal distribution with the major mode at 2 ϕ and a minor mode at 4 ϕ. All reddish-brown organic-rich sands have bimodal distributions. One has a major mode at 3.5 ϕ and a minor mode at 5 ϕ. The other two have major modes at 4 ϕ and minor modes at 2 ϕ. The total percent weight loss of water and organic matter for these eight samples range from 58% to 97%, with an average of 77%. (Appendix D).

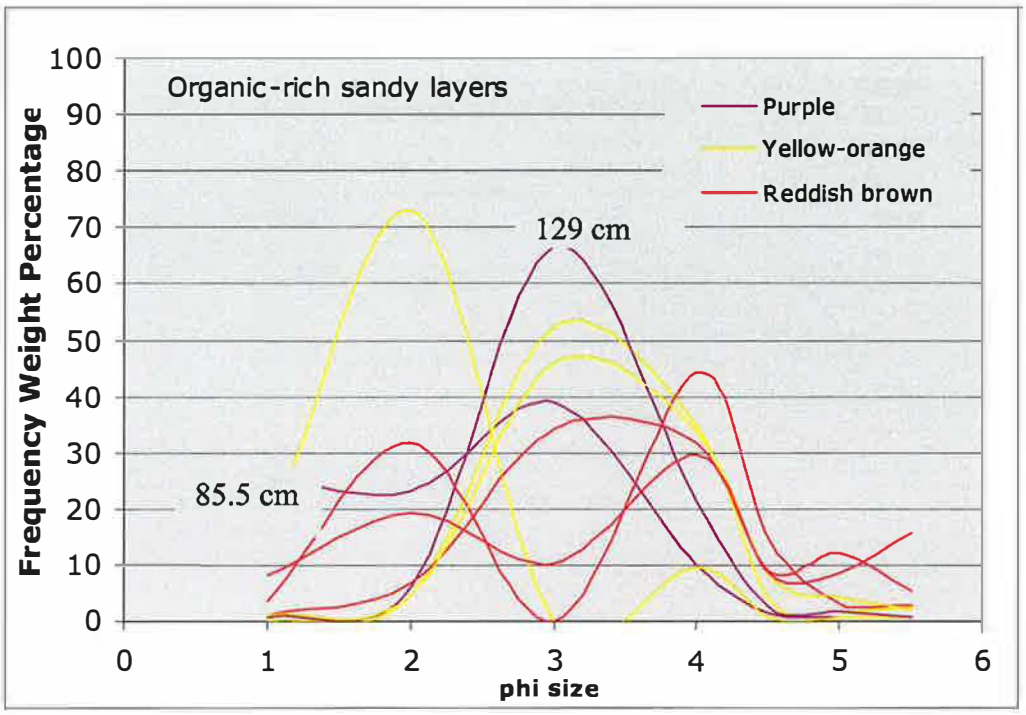

Figure 2.8. Grain size distribution of organic-rich sands.

Sand

Three types of sand are distinguished on the basis of color: white, yellowish-orange, and red (Table 2.2 and Figs. 2.2 and 2.4). Sand defined by this study consists of >60% sand, 5% mud, and 5 to 35% organic matter. White and yellow-orange sands occur in the sludge and sand-dominated intervals. The differences between these two sands are that the yellow-orange sand contains a significantly higher percentage of orange-coated grains, tends to be slightly coarser grained than the white sand, and has greater maximum and average thicknesses. Red sand occurs in the lower portion of the sand-dominated interval and throughout the lower organic-rich sand interval. The red sand is very fine- to fine-grained, whereas most layers of the other two sands are fine- to medium-grained.

Twenty-four sands were bleach treated and sieved: processed for isotopic analysis: 17 white, 5 yellow orange, and 2 red. Fifteen of the white sands have unimodal

distributions with mode at 3 ϕ to 3.5 ϕ (Fig. 2.9). One is only moderately sorted, with a poorly defined mode at 4 ϕ, and one has a bimodal distribution with a mode at 3 ϕ and a second mode not defined by the sieve sizes, but at least 1 ϕ. Three of the yellow-range sands have unimodal distributions with modes between 2.5 ϕ and 2 ϕ. The other two do not have modes defined by the sieve sizes, but are at least 1 ϕ. The two of the red sands have unimodal distributions, one with a mode of 3.5 ϕ and the other of 4 ϕ.

The total percent weight loss of water and organic matter for all sand samples ranges from 3 to 84% (Appendix D). The high values are from samples that are borderline between sand and organic-rich sand.

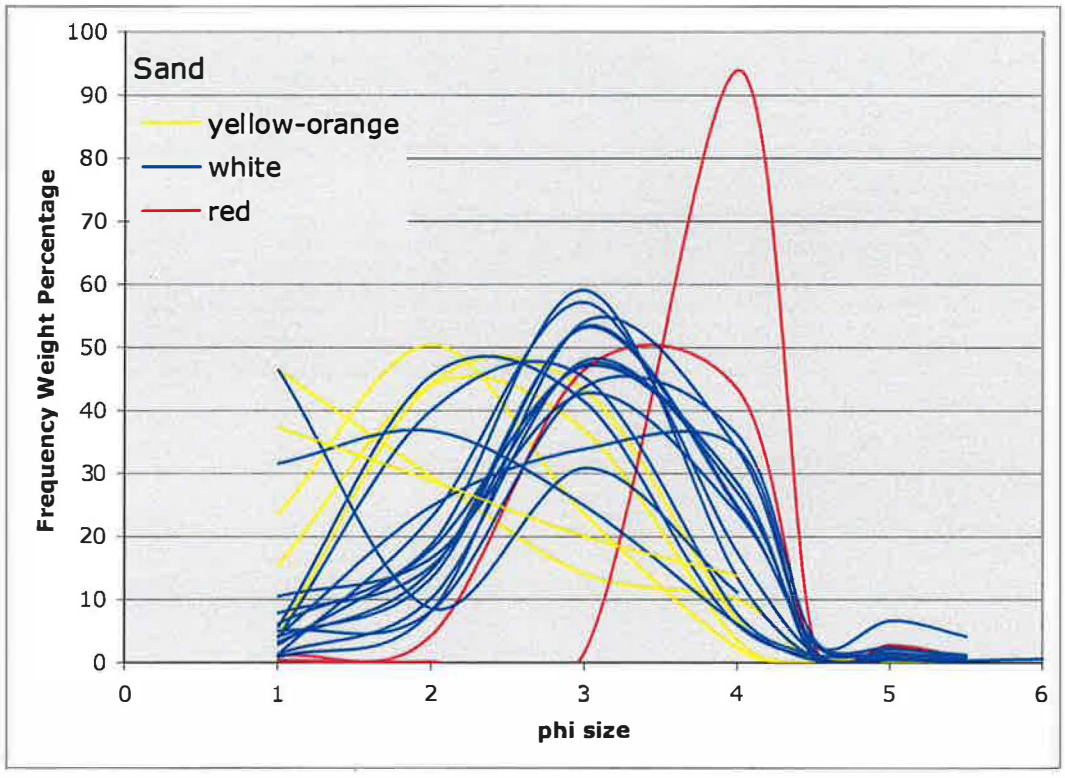

Figure 2.9. Grain size distribution of sand.

X-RAY DIFFRACTION

X-ray diffraction (XRD) analyses were made on 15 sieved sand fractions from selected samples in core 2 (Fig. 2.10). The 3ϕ fraction was used, unless there was not enough material for the analysis, in which case several size fractions were combined. For nine of these samples, enough material from the <20-μm fraction was also available for XRD analyses (Fig. 2.11). One additional <20-μm sample, for which there was insufficient sand-size material, was analyzed. The only two minerals detected in the sand and fine fractions were aragonite and Mg-calcite. The Mg-calcite in both fractions contains 9 to 12.5 mole% $MgCO_3$. No vertical changes in mineralogy in either the sand or fine fraction were defined by the limited sampling of the core.

Ten of the 15 sand samples are pure aragonite. The other five range from 57% to 78% aragonite and 22% to 43% Mg-calcite. Four of the fine fractions are identical to the sand fraction in the same sample, being pure aragonite. The other five analyses of fine samples that had analyses of sand from the same sample differed in having more Mg-calcite than the sand. For example, the sand in the sample at 180 cm was all aragonite, whereas the fine fraction was 75% Mg-calcite and 25% aragonite.

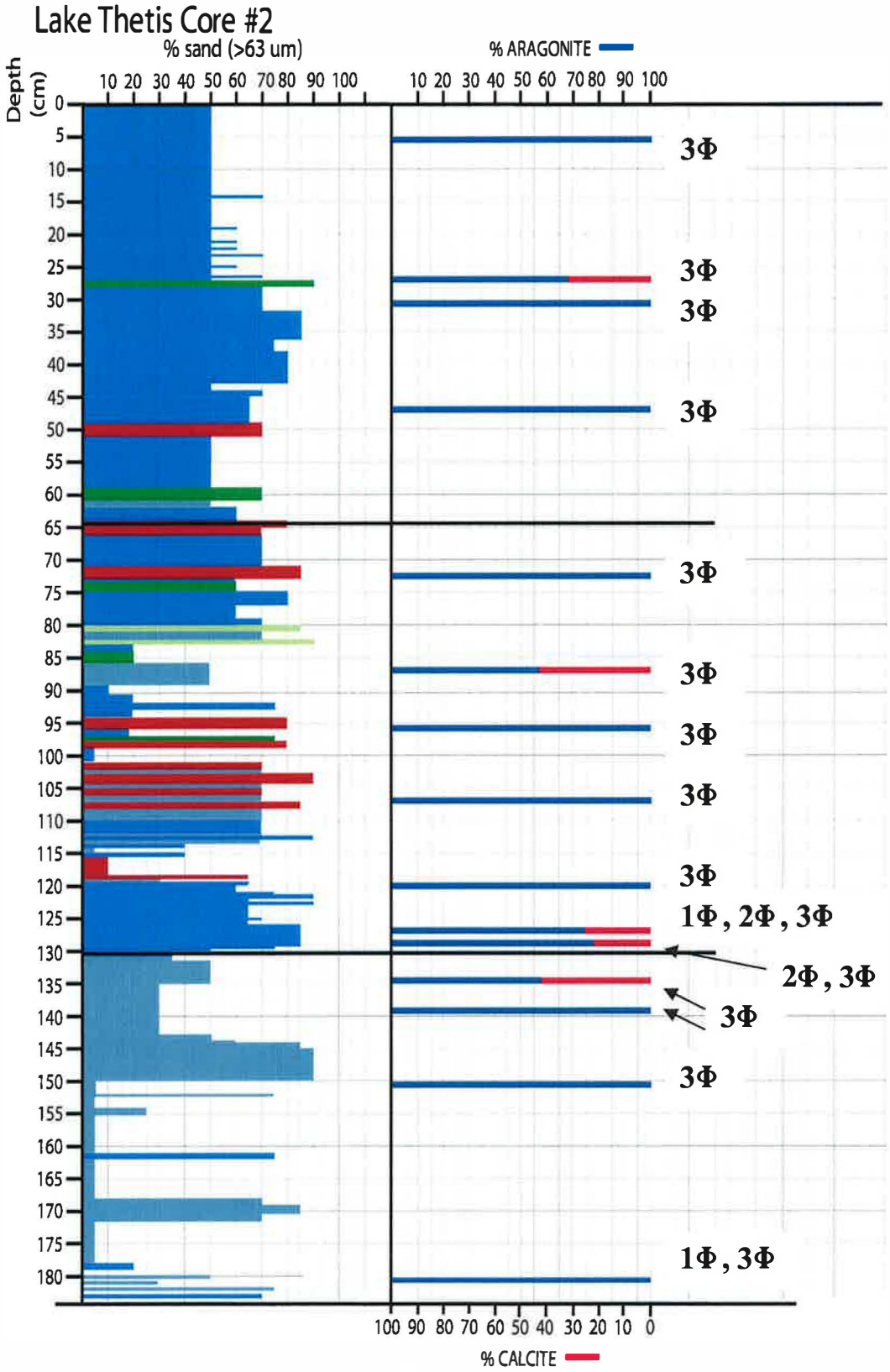

Figure 2.10. Distribution of aragonite and Mg-calcite in sand in Lake Thetis core 2.

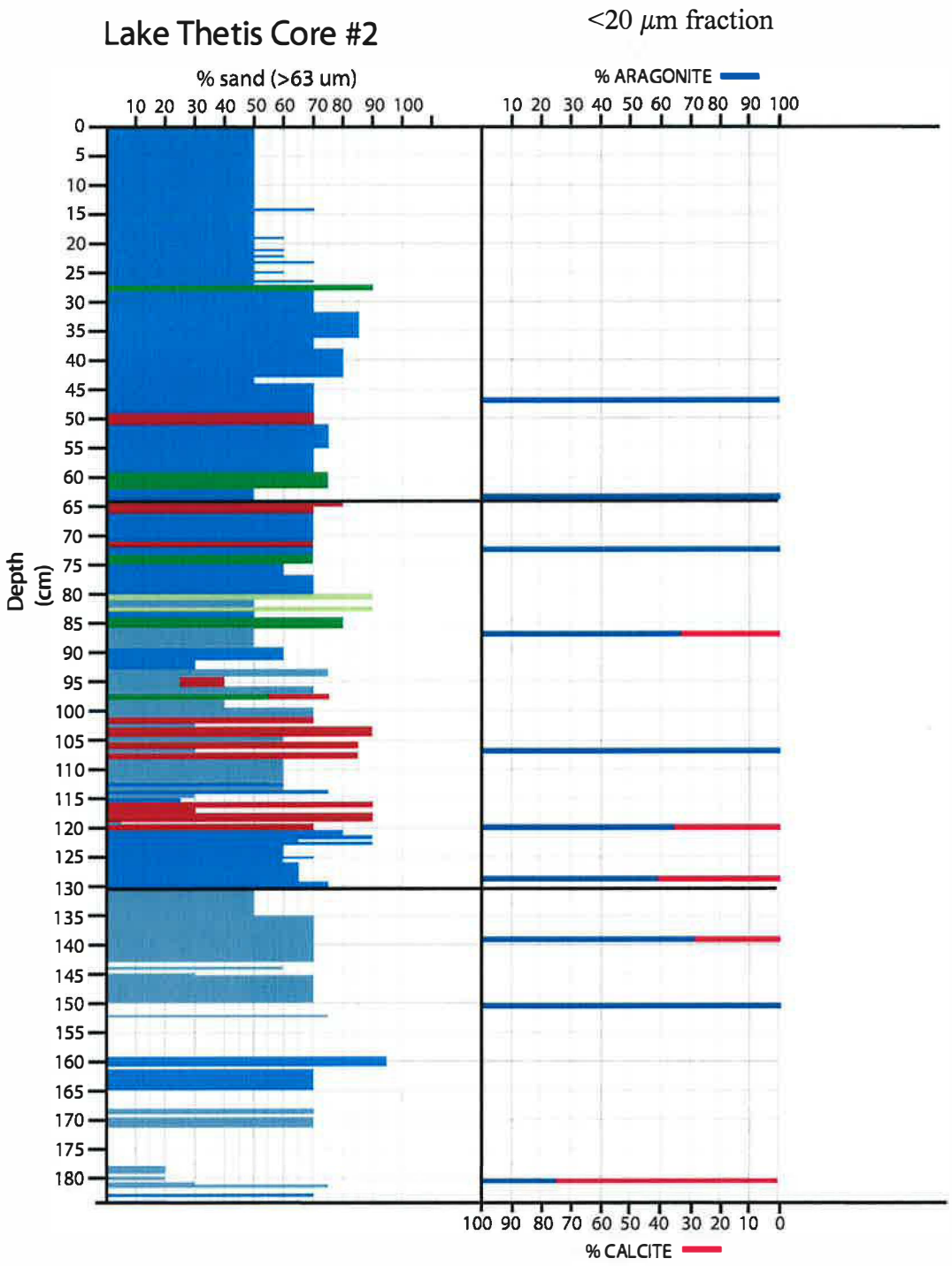

Figure 2.11. Distribution of aragonite and Mg-calcite in the <20 μm fraction in Lake Thetis core 2.

ASSEMBLAGE OF BIOTA IN LAKE THETIS CORES

The cores from Lake Thetis contain skeletal remains of ostracodes, gastropods, diatoms, charophytes, and sponges. Pollen was also separated from a few samples.

Ostracodes

Ostracodes were collected from 40 samples in core 2 and 10 samples in core 1. Representative specimens were sent to Dr. Patrick De Deckker, a well known expert of nonmarine ostracodes at the Australian National University in Canberra, for identification. He confirmed that two species were represented: *Cyprideis australiensis* (Fig. 2.12) and *Mytilocypris ambiguosa* (Fig. 2.13). He notes that samples contain both adults and juveniles, which is evidence for the lack of re-working of the sediment (De Deckker, 1988). He also notes that the *Mytilocypris ambiguosa* in the Lake Thetis samples are quite small for this species, which might be a function of high temperature or salinity close to their environmental limit.

In core 2, *Cyprideis australiensis* occurs throughout the core, whereas *Mytilocypris ambiguosa* occurs only below 127 cm, close to the boundary at 131 cm that divides the sand-dominated interval from the sandy, organic-rich layers (Fig. 2.4). In core 1, *Cyprideis australiensis* occurs throughout the core, whereas *Mytilocypris ambiguosa* occurs only below 135 cm at the boundary that divides the sand-dominated interval from the organic-rich sand interval (Fig. 2.5). Although ostracodes occur in nearly every layer of the cores, the abundance of carapaces ranges from trace (<10% of the volume of the layer) to abundant (>70% of the sediment volume)(Figs. 2.14 and 2.15).

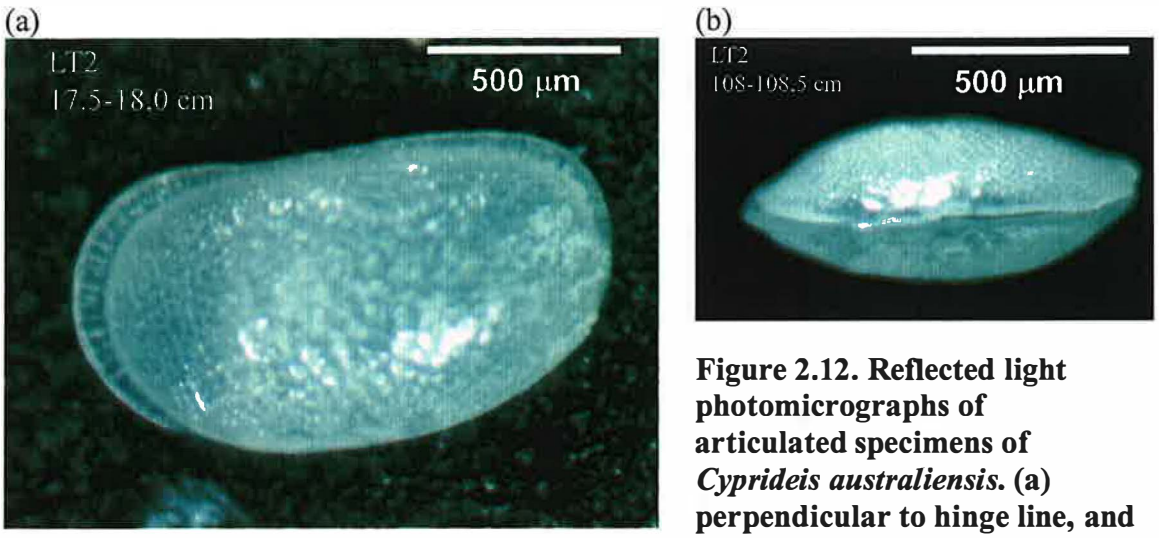

Figure 2.12. Reflected light photomicrographs of articulated specimens of *Cyprideis australiensis*. (a) perpendicular to hinge line, and (b) parallel to hinge line.

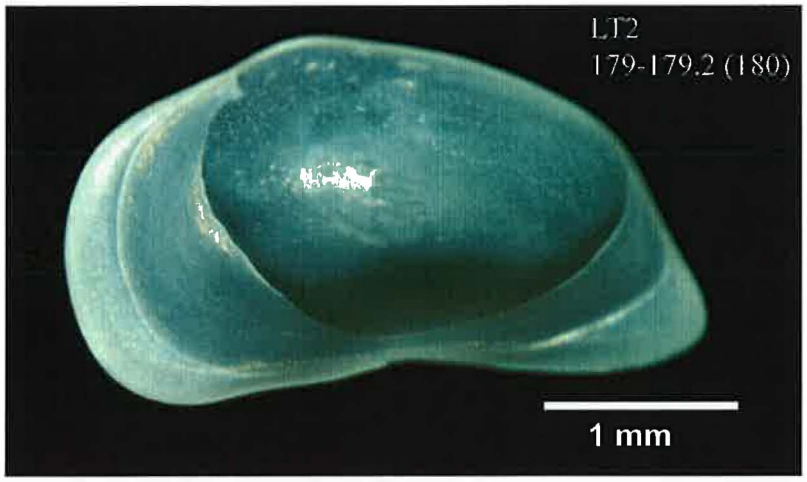

Figure 2.13. *Mytilocypris ambiguosa* carapace from core 2.

De Deckker (1983) and De Deckker and others (1999) described ecological and environmental information about the two species of ostracodes found in Lake Thetis. These extant species are common halobionts (organisms that live in salty environments) in saline lakes. The euryhaline (wide tolerance of salinity) ostracode, *Cyprideis australiensis*, is a free-swimmer of marine ancestry and is endemic to many shallow, athallasic (high-solute water of nonmarine origin) Australian lakes. Its eggs cannot exist in ephemeral lakes because they cannot withstand long periods of desiccation. Therefore, *Cyprideis australiensis* requires permanent standing water to reproduce. In contrast,

Mytilocypris ambiguosa is also a good swimmer, but benthic and swims near the bottom of ephemeral and permanent lakes. De Deckker (1983) reported that neither of these species occurs in highly saline lakes where saline levels are >60 per mil. They require salinities less than this for reproduction or longer lives. The hatching of eggs may be triggered by the salinity levels of the lake waters; hatching usually occurs during times of low salinity. Variations in temperature, salinity, oxygen, food supply, and water chemistry may be controlling size, shape, and ornamentation of ostracode shells.

Gastropods

Shells of the nonmarine gastropod *Coxiella exposita* (Fig. 2.16) occur in three white sands in core 2 between 61 and 61.5 cm, 76 and 76.5 cm, and 108 and 108.5 (Fig. 2.17). The identification was made by Dr. George Kendrick, a gastropod expert at the University of Western Australia, by comparing the specimens from Lake Thetis to those in the modern and fossil collections of the Western Australian Museum. *Coxiella* gastropods are found in southwestern Western Australia, in coastal lakes of South Australia, throughout Victoria, and in Tasmania. Members of this genus are long-lived and produce few offspring. They inhabit lakes where pH is >4.5, salinity is between 6 and 124 g/L, and temperatures are between 20°C and 45°C (Williams and Mellor, 1991). They are able to withstand episodes of desiccation and anoxia. G. Kendrick (pers. communication) notes that *C. exposita* is common living in and marginal to saline to brackish inland waters of the coastal plain of southwestern Western Australia.

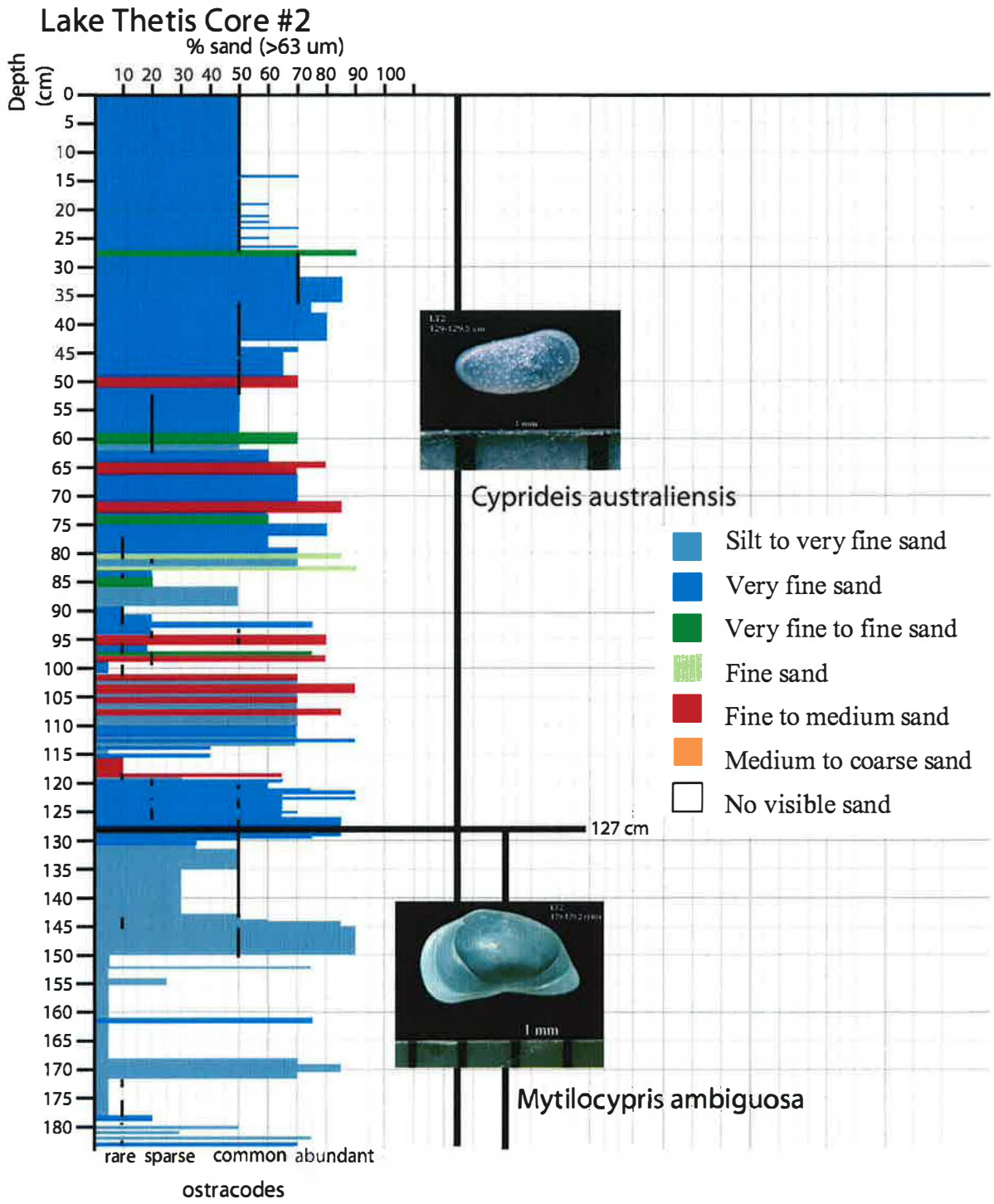

Figure 2.14. Ostracode abundance and distribution in core 2. Rare is between 10 and 20%; sparse between 20 and 50%; common between 50 and 70%; abundant above 70%. Trace amounts less than 10% are not shown in figure.

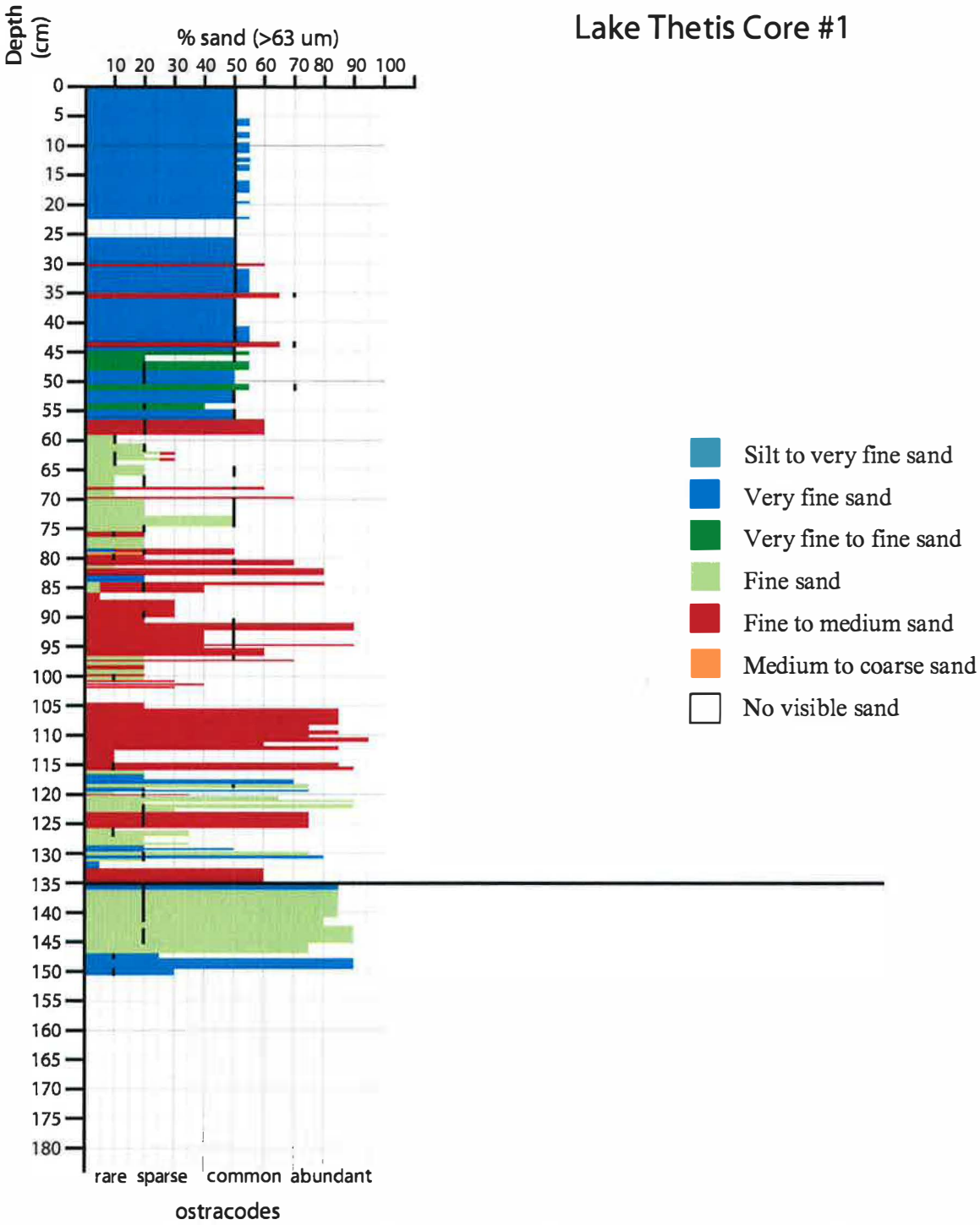

Figure 2.15. Ostracode abundance in core 1. Rare is between 10 and 20%; sparse between 20 and 50%; common between 50 and 70%; abundant above 70%. Trace amounts less than 10% are not shown in figure.

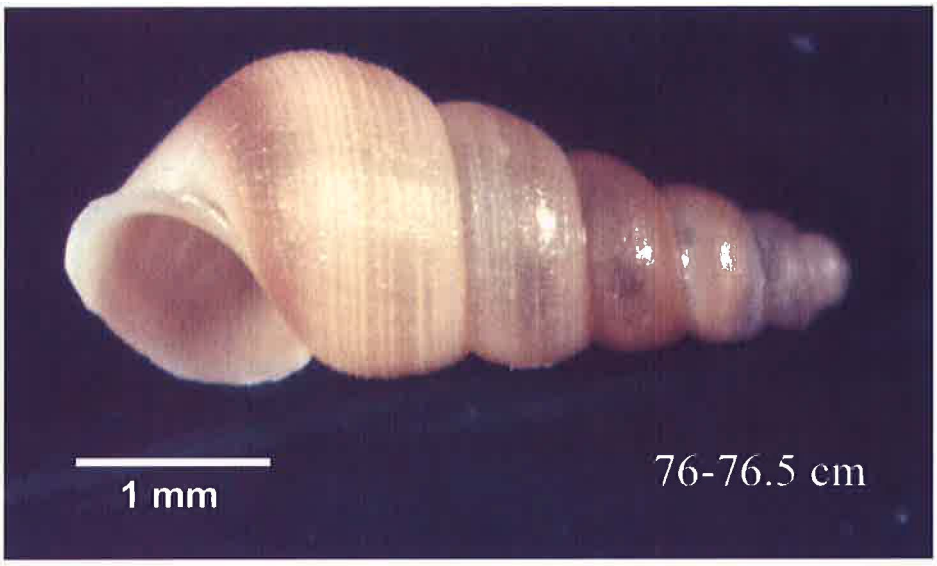

Figure 2.16. *Coxiella exposita* gastropod shells from core 2.

Charophytes

Charophytes are nonvascular hydrophytes and are unique in the fact that their biological characteristics are intermediate between green algae and bryophytes (Bold and Wynne, 1985). Oogonia, the reproductive bodies of the charophytes, occur in both cores, but only in one white sand layer in each core in the same stratigraphic horizon, 107 cm in core 2 (Fig. 2.17) and 105 cm in core 1. Only a few of the 0.5- to 1.0-mm long spiral structures (Fig. 2.18) occur in the sand layers.

Charophytes are nonmarine and are mostly found in fresh water, but they can tolerate brackish conditions. Charophytes prefer calm water, can anchor themselves on muddy, sandy, and hard limestone substrates, and can inhabit depths to 10 to 15 m (Tucker and Wright, 1990). They also readily induce calcification of their tissues.

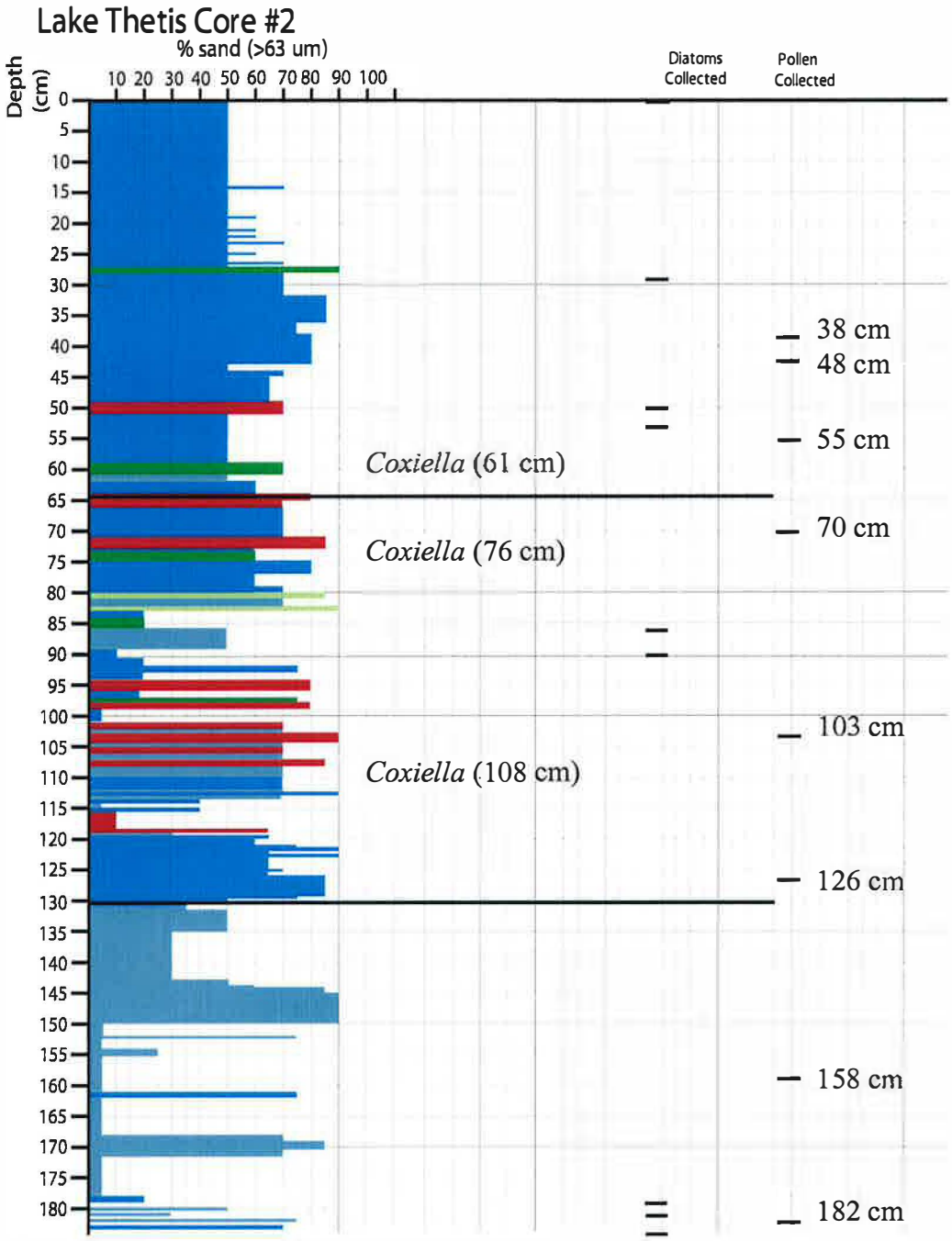

Figure 2.17. Distribution of gastropods in core 2. Also shown are the locations of samples processed for diatoms and pollen.

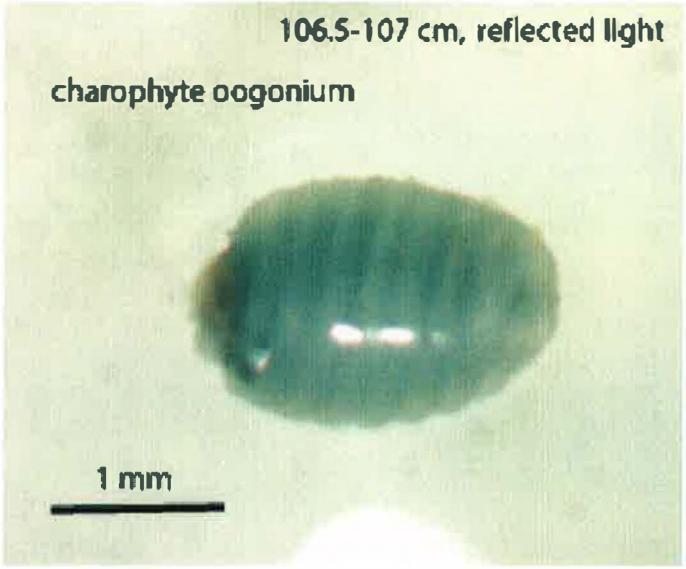

Figure 2.18. *Charophyte oogonium* from core 2

Diatoms

Eight samples from core 2 were processed to isolate diatom and other non-carbonate biotic remains by diatom expert, Dr. Sandie McHugh at the University of Western Australia. She identified 13 species in 11 genera (Table 2.3). Observations from smear slides by this study provide additional information concerning the distribution of diatoms throughout core 2.

Well preserved diatoms are abundant between 0 and 5 cm (Table 2.3). The assemblage is moderately diverse, consisting of five species in five different genera. *Plagiotropis lepidoptera* is the most abundant, forming 50% of the assemblage (Fig. 2.19). The remainder of the diatoms consists of *Amphora veneta*, *Navicula* sp., *Pinnularia* fragments, and *Cymbella* sp. The occurrence of *Plagiotropis lepidoptera* indicates alkaline, saline waters (Burke and Knott, 1997). The other species

Table 2.3. Diatom abundance and distribution compiled by this study (shaded) and Dr. S. McHugh, University of Western Australia (unshaded).

Depth (cm)	Description	Occurrence	Diatom Assemblage
0	Dusky-red sludge	Diatoms abundant and well preserved	*Plagiotropis lepidoptera* abundant (50%) Remainder consists of *Amphora veneta*, *Navicula* sp., *Pinnularia* fragments, *Cymbella* sp.
2.5-5	Dusky-red sludge	Diatoms abundant and well preserved	Same as above
5	Dusky-red sludge	sparse	
6.5-8.5	Dusky-red sludge	rare	
9.5-160	See Appendix A	absent	
28.4-32.0	White sand	Diatoms absent, rare chryosphyte cysts	
51.0-54.2	Dusky-red sludge	Very rare diatom fragments	
86.2-88.3	Yellowish-orange organic-rich sand	Very rare diatom fragments, evidence of valve dissolution, rare sponge spicules	
88.3-89.2	Yellowish-orange organic-rich sand	Very rare diatom fragments, evidence of valve dissolution	
160.0-179.0	See Appendix A	Diatoms sparse; mostly in fragments	*Anomoeoneis sphaerophora* (30%) and *Campylodiscus* sp.(?) (>50%)
179.0-179.2	Reddish-brown organic-rich sand	Diatoms abundant and well preserved; Chrysophyte cysts relatively common	*Amphora coffeaeformis* (>60%), *Amphora veneta* (25%), *Navicula* sp., *Mastagloia elliptica, Anomoeoneis sphaerophora, Campylodiscus* sp., *Brachysira manfredii* (rare), *Brachysira. procera* (rare)
179.2-180.0	Reddish-brown organic-rich sand	Diatoms abundant and well preserved	*Amphora veneta* (>50%), *Amphora coffeaeformis* (25%), also *Mastagloia* sp., *Synedra* sp., *Anomoeoneis sphaerophora, Brachysira manfredii, Campylodiscus* sp.
184.2-186.7	Red sand	Diatoms abundant and well preserved; Chrysophyte cysts common	*Amphora coffeaeformis* (50%), *Amphora veneta* (25%), and *Navicula* sp., *Anomoeoneis sphaerophora*, *Nitzschia* sp., *Brachysira manfredii* (rare)

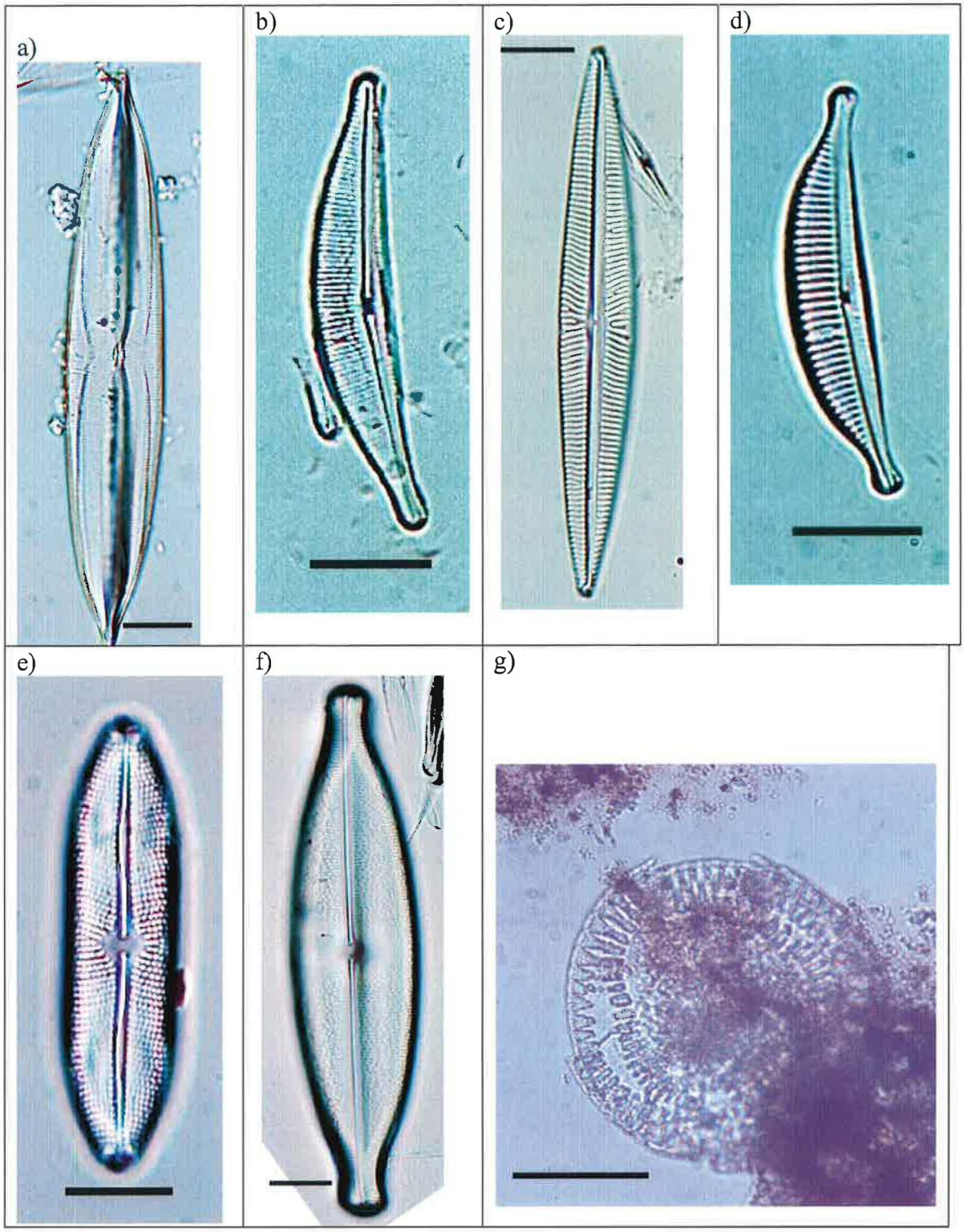

Figure 2.19. Diatoms in core 2. Scale bar is 10 μm. a) *Plagiotropis lepidoptera;*. b) *Amphora veneta;* c) *Navicula* sp.; d) *Amphora coffeaeformis;* e) *Mastagloia* sp.; f) *Anomoeoneis sphaerophora;* g) *Campylodiscus* (?) sp., showing partial dissolution.

are indicative of near-neutral to alkaline waters that range from fresh to slightly saline (John, 1998, Sonneman and others, 2000). The dominance of *Plagiotropis lepidoptera* suggests that the salinity is relatively high, near the limit of the tolerance of the other species. Between 5 cm and 179 cm, diatoms are rare to absent. Generally, only fragments of partially dissolved diatoms are found in this interval (Fig. 2.19G).

From 179 cm to the base of the core at 186.7 cm, diatoms are again abundant and well preserved. There are ten species represented and eight genera. The two dominant species are *Amphora coffeaeformis* and *Amphora veneta. Amphora coffeaeformis* indicates saline, alkaline waters (Sonneman and others, 2000). *Amphora veneta* has wider environmental tolerance of near neutral to alkaline, fresh to saline waters. The rare occurrence of *Brachysira manfredii*, which is indicative of slightly acidic waters, is at odds with the dominant species.

Sponge Spicules

Sponge spicules occur in trace amounts in core 2. They are recognized in the smear slides and have arms at angles of 120° to each other (Fig. 2.20). The environmental significance of their occurrence is unknown.

Figure 2.20. Sponge spicules in core 2 from a sample at 80 cm.

Pollen

Dr. John Backhouse, a pollen expert at the University of Western Australia, processed eight samples from Core 2 for identification and counts of pollen. For each sample, 160 pollen grains were counted, including distinctive fern pollen added to samples as a "dope" for statistical counting purposes. All pollen grains are from modern species (<10,000 years) and are consistent with flora of the area (J. Backhouse, pers. communication) (Table 2.4). Backhouse also reports that all samples contain charcoal and fungal spores, but no obvious marine remains like dinocysts.

The dominant groups are Casuarinaceae, Chenopodiaceae, Cyperaceae, Epacridaceae, Melaleuca, and Asteraceae. Much of the pollen of the salt marsh vegetation of Chenopodiaceae, as well as the wetland rushes of Cyperaceae and paperbarks of Melaleuca, are likely from the local area surrounding Lake Thetis. The assemblages are generally similar throughout the core, and no compositional changes can be clearly defined. However, the Cyperaceae, sedges that favor less saline conditions than Chenopodiaceae (Backhouse, 1993), increase upward.

STABLE ISOTOPES FROM CORE 2

Intra-sample variation

Carbon and oxygen isotopes were analyzed in *Cyprideis australiensis* from 33 layers, *Mytilocypris ambiguosa* from 6 layers, and micrite from the <20-μm fraction in 25 layers. In order to evaluate the significance of isotopic variations between layers, the intra-sample variation within a layer was evaluated from the duplicate to quintuplicate analyses of both ostracodes and micrite. Table 2.5 shows the minimum and maximum

Table 2.4. Lake Thetis core 2 pollen counts done by Dr. J. Backhouse, University of Western Australia

Depth cm	Sediment Type	Lycopodium (dope)	Asteraceae	Banksia	Casuarinaceae	Chenopodiaceae	Cyperaceae	Epacridaceae	Eucalyptus	Form 1	Goodeniaceae	Gyrostemonaceae	Haloragaceae	Indeterminate	Melaleuca	Pine pollen	Poaceae	Proteaceae	total count
38	white sand	63	11		34	31	23	19	3	1	4	5	2	9	16	1		1	160
43	dusky red sludge	55	10		25	14	30	29	7		2	5	5	17	8	1	5	2	160
55	dusky red sludge	36	15	1	20	19	15	18	14		1	4	5	33	12		2	1	160
70	yellowish orange sand	12	15		32	26	15	19	7		1	9	3	21	8		1	3	160
103	yellowish orange sand	30	11		34	23	17	12	9	4	4	6	2	24	9		5		160
126	white sand	65	22	1	46	23	4	23	3	8	6	8	2	5	7		2		160
158	red-brownish organic-rich sand	62	21		46	23	6	13	8	4	4	7	1	12	10		4	1	160
182	red sand	44	19	1	22	35	7	8	3	2	9	23	2	13	9		4	3	160

Additional comments:

Lycopodium (dope): Distinctive fern pollen added to the sample for statistical purposes as a tablet.
Asteraceae: Daisies, thousands of species, all pollen look very similar
Banksia: Banksias, they all look the same as pollen, related to Proteaceae
Casuarinaceae: Usually very numerous as they are wind pollinated and need to produce huge quantities of pollen.
Chenopodiaceae: Salt marsh vegetation, e.g as seen on salt marshes at Rottnest
Cyperaceae: Rushes, usually bordering wetlands
Epacridaceae: numerous genera of heath-type small shrubs found in a range of habitats, including the coastal zone
Eucalyptus: on the coastal plain likely to be red gums and tuart, with a few others less common, produce a lot of pollen
Melaleuca: Pollen similar to eucalypts but generally smaller. Typical Melaleucas are paperbarks found round wetlands
Pine pollen: Recent introduction since European settlement. Unlikely to be many around before late 1800s
Poaceae: Grass pollen (native grasses in this case)
Proteaceae:Huge family, vast number of pollen types. Usually make up small proportion of assemblage as they are insect pollinated

variations in individual layers for both $\delta^{13}C$ and $\delta^{18}O$ and the mean variation of all the layers.

It is also important to note that the intra-sample variation in $\delta^{18}O$ and $\delta^{13}C$ in the ostracodes is not a function of size. For example, the minimum difference in $\delta^{18}O$ between carapaces of *Cyprideis australiensis* of 1 ϕ and 2 ϕ sizes is 0.04 ‰ and the maximum is 1.1 ‰. These values are within the total range exhibited by carapaces of all one size within a given layer. The same is true of $\delta^{13}C$ in the *Cyprideis australiensis* and for both isotopes in the *Mytilocypris ambiguosa.*

TABLE 2.5. Intra-sample variation in carbon and oxygen isotopes.

Sample	Minimum and maximum variation in $\delta^{18}O$ (‰)	mean variation $\delta^{18}O$ (‰)	Minimum and maximum variation in $\delta^{13}C$ (‰)	mean variation $\delta^{13}C$ (‰)
Cyprideis australiensis	Min: 0.01 Max: 1.86	0.6	Min: 1.27 Max: 3.47	1.1
Mytilocypris ambiguosa	Min: 0.16 Max: 1.36	0.8	Min: 0.67 Max: 3.04	1.5
micrite	Min: 0.076 Max: 2.61	0.5	Min: 0.03 Max: 1.8	0.5

Comparison of Different Sample Types

The results of all analyses (including multiple analyses within each layer) are shown in Figure 2.21 and in Appendix E. The three sample types form distinct fields on the $\delta^{13}C$ versus $\delta^{18}O$ plot. The *Mytilocypris ambiguosa* has the highest $\delta^{18}O$ values and $\delta^{13}C$ values similar to those of micrite. The micrite has $\delta^{18}O$ values similar to those of *Cyprideis australiensis,* but has it significantly higher $\delta^{13}C$ values than this species of ostracode. The *Cyprideis australiensis* is distinct from the *Mytilocypris ambiguosa* and the micrite by its low $\delta^{13}C$ values.

Variation in Isotopic Composition with Depth

Multiple analyses of the samples were averaged for each species of ostracode and for micrite and plotted versus depth in Figures 2.22 and 2.23. The mean intra-sample variations from Table 2.5 are also plotted on these figures. Variations equal to or less than these values between layers cannot be interpreted as significant.

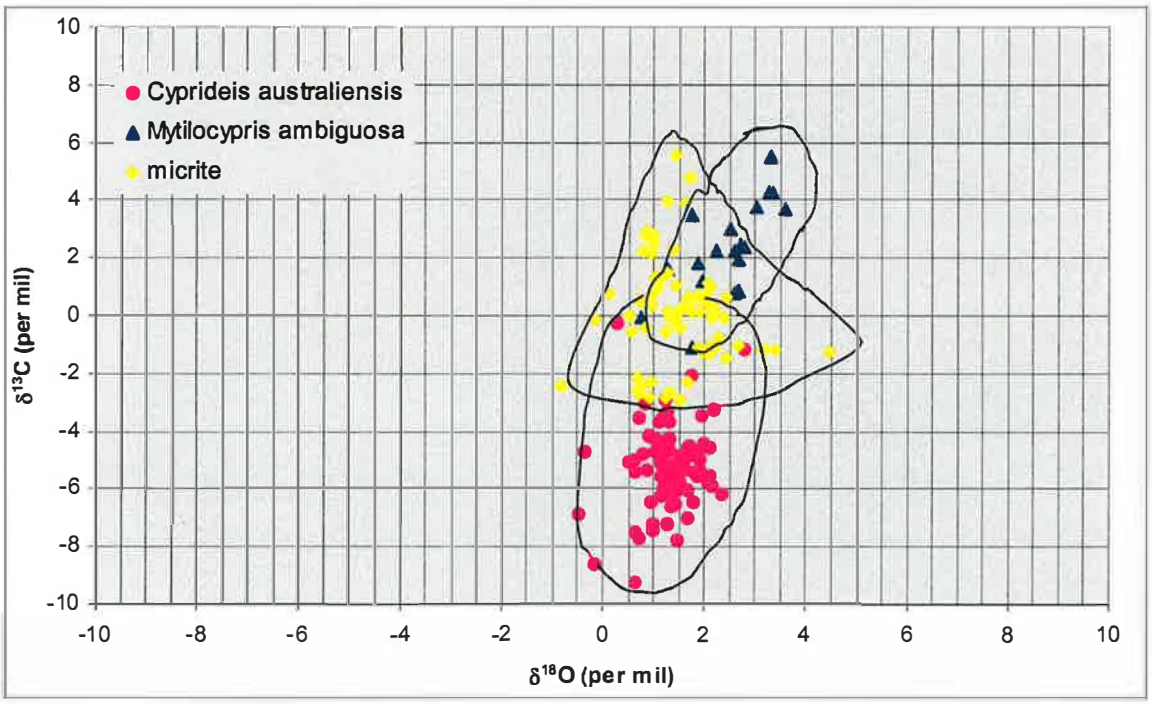

Figure 2.21. Plot of all isotopic analyses of the study.

The $\delta^{18}O$ does not vary much over the entire core (Fig. 2.22), but there is a slight increase of about 0.5 to 1 ‰ from the base to the top in the micrite and *Cyprideis australiensis*. The major shift occurs between 110 and 80 cm. The $\delta^{18}O$ values for *Cyprideis australiensis* range between 0.1 and 2.1 ‰, with an average of 1.3 ‰. Those of *Mytilocypris ambiguosa* range between 1.8 and 3.2 ‰, with an average of 2.6 ‰. Those of micrite range between 0.6 and 2.6 ‰, with average of 1.5 ‰.

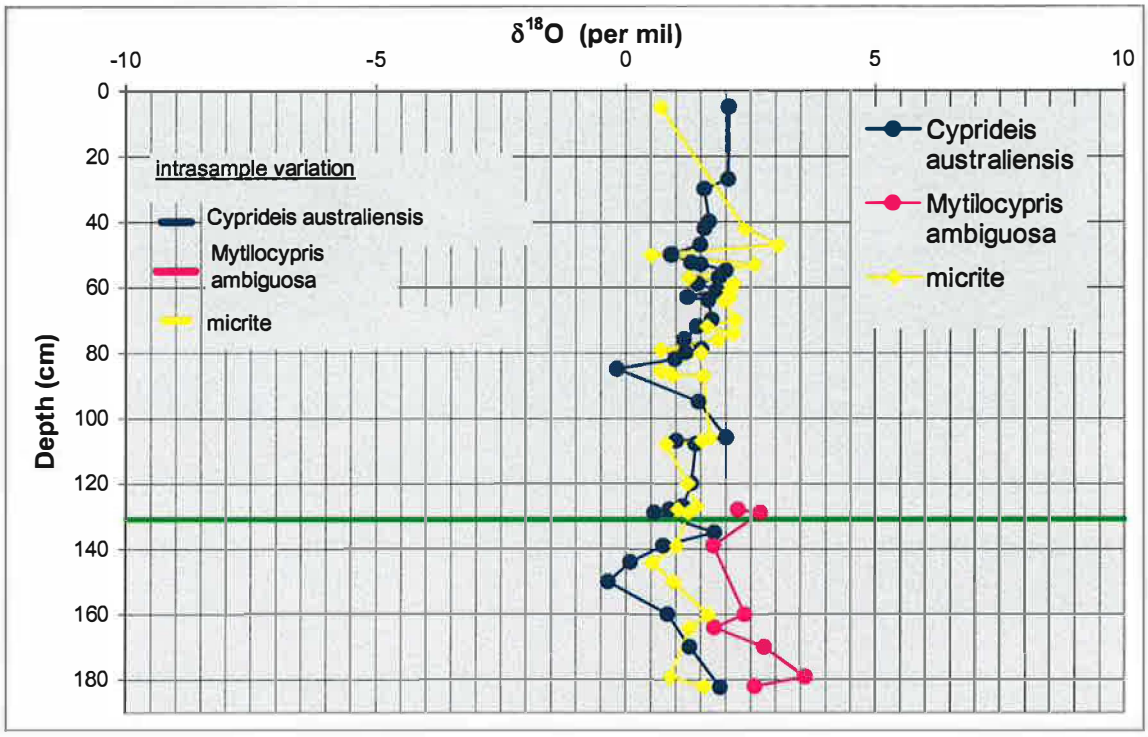

Figure 2.22. Variation in $\delta^{18}O$ versus depth. The green line shows the depth were the sediment type changes from sand-dominated to organic-rich sand dominated.

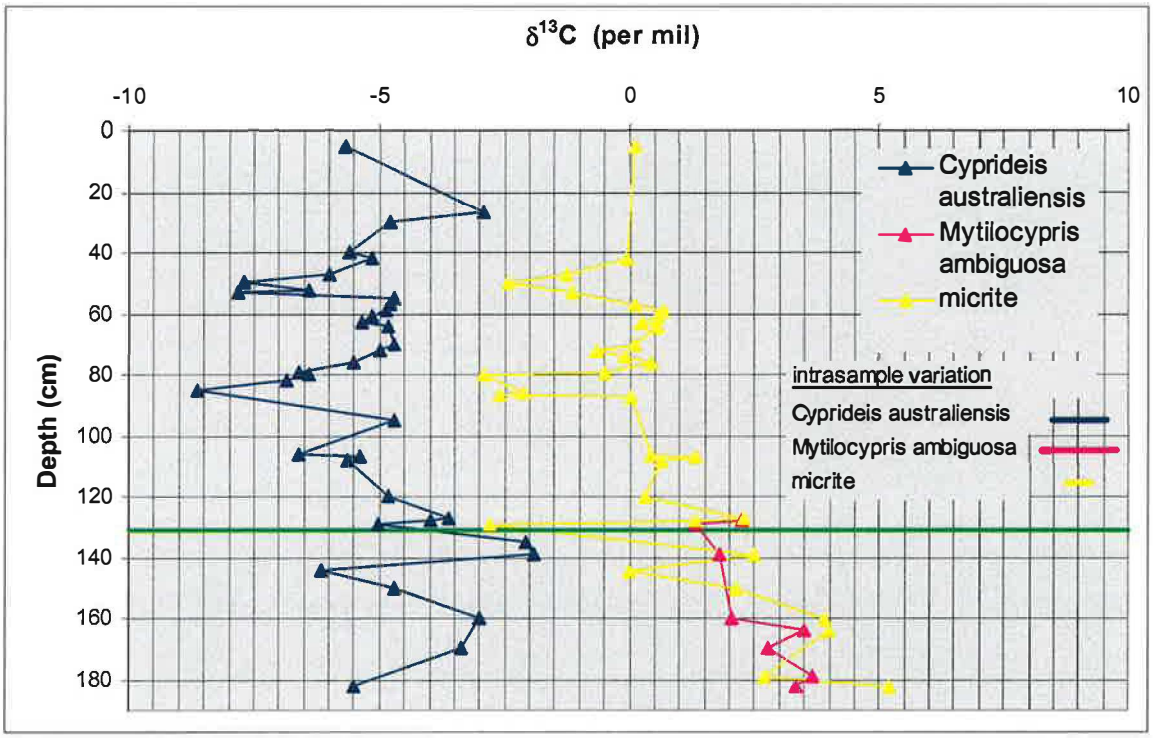

Figure 2.23. Variation in $\delta^{13}C$ versus depth. The green line shows the depth were the sediment type changes from sand-dominated to organic-rich sand dominated.

The $\delta^{13}C$ values in each sediment type (Fig. 2.23) show more variation than they do in $\delta^{18}O$. The *Mytilocypris ambiguosa* occurs in core 2 only below 130 cm. In this interval, the $\delta^{13}C$ values decrease 3 ‰ in this ostracode species. The $\delta^{13}C$ values of the micrite show an overall decrease throughout the core of about 5 ‰, with several significant negative excursions at 180, 130 cm, 88 cm, and 50 cm. The *Cyprideis australiensis* show neither an upward decrease or increase, but do show several significant negative excursions at 144 cm, 85 cm, and 50 cm. The suite of analyses of the *Cyprideis australiensis* are not exactly the same as those of the micrite, but the general structure of the two curves positively covary. The $\delta^{13}C$ values for *Cyprideis australiensis* range between -7.6 and -2.5 ‰, with an average of -5.3 ‰. Those of *Mytilocypris ambiguosa* range between 1.3 and 4.5 ‰, with an average of 2.7 ‰, and those of micrite range between -2.4 and 5.4 ‰, with average of 0.6 ‰.

AMS AGES

Table 2.6 shows the ten AMS radiocarbon ages from bulk organic matter in core 2 and the calculated rate of sedimentation between each adjacent pairs of samples. Ages get progressively older with depth, and therefore make stratigraphically sense, until the sample at 163.7 cm. This sample shows an age reversal, with an apparent age that is ~200 years younger than the sample above it. This sample also yields the same age as the sample that is 16 cm below it. The sedimentation rate for the interval between 0 cm and 163.7 cm varies between 3 and 6 cm/100 years, whereas that below this horizon is at least an order-of-magnitude greater. Interestingly, the changes in stratigraphic sense of the ages and in sedimentation rate occur over the boundary between the sand-dominated and organic-rich-sand-dominated intervals.

Table 2.6. AMS-radiocarbon ages of bulk organic matter in core 2

Depth	sediment type	Age	sedimentation rate (cm/100 y)
0	dusky red sludge	491±34	
28.4-32.0	white sand	1451±36	
51.0-54.2	dusky red sludge	2128±37	
86.2-88.3	yellowish-orange organic-rich sand	2772±38	
105.2-106.3	white sand	3372±50	
119.2-119.5	white sand	3648±51	
143.2-144.7	purple organic-rich sand	4076±44	
163.7-164.0	red sand	3875±48	
179.2-180.0	reddish-brown organic-rich sand	3876±62	
185.8-186.2	reddish-brown organic-rich sand	4126±71	

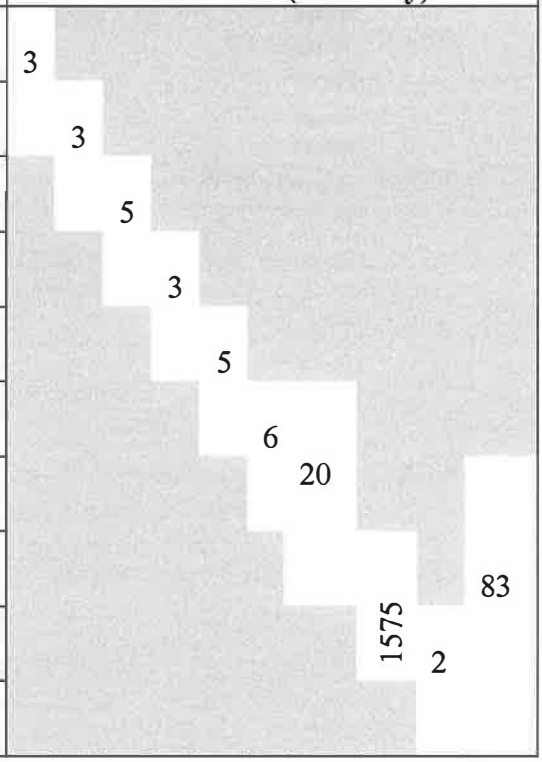

The measured age of the top of the core is ~500 years and the base of the core 4126 years. Because the top does not yield a modern age and the lower interval has some problematic ages, the accuracy of the ages must be examined. There are three likely factors that could contribute to the apparent ~500-year-too-old age of the bulk organic matter at the top of the core:

1) The sample contains flecks of windblown charcoal derived from the combustion of older plant material, as noted in all samples examined by J. Backhouse (see Pollen section above).

2) The benthic mat community is a flocculent, irregular mass, with fragile cohesion and a texture like gooey cottage cheese (Chapter 1). It can be physically mixed by bioturbation by the telost fish that feed on it and by bottom currents that might be generated by storms.

3) Addition of CO_2 derived from the upward diffusion of the gas from anaerobic decomposition of the older underlying organic matter can be incorporated by the modern microbes.

All of these factors probable contribute to the "old age" of the modern sample. The high volume of organic material in the core indicates that the benthic microbial mat was present throughout the time interval represented by the core. Therefore, these same three factors have also probably operated throughout the accumulation of the sediment column. However, it cannot be assumed that the extent and proportion of these factors has been constant through time; and, therefore, a correction of 500 years cannot be applied to ages. The ~500-year correction is a reasonable first-order approximation. Therefore the age of the base of the core is likely somewhere between the measured age of 4,126 years and a "corrected age" of 3635 years.

CHAPTER 3 -- DISCUSSION AND CONCLUSIONS

SEDIMENT RECORD OF LAKE THETIS

The sediment pile in Lake Thetis forms an *in situ* (non-reworked) record of deposition for the past ~4000 years, as demonstrated by well defined lamination and the assemblage of adult and juvenile ostracodes within layers that host them. The sediment consists of three main components: organic matter, carbonate sand, and carbonate mud (micrite).

Origin of Organic Matter

Partly decomposed organic matter forms the largest volume of the sediment pile in Lake Thetis indicated by the large percent weight loss in all sediment types following bleach treatment. A benthic microbial community, similar to that of today, must have existed throughout the interval of time represented in the core. Then, as now, it produced an anoxic environment below the first centimeter of the mat, as demonstrated by preservation of the large volume of organic matter and the hydrogen sulfide odor that lingered several days after the cores were opened.

Origin of Sand

The carbonate sand in the lake-center cores have two possible sources: the surrounding calcareous Holocene Safety Bay Sand, well exposed in the abandoned quarry just north of the lake (Fig. 1.4 and Fig 1.8), and stromatolites on the terraces of Lake Thetis (Fig. 1.7). The minor siliciclastic component in the sand fraction must be derived from the Safety Bay Sand, which has a significant component of detrital quartz (Kern, 1993). Therefore, some or most of the carbonate sand must also have come from this source. It is likely that little of the carbonate sand was locally derived from wave erosion

of the stromatolites on the terraces. No loose sand was observed on the terraces during field work in June 2004, and wave erosion of the stromatolites would be expected to produce a range of sediment size from very fine sand to gravel. It is possible that sediment at the base of the slope might contain material derived from stromatolites; but a grain flow from the terrace will not travel far into the lake center.

As there are no streams entering the Lake Thetis drainage, deposition by wind is the most likely transport agent for the sand. The vast majority of sands have a unimodal distribution of well sorted sand with a dominant mode of 3 ϕ. These characteristics are typical of sand deposited by eolian processes (Reineck and Singh, 1980). The dominant wind direction is from the west and the south (Chapter 1). It is likely that eolian deposition of sand in the lake follows this pattern, and that the greatest volume of sand occurs near the western and southern margins of the lake. The cores of this study are too few to confirm this hypothesis, but the "western" core 1 does contain coarser-grained sand and more sand, especially in the lower intervals, than the "eastern" core 2 (Figs. 1.8, 2.4, 2.5 and Appendix B).

Origin of Mud

Carbonate mud forms only a small volume of the total sediment in Lake Thetis, not more than 5% of any layer, regardless of sediment type. The important question to determine is whether the mud is windblown detritus or endogenic carbonate formed in the lake. Textural, mineralogical, and geochemical evidence support an endogenic origin. Both sand- and clay- size particles are encased within gelatinous organic matter in the sediment. However, much of the clay-size carbonate has specific orientation, particularly the radial orientation shown in Figure 2.3, suggesting that it formed *in situ* within the

organic matter through bacterial mediation. Detrital material would be randomly oriented. Other textural evidence is the lack of significant silt-size fractions between sand and micrite. Windblown detrital material would be expected to occur in all size fractions in a Gaussian distribution from sand to fine-grained material.

The higher proportion of Mg-calcite in the micrite compared to the sand (Fig. 2.11) suggests that the sources of the two size fractions are not the same. Although aragonite is the dominant mineral of the micrite as well as of the sand, the different proportions of the aragonite and Mg-calcite in the two size fractions in many samples suggests the fact that micrite is made in the lake and is not detrital like the sand. The calcium carbonate phase that precipitates from a fluid is largely a function of the Mg:Ca ratio of the fluid (Given and Wilkinson, 1985). Typically, aragonite is formed during times of high salinity and Mg-calcite during times of slightly less salinity (Spencer and others, 1984; McKenzie and Eberli, 1987). The two minerals are not co-genetic, but the sampling resolution of the study of ~5 mm includes years to decades, given the sedimentation rates determined from the AMS ages (Table 2.6).

The values and depth profiles of the stable isotopes measured in micrite (Figs. 2.22 and 2.23) are unlike those expected for detrital micrite derived from the marine Safety Bay Sand. Grey and others (1990) analyzed three limestone samples of the Safety Bay Sand from the abandoned quarry north of Lake Thetis (Fig. 1.8). These marine limestone samples have $\delta^{18}O$ values between 0.2 ‰ and 0.4 ‰ (VPDB), which are lower than those of the Thetis micrite, and $\delta^{13}C$ values between –0.7 ‰ and +0.4 ‰ (VPDB), which are similar to only a few analyses of the Thetis micrite. The $\delta^{13}C$ values in the Thetis micrite are highly variable and generally decrease upward in the core, whereas

those of shallow, open-marine inorganic Holocene carbonate (e.g., the Safety Bay Sand) vary little (Tucker and Wright, 1990). Finally, the $\delta^{18}O$ and $\delta^{13}C$ of the Thetis micrite generally shows positive covariance with the $\delta^{18}O$ and $\delta^{13}C$ of the ostracodes. This could only result if the micrite formed in the lake water. Therefore, a detrital origin for the micrite is ruled out.

BIOTIC RECORD OF LAKE THETIS

Ostracodes

Before interpreting the ostracode record of Lake Thetis, two unusual things about the occurrence of this organism must be noted. The ostracode fauna in the Lake Thetis cores is remarkable in its lack of diversity. Rarely do more than one species of ostracode occur in a given horizon. A similar occurrence is noted by Coshell and Rosen (1994) in Lake Hayward, one of the Yalgorup lakes south of Perth (Fig. 1.10). These authors state that *Cyprideis australiensis* is the only ostracode that made the transition from the marine inlet phase to the lacustrine phase. In Lake Thetis, this species and *Mytilocypris ambiguosa* coexisted in the early phase of the lake.

The other unusual thing about the ostracode fauna in Lake Thetis is that *Cyprideis australiensis*, the species of ostracode found in the surface sample, as well as throughout the entire core, should not be able to exist in water as saline as that of Lake Thetis. The known range of salinity tolerance of this species is 2 g/L to 35 g/L (Yassini and Kendrick, 1988), whereas the measured salinity of Lake Thetis in 1985, 1987, and 2004 ranged from 39 to 53 (see Tables 1.1 and 1.2). Either *Cyprideis australiensis* has not been extant in the lake since at least the mid-1980s or its salinity tolerance is greater

than previously known. Grey and others (1990) included ostracodes in the list of fauna present in the lake. Furthermore, the abundance of *Cyprideis australiensis* is highly variable in cores 1 and 2 (Figs. 2.14 and 2.15). The variability might be an indicator of salinity fluctuations over the time period represented by the core. Although Grey and others (1990) stated that ostracodes are part of the fauna of the lake, the abundance of this organism was not noted.

Mytilocypris ambiguosa is less tolerant of high salinity than *Cyprideis australiensis*. The known salinity tolerance of *Mytilocypris ambiguosa* is 5 g/L to 10 g/L (De Deckker, 1983; 1988). The absence of *Mytilocypris ambiguosa* above 127 cm indicates that waters became too saline for this species.

Diatoms

It is unfortunate that diatoms are dissolved throughout most of the cores because the abundance, types, and diversity of species are sensitive to changes in salinity (Reed, 1998). The occurrence of well preserved diatoms in the cores might have been useful to indicate changes in salinity. However, it is not unusual for diatoms to be absent to partly dissolve in the sediment record of saline lakes. Factors that lead to diatom dissolution within lake water and sediment are high salinity, temperature, pH, calcium carbonate content, and silica diffusion rates (review in Reed, 1998). The absence of abundant, well preserved diatoms between 5 cm and 179 cm suggests that one or more of these factors existed throughout the accumulation of the sediment. Dissolution requires movement of fluid in order to remove the dissolved ions and bring in new fluid undersaturated with respect to the dissolving phase. The rapid decrease of preserved diatoms below 5 cm

suggests that dissolution takes place in the sludge phase before compaction reduces the porosity and turns sludge into packed sand and organic-rich sand. During the sludge phase, the permeability and porosity are high.

The occurrence of well preserved diatoms below 179 cm to the base of the core indicates that conditions in the lake during this time were unlike those of today. The factors that promote dissolution are high salinity, temperature, pH, calcium carbonate content, and silica diffusion rates. The factor most likely to have been significantly different than today is salinity because calcium carbonate sand and mud are present in these layers and shows no evidence of dissolution. The lower salinity is consistent with the occurrence of *Mytilocypris ambiguosa* in this interval.

Other Biota

Charophytes cannot tolerate salinity above brackish levels, hence the occurrence of oogonia in other one horizon suggests that Lake Thetis was almost always more saline than brackish, or that oogonia were rarely preserved in the sediment record. Charophytes need clear water and hence would have lived on the terraces, not in the lake center. However, if they were common components of biota in the past, their robust oogonia would certainly have been carried throughout the surface water to settle as part of the sediment record. The significance of the occurrence of so few specimens in the one horizon is unknown. It does not correlate to an abundance of *Cyprideis australiensis* as might be expected if salinity was low. Perhaps the oogonia are detrital grains, blown in from a nearby, short-lived freshwater pond.

The gastropods are tolerant of a wide range of environmental conditions. This coupled with their sparse occurrence provide no insight into environmental condition of the lake through time. The spatial resolution of the pollen study is too limited to define trends. The only apparent increase is in Cyperaceae, sedges that are less tolerant of saline conditions than salt marsh vegetation of the Chenopodiaceae group (Backhouse, 1993). The fact that Cyperaceae pollen increases upper in the core is at odds with the ostracode and diatom data, which suggest that salinity increases through time.

C AND O ISOTOPE RECORD IN CORE 2

The two ostracode species from the same layers have different C and O isotopic compositions. The $\delta^{13}C$ is 0.5 ‰ to 1.0 ‰ greater and the $\delta^{18}O$ is 4 ‰ to 6 ‰ greater in *Mytilocypris ambiguosa* than in *Cyprideis australiensis*. Both ostracodes are swimmers and inhabit the same environment, so differences must reflect different degrees of biological fractionation of the two isotopes in the different genera.

The vertical profiles of $\delta^{18}O$ in *Cyprideis australiensis* and endogenic micrite show a small (0.5 ‰ to 1.0 ‰) increase above 80 cm in core 2 (Fig. 2.22). In addition, there are several small excursions greater than intrasample variability between 160 and 140 cm, 110 and 90 cm, 80 and 70 cm, and 60 and 50 cm. In a hydrologically closed, non-stratified shallow lake, the balance between inflow and evaporation controls the $\delta^{18}O$ isotopic composition of the water on a seasonal and year-to-year basis (Spencer and others, 1984; McKenzie and Eberli, 1987; and Talbot, 1990). Increase in $\delta^{18}O$ in carbonate minerals formed in such lakes is interpreted to represent periods of low lake level, decreased freshwater inflow, and increased salinity. Conversely, decrease in $\delta^{18}O$ is

interpreted to represent high lake level, increased freshwater inflow, and decreased salinity.

The small excursions in the $\delta^{18}O$ record of Lake Thetis interpreted represent changes in the balance between inflow and evaporation, i.e., drought-wet cycles. As noted in Chapter 1, because the $\delta^{18}O$ of the meteoric water in the area of Lake Thetis is only slightly negative relative to seawater (0 ‰ (VSMOW)) and because water-rock interaction in the shallow groundwater system will act to the further increase the $\delta^{18}O$ of the meteoric water, only large volumes of meteoric inflow will be easily detected in the lake. Furthermore, in order to be detected in the sediment record, such isotopic conditions must persist for a period of time long enough to form endogenic sediment and/or ostracode carapaces; and the sampling interval must also be of sufficient resolution to sample the changes. The overall upward increase above 80 cm in $\delta^{18}O$ in core 2 indicates that the lake is likely smaller and more saline than it was during deposition of most the previously deposited sediment.

The following discussion focuses on the micrite formed in Lake Thetis because the isotopic composition of the micrite is not influenced by biological fractionation, as it is for the ostracode carapaces. Theoretical considerations (Andrews and others, 1993) and empirical data (Abell and others, 1982; Cohen and others, 1997) indicate that microbially precipitated calcium carbonate forms in isotopic equilibrium with the water.

The isotopic composition of aragonite, the dominant mineral of the micrite, depends on the $\delta^{18}O$ composition of the water and the temperature at which the aragonite forms. The equation,

$$T(°C) = 20.6 - 4.34\ (\delta_a - \delta_w),$$

where δ_a is the $\delta^{18}O$ (VPBD) of aragonite and δ_w is the $\delta^{18}O$ (VSMOW) of the water, relates these three variables (Grossman and Ku, 1986). Using the average summer temperature of 22°C (Fig. 1.9) and $\delta^{18}O = 1$ ‰ for micrite below 80 cm (Fig. 2.22), the $\delta^{18}O$ of the water would have been ~+1.3 ‰ (VSMOW). To form the micrite above 80 cm with an average values of 2 ‰, the water would have been ~+2.3 ‰ (VSMOW). These estimates indicate that the water in Lake Thetis during the time represented by the sediment in core 2 was generally greater than that of standard mean ocean water, 0 ‰ (SMOW) and greater than the average meteoric precipitation in the area, -2.9 ‰ (SMOW). The higher values of the Lake Thetis water indicate that no matter what the source(s) of water to the lake, either all meteoric or mixed meteoric and seawater, evaporation generally exceeded precipitation; and Lake Thetis was never a freshwater lake during the time represented in core 2 sediment. The small excursions to the values of micrite greater or less than the average values of the micrite indicate changes in the balance of evaporation and inflow of the lake.

The $\delta^{13}C$ vertical profile of micrite in core 2 (Fig. 2.23) shows a ~7 ‰ overall decrease upward in the core. Furthermore, unlike $\delta^{18}O$, the $\delta^{13}C$ shows numerous excursions of at least 2 ‰. The $\delta^{13}C$ of calcium carbonate formed in the lake is dependent on the types and extent of exchanges of carbon between different natural reservoirs, particularly CO_2 in the atmosphere, carbonate in carbonate rocks, and carbon in organic matter. The $\delta^{13}C$ of marine carbonate measured by Grey and others (1990) in the surrounding Safety Bay Sand ranges from –0.7 ‰ to +0.4 ‰ ~0 ‰ (VPDB). Therefore, dissolved HCO_3^- from carbonate rocks contributed by shallow groundwater through water-rock interaction cannot be a controlling factor in the $\delta^{13}C$ of the lake

water. The two remaining possible sources of carbon, therefore, are from the atmosphere and organic matter.

The calculated $\delta^{13}C$ of the pre-industrial atmosphere is –6.4‰ (VPDB) (Zhang and others, 1995). Using the temperature-dependent functions of equilibrium fractionation factors between aqueous HCO_3^- and CO_2 gas of Zhang and others (1995) and aqueous HCO_3^- and calcite of Romanek and others (1992), the calculated $\delta^{13}C$ composition of calcite formed in equilibrium with pre-industrial atmospheric CO_2 at 25°C is +1.7‰ (VPDB). Therefore, the $\delta^{13}C$ of the calcium carbonate formed in Lake Thetis cannot have been controlled by the exchange of carbon between the lake water and atmosphere. Hence, the changes in $\delta^{13}C$ must result from changes related to organic productivity and organic decomposition in the lake and lake sediment. .

Photosynthesis results in the preferential incorporation of ^{12}C relative to ^{13}C, which increases the $\delta^{13}C$ of the lake water (Faure, 1986). The $\delta^{13}C$ of micrite formed in the lake might then be expected to have values higher than calcite formed in equilibrium with atmospheric carbon in a lake were photosynthesis is the dominant control on $\delta^{13}C$. The high values measured in micrite in the core below 130 cm probably indicate that photosynthesis was the dominant control. This interval is coincident with the high rates of accumulation of organic-rich sand. Therefore, photosynthesis of the benthic mat community during this time was the major control on $\delta^{13}C$ of the lake water.

Benthic mat communities continued to thrive throughout the history of Lake Thetis, as demonstrated by the large volume of partly decomposed organic matter throughout the cores, into the present day. However, the trend to increasingly light $\delta^{13}C$ values in the micrite show that photosynthesis stopped being the dominant control on

$\delta^{13}C$ of the lake. The $\delta^{13}C$ composition of organic carbon is isotopically light (Kendall and Caldwell, 1998), with an average value of -25‰ (VPDB) (Sharp, 2005). The low values of micrite above 130 cm indicate the influence of addition of isotopically light carbon derived from organic decomposition. Continued anaerobic decomposition of the large volume of organic matter buried in the sediment generates gases with isotopically light carbon, which is incorporated into the micrite. The large excursions to very light $\delta^{13}C$ values at 145 cm, 130 cm, 80 cm and 50 cm (Fig. 2.23) could represent episodic large releases of gases from the sediment pile. Hence, the $\delta^{13}C$ composition of the micrite shows a change from photosynthesis to organic decomposition as the dominant control of the $\delta^{13}C$ of the lake.

SIGNIFICANCE OF THE STUDY TO CLIMATE CHANGE

The interval of time represented by the cores of this study is ~4100 y (Table 2.6). The record does not extend back far enough to compare to changes observed by Zheng and others (2002) and Backhouse (1993) that were described in Chapter 1. It does include the period between 3000 and 2000 years BP described by Shepherd and Eliot (1995) as a time of increased occurrence and/or frequency of either tropical cyclones or winter cyclonic storms in the Cervantes area. The change from organic-sand dominated to sand-dominated sediment in Lake Thetis occurs between 4076 y and 3372 y. Possibly, the increase in cyclonic storms contributed to this change, favoring the accumulation of sand in proportion to accumulation of organic matter.

The occurrence of *Mytilocypris ambiguosa* below 130 cm in core 2 (Fig. 2.14), the preservation of diatoms below 179 cm (Fig. 2.17), and the abundant Mg-calcite in

micrite at 180 cm (Fig. 2.11) suggest that salinity was low between at ~3876 y and 4126 y (Table 2.6) compared to later times in Lake Thetis. This might coincide with the maximum lake level preserved by relict shorelines (Fig. 1.8); but until the full sediment record is cored and studied, this is only speculation. The small excursions in $\delta^{18}O$ in the micrite indicate that the occurrence of drought–wet cycles in the area during the past 4100 y, but additional work is needed to document the magnitude and frequency of these events. The small increase in $\delta^{18}O$ of the micrite from an average of +1 ‰ to +2 ‰ at about ~80 cm (Fig. 2.22) and 2772 y, suggests increased aridity and increased evaporation compared to conditions during the earlier part of the sediment record. The increase in sand deposition, which starts earlier than this at ~130 cm and between 4000 and 3650 y, is consistent with increasing aridity. Eolian sand processes are dominant when the baffling effect of extensive vegetation is absent.

FUTURE WORK

Origin of Orange-Coated Grains

The origin of the "orange coats" on the carbonate grains cannot be resolved until the mineralogy is known and a more comprehensive study of diagenesis in undertaken. The addition of cold 10% HCl to samples with orange-coated grains dissolved the carbonate and turned the samples colorless. The dissolution of the orange mineral phase by this process suggest that the mineral is an amorphous Fe-oxide (Charette and Sholkovitz, 2002), but additional work must be done to prove this. In addition, a comprehensive study of diagenesis must resolve is whether the grains were coated prior to deposition or were coated *in situ* after deposition.

Formation of coats prior to deposition requires a change in environmental conditions in the source area that would episodically result in the production of a large volume of coated grains. As these are eolian sands, the process would have to be a surface process. Fe-oxide coating on sand is prevalent in red desert sands in the form of "desert varnish," which may form biologically and/or inorganically. Most researchers support the idea of biologically-formed desert varnish, where colonies of microscopic bacteria living on the rock surface for thousands of years absorb trace amounts of manganese and iron from the atmosphere and precipitate it as a black layer of manganese oxide or reddish iron oxide (Dorn and others, 1981; Krumbein and Jens, 1981; Taylor-George and others, 1983; Palmer and others, 1986; Perry and others, 2002). Some researchers support the idea of inorganic origins of desert varnish (Potter and Rossman, 1977; Elvidge, 1979), where clay minerals interact with Mn- and Fe- oxides to produce a thin veneer of cryptocrystalline orange-coats on the surface of rocks as a result of chemical weathering (Potter and Rossman, 1977; Elvidge, 1979).

In situ formation of the orange coats requires interaction with oxygenated pore water in these limited horizons. The preservation of abundant organic matter and the H_2S odor of the freshly cut cores indicates strongly anoxic conditions that are clearly at odds with the formation of iron-oxide minerals. A study by Charette and Sholkovitz (2002) described the formation of iron oxides (ferrihydrite, lepidocrocite, and goethite) on shallow-subsurface grains in aquifers where reduced meteoric water mixed with oxygenated seawater near the groundwater-seawater interface. Possibly, the coatings on the grains might have formed during episodes when anoxic pore waters were replaced with oxygenated groundwater. The coarser sand layers, which tend to have the highest

concentrations of orange-coated grains, would have been the most porous and permeable layers and therefore be most affected by diagenesis.

HIGHER SPATIAL RESOLUTION STUDY OF STABLE ISOTOPES, MINERALOGY, POLLEN AND OSTRACODE ABUNDANCE

The vertical profiles in $\delta^{18}O$ and $\delta^{13}C$ show excursions that are particularly well defined over intervals of closely spaced samples (see Figs. 2.22 and 2.23). The vertical profiles of Mg-calcite to aragonite in the endogenic micrite has such poor spatial resolution that changes in mineralogy that could be related to change in Mg:Ca ratio and overall salinity cannot be detected. C and O isotope and mineralogical data from additional samples in the core at a spacing of no more than 2 cm must be obtained. These data, coupled with more detailed study of pollen and ostracode abundance are needed to define possible decadal-scale drought-wet cycles.

The limited pollen analyses at low spatial resolution are not adequate to determine trends or changes in pollen existing in the Thetis sediment record. Future work that will process closely spaced samples throughout core for pollen is needed to see if changes in total abundance and in species might provide better insight into drought/wet cycles in the area of Lake Thetis. Particularly, the hypothesis that increase in aridity might account for increase in sand deposition between 4000 and 3650 y could be tested by a significant decrease in pollen abundance.

The ostracode *Cyprideis australiensis* occurs throughout the core, but not in the same abundance in every layer. Quantitative, high-spatial-resolution counts of carapaces in each layer will provide important data on the times of environmental conditions that

were favorable and unfavorable for ostracode survival and reproduction. Synthesis of these data with other data from the study will provide better understanding of the nature of the changes in environmental conditions (e.g., salinity changes, pH).

IMPROVEMENT OF GEOCHRONOLOGY

As noted in Chapter 2, the ~500-y age of the top of the core and some problematic ages between 140 cm and 180 cm requires that more radiocarbon ages be obtained in order to obtain a better geochronology of the Lake Thetis sediment record. One possible cause of the too-old age of the top of the core, which could also be a factor in all intervals, is the occurrence of flecks of windblown charcoal. Future samples to be analyzed should be examined under reflected-light microscopy and any flecks of charcoal removed. The majority of pollen in the samples reflects local vegetation. In layers that contain abundant pollen, the sample could be split. One split can be processed to obtain an age only on the refractory pollen fraction of the organic matter, and the other on the bulk organic (minus the charcoal). This might provide some insight into the problematic ages, particularly in the organic-rich sand interval, because pollen is not affected by incorporation of CO_2 derived from older organic matter (Chapter 2). Finally, the addition of analyses at higher spatial resolution will also help defined sedimentation rates over the entire interval.

COLLECTION OF MORE AND LONGER CORES

Longer cores to basement are needed to compile the entire history of sedimentation, biota, and C and O isotope record of Lake Thetis. Cores should be taken across a transect line from base of slope on the west side, across center to the base of

slope of the east side. This will identify facies changes that might occur, such as changes in volume of sand from west to east and or possible debris aprons at the bases of the slope that contain locally derived stromatolite debris.

CONCLUSIONS

The sediment record of Lake Thetis obtained in two cores spans the past ~4100 y and shows changes in sediment type, sedimentation rate, biota, and C and O isotopes that are related to climate change and the evolving nature of the lake. The oldest sediment is dominated by organic-rich sand, which is compacted, partly decomposed organic matter derived from thick microbial mats that covered the lake bottom and which accumulated at rates of >20 cm/100 y. During the phase of sedimentation dominated by accumulation of organic-rich sand, the control on $\delta^{13}C$ of the lake changed from photosynthesis to addition of isotopically light carbon derived from organic decomposition, shown by the significant decrease in $\delta^{13}C$ in endogenic micrite. The $\delta^{18}O$ of endogenic micrite at the base of the sediment record has an average value of +1.0 ‰, which indicates that it formed from water that had a higher $\delta^{18}O$ value than either seawater or meteoric water of the region. Therefore, during this period of time, evaporation must have slightly exceeded precipitation and inflow. However, the base of organic-rich sand interval contains abundant, well preserved diatoms and ostracode species *Mytilocypris ambiguosa*. These observations constrain the salinity of the lake to be only brackish (<10 g/L). This period likely represents the lowest salinity and largest lake size of the time represented in the cores.

Between ~4000 y and 3650 y, sand deposition increased and organic-rich sand deposition decreased. Since this time, sand and organic-rich sand (and uncompacted organic-rich sand, i.e., sludge) have accumulated at rates between 3 and 6 cm/100y. The increase in eolian sand brought to the lake suggests that the vegetation in the area surrounding Lake Thetis decreased owing to increasing aridity. Concomitant with the change in sedimentation is the disappearance of *Mytilocypris ambiguosa* from the sediment record, which signals that the lake reached a salinity level above the biological tolerance of this species. The average size and salinity of the lake have probably been similar to those of today for the past ~3800 y, particularly after ~2770 y when the average $\delta^{18}O$ of the micrite increased from +1 ‰ to its modern value of +2 ‰. Today, evaporation greatly exceeds precipitation. The lake water is hypersaline, generally>40 g/L, exceeding the documented tolerance level of *Cyprideis australiensis*, the only ostracode extant in the lake. Biodiversity is low, indicating that the lake is inhospitable to many species.

The $\delta^{18}O$ of endogenic micrite maintains an average value of +1 ‰ from ~4100y to 2770 y, despite the evidence of increasing salinity shown prior to 3670 y shown by the disappearance of *Mytilocypris ambiguosa.* An increase would be expected owing to higher evaporation rates, unless it was offset by increase in the proportion of isotopically light water added to the lake. The lack of increase in $\delta^{18}O$ in micrite between ~3670 y and 2770 y might represent an end of to the addition of seawater through deeper aquifers, sealed off by the accumulation of relatively impermeable organic-rich sand, and the change to meteoric water as the sole source of lake water.

Superposed on the overall history of increasing salinity and decreasing lake size are small excursions that mark short-term increases and decreases in salinity and lake size. These excursions are recorded in small (~1 ‰) changes in $\delta^{18}O$ of micrite and in abundance of *Cyprideis australiensis*. The excursions are likely associated with drought/wet cycles in the area of Lake Thetis. Definition of the magnitude and frequency of drought/wet cycles requires additional high-resolution temporal and spatial studies. These include the collection of cores that contain the complete sediment record along an east to west transect, analyses of $\delta^{18}O$ and mineralogy of endogenic micrite at 1 to 2 cm intervals, quantitative data of *Cyprideis australiensis* and pollen abundances at 1 to 2 cm intervals, and additional AMS-radiocarbon ages from bulk organic matter and from pollen separates.

References

Abell, P., S. Awramik, R. Osbourne, and S. Tomellini, 1982, Plio-Pleistocene lacustrine stromatolites from Lake Turkana, Kenya: Morphology, stratigraphy, and stable isotopes: Sedimentary Geology, v. 32, p. 1-26.

Alin, S.R., and Cohen, A.S., 2003, Lake-level history of Lake Tanganyika, East Africa, for the past 2500 years based on ostracode-inferred water-depth reconstruction, Palaeogeography, Palaeoclimatology, Palaeoecology: v. 199, p. 31-49.

Andrews, J.F., R. Riding, and P.F. Dennis, 1993, Stable isotopic compositions of Recent freshwater cyanobacterial carbonates from the British Isle: local and regional environmental controls: Sedimentology, v. 40, p. 303-314.

Australian Bureau of Statistics, 2002, Year Book Australia 2002: Belconnen, Australia, http://www.abs.gov.au/Ausstats/abs@.nsf/94713ad445ff1425ca25682000192af2/fe3fa39a5bf5aa5aca256b350010b3fd!OpenDocument, accessed 23 July 2005.

Backhouse, J., 1993, Holocene vegetation and climate record from Barker Swamp, Rottnest Island, Western Australia, Journal of the Royal Society of Western Australia: v. 76, p. 53-61.

Bold, H. C., and Wynne, M. J., 1978, Introduction to the Algae: structure and reproduction, second edition, 720p.

Bold, H.C. and M.J. Wynne. 1985. Introduction to the Algae, Structure and Function. 2nd ed. Prentice-Hall, Inc., Englewood Cliffs, N.J.

Bookman, R., Enzel, Y., Agnon, A., Stein, M., 2004, Late Holocene lake levels of the Dead Sea, Geological Society of America Bulletin: v. 116, no. 5/6, p. 555-571.

Burke, C. M., and Knott, B., 1997, Homeostatic interactions between the benthic microbial communities and the waters of a hypersaline lake, Lake Hayward, Western Australia, Marine Freshwater Research: v. 48, p. 623-631.

Burne, R.V., and Bauld, J., 1985, The origin and preservation of microbial organic facies in coastal saline lakes of South Australia and Western Australia, abstract, in Lacustrine Petroleum Source Rocks, Programme & Abstracts, p. 18-19.

British Columbia Water Quality Report, 1997, Ambient water quality for dissolved oxygen, overview report, compiled by the Ministry of Environment, Government of British Columbia, http://wlapwww.gov.bc.ca, accessed 23 July 2005.

Charette, M.A., and Sholkovitz, E.R., 2002, Oxidative precipitation of groundwater-derived ferrous iron in the subterranean estuary of a coastal bay, Geophysical Research Letters: v. 29, no. 10, p. 1-4.

Cohen, A.S., M.R. Talbot, S.M. Awramik, D.L. Dettman, and P. Abell, 1997, Lake level and paleoenvironmental history of Lake Tanganyika, Africa, as inferred from late Holocene and modern stromatolites: Geological Society of America Bulletin, v. 109, p. 444-460.

Cohen, A. S., 2003, Paleolimnology, The history and evolution of lake systems, Oxford University Press, 500 p.

Coshell, L., and Rosen, M. R., 1994, Stratigraphy and Holocene of Lake Hayward, Swan coastal plain wetlands, Western Australia, *in* Special Publication - SEPM Society for Sedimentary Geology: v. 50, p.173-188.

Cuffey, K.M., and G.D. Clow, 1997, Temperature, accumulation, and ice sheet elevation in central Greenland through the last deglacial transition; Journ. of Geophysical Research: v. 102, no. C12, p. 26,383-26,396.

De Deckker, P., 1983, Notes on the ecology and distribution of non-marine ostracods in Australia, Hydrobiologia: v. 3, no. 106, p. 223-234.

De Deckker, P. (1988). An account of the techniques using ostracods in palaeolimnology in Australia. Palaeogeography, Palaeoclimatology, Palaeoecology **62,** 463-475.

De Deckker, P., Chivas, A. R., and Shelley, J. M. G., 1999, Uptake of Mg and Sr in the euryhaline ostracod Cyprideis determined from in vitro experiments, Palaeogeography, Palaeoclimatology, Palaeoecology: v. 148, p. 105-116.

Dickin, A. P., 1995, Radiogenic Isotope Geology, New York: Cambridge University Press, 490 p.

Dorn, R.I., and Oberlander, T.M., 1981, Microbial origin of desert varnish, Science: v. 213, no. 4513, p. 1245-1247.

Duranceau, S.J., and Henthorne, L.R., 2004, Membrane pretreatment for seawater reverse-osmosis desalination, Florida Water Resources Journal, p. 33-37.

Edward, D. H. D., 1983, Inland waters of Rottnest Island, Journal of the Royal Society of Western Australia: v. 66, p. 41-47.

Elvidge, C.D., 1979, Distribution and formation of desert varnish in Arizona, M.Sci. Thesis, University of Arizona, Phoenix.

Faure, G., 1986, Principles of isotope geology, John Wiley and Sons, p. 429-455.

Freeman, M. J., George, A. D., Marshall, A., and Dunphy, J. M., 1998, The Prider fieldtrip – The rock cycle and geology of the Perth metropolitan area, Geological Society of Australia Excursion Guidebook No. 10, 72 p.

Given, R.K., and Wilkinson, B.H., 1985, Kinetic control of morphology, composition, and mineralogy of abiotic sedimentary carbonates: Journal of Sedimentary Petrology, v. 55, p. 109-119.

Grey, K., Moore, L. S., Burne, R. V., Pierson, B. K., and Bauld, J., 1990, Lake Thetis, Western Australia: an Example of Saline Lake Sedimentation Dominated by Benthic Microbial Processes: Australian Journal of Marine and Freshwater Research, v. 41, p. 275-300.

Grossman, E. L., and T.-L. Ku, 1986, Oxygen and carbon isotope fractionation in biogenic aragonite: Temperature effects, Chem. Geol.: v. 59, p. 59 – 74.

Hallam, A., 1992, Phanerozoic sea-level changes, New York: Columbia University Press, p. 154-155.

Hawkins, L.V., Hennion, J.F., Nafe, J.E., and Thyer, R.F., 1965, Geophysical investigations in the area of the Perth Basin, Western Australia, Geophysics, v. 30, no.6, p. 1026-1052.

Hearty, P. J., 2003, Stratigraphy and timing of eolianite deposition on Rottnest Island, Western Australia, Quaternary Research: v. 60, p. 211-222.

Hoffmeister, W.S., 1960, Sodium hypchlorite, a new oxidizing agent for the preparation of microfossils, in: Oklahoma geology notes, Oklahoma Geological Survey, v. 20, p. 34-35.

IAEA (2004), Isotope Hydrology Information System, Global Network of Isotopes in Precipitation (GNIP) and Isotope Hydrology Information System (ISOHIS), The ISOHIS Database. Accessible at: http://isohis.iaea.org/, accessed 23 July 2005.

John, J., 1998, Diatoms: Tools for Bioassessment of River Health. Report to Land and Water Resources Research and Development Corporation, Canberra, 388p.

Katz, A.. and Kolodny, N., 1988, Hypersaline brine diagenesis and evolution in the Dead Sea-Lake Lisan system (Israel), Geochimica et Cosmochimica Acta: v. 53, no. 18, p. 59-67.

Kendall, C., and Caldwell, E.A., 1998, Fundamentals of Isotope Geochemistry *in* Kendall, C., and McDonnell, J.J., (eds), 1998, Isotope Tracers in Catchment Hydrology, Elsevier Science B.V., Amsterdam, p. 51-86.

Kern, A. M., 1993, The geology and hydrogeology of the superficial formations between Cervantes and Lancelin, Western Australia, Professional Papers Report 34, Geological Survey of Western Australia, Perth, 26 p.

Kilian, M.R., van der Plicht, J., van Geel, B. and Goslar, T. 2001. Problematic ^{14}C -AMS dates of pollen concentrates from Lake Gosciaz (Poland). Quaternary International 88, p. 21-26.

Krumbein, W.E., and Jens, K., 1981, Biogenic rock varnishes of the Negev Desert (Israel): an ecological study of iron and manganese transformation by cyanobacteria and fungi, Oecologia: v. 50, p. 25-38.

Lenntech Water Treatment & Air Purification Holding B.V., http://www.lenntech.com, accessed 23 July 2005.

Lister, G. S., 1988, Stable isotopes from lacustrine ostracoda as tracers for continental palaenvironments, in: De Deckker, P., Colin, J. P., and Peypouquet, J. P., (Eds.), Ostracoda in the Earth Sciences, Elsevier, New York, p. 201-218.

Leng., M., Barker, P., Greenwood, P., Roberts, N., and Reed, J., 2001, Oxygen isotope analysis of diatom silica and authigenic calcite from Lake Pinarbasi, Turkey, Journal of Paleolimnology: v. 25, p. 343-349.

Los Angeles Department of Water and Power, Annual Water Quality Report, 2004, 16p. http://www.ladwp.com/ladwp/cms/ladwp001965.jsp, accessed 23 July 2005.

Luton, G. C., and Johnston, G. M., 2001, AHD71, AUSGEOID and GPS: A heightening odyssey, Australian Surveying and Land Information Group, *in* 2001 – A Spatial Odyssey: 42nd Australian Surveyor's Congress.

McKenzie, J.A., and Eberli, G.P., 1987, Indications for abrupt Holocene climatic change: late Holocene oxygen isotope stratigraphy of the Great Salt Lake, Utah: in Berger, W.H., and Labeyrie (eds.), Abrupt Climate Change, D. Reidel Publishing Company, p. 127-136.

MDBMC, 1987, Murray-Darling Basin Environmental Resources Study, Murray-Darling Basin Miniterial Council (MDBMC), Canberra.

Moore, L. S., 1987, Water chemistry of the coastal saline lakes of the Clifton-Preston Lakeland system, south-Western Australia, and its influence on stromatolite formation, Australian Journal of Marine Freshwater Research: v. 38, p. 647-660.

Morton, R. A., and Suter, J. R., 1996, Sequence Stratigraphy and Composition of Late Quaternary Shelf-Margin Deltas, Northern Gulf of Mexico. American Association et Petroleum Geologists Bulletin: v. 80, p. 505-530.

Moss, S. J., Freeman, M., George, A. D., Marshall, A., & Dunphy, J. M., 1998, The

Neal, J.W., 1988, Ostracods and paleosalinity reconstruction, in: De Deckker, P., Colin, J.P., and Peypouquet, J.P., Ostracoda in the Earth Sciences, Elsevier, London, p. 125-154.

O'Reilly, C.M., Alin, S.R., Pilsner, P.D., Cohen, A.S., and McKee, B.A., Climate change decreases ecosystem productivity of Lake Tanganyika, Africa, Nature: v. 424, p. 766-768.

Pack, S.M., Miller, G.H., Fogel, M.L., Spooner, N.A., 2003, Carbon isotopic evidence for increased aridity in northwestern Australia through the Quaternary, Quaternary Science Reviews: v. 22, p. 629-643.

Prider Field Trip– the rock cycle and geology the Perth metropolitan area. A Professional Development Day for High School Geology and Science Teachers. Geological Society of Australia (WA Division), Excursion Guidebook, No. 10, 72 p.

Palmer, F.E., Staley, J.T., Murray, R.G., Counsell, T., and Adams, J.B., 1986, Identification of manganese-oxidizing bacteria from desert varnish, Geomicrobiology Journal: v. 4, no. 4, p. 343-360.

Perry, R.S., Dodsworth J., Staley, J.T., and Gillespie A., 2002, Molecular analyses of microbial communities in rock coatings and soils from Death Valley California, Astrobiology: v. 2, no. 4, p. 539.

Playford, P. E., and Leech, R. E. J., 1977, Geology and hydrology of Rottnest Island, Western Australia Geological Survey Report No. 6.

Playford, P.E., 1988, Guidebook to the geology of Rottnest Island, Geological Society of Australia Western Australia Division, Excursion Guidebook No. 2, 67p.

Playford, P.E., 1997. Geology and hydrology of Rottnest Island, Western Australia, in: Vacher, H.L., T. Quinn, (Eds.), Geology and Hydrology of Carbonate Islands, Developments in Sedimentology 54, Elsevier, London, p. 783-810.

Potter, R.M., and Rossman, G.R., 1977, Desert varnish: the importance of clay minerals, Science: v. 196, no. 4297, p. 1446-1448.

Schmidt, G.A., G. R. Bigg and E. J. Rohling. 1999. "Global Seawater Oxygen-18 Database". http://data.giss.nasa.gov/data, http://data.giss.nasa.gov/o18data/, accessed 23 July 2005.

Reed, J.M., 1998, Diatom preservation in the recent sediment record of Spanish saline lakes: implications for paleoclimate study, Journal of Paleolimnology: v. 19, p. 129-137.

Reineck H.E., and Singh, I., 1980, Depositional Sedimentary Environments. Springer Verlag. Berlin, 549p.

Romanek, C.S., Grossman, E.L., Morse, J.W., 1992. Carbon isotopic fractionation in synthetic aragonite and calcite: effects of temperature and precipitation rate. Geochim. Cosmochim. Acta 56, 419–430.

Romeny, J. L., 1995, Lake Thetis-WA084, in a Directory of Important Wetlands in Australia – Database, Department of Conservation and Land Management, Busselton, revised in 2000 by Elscot, S., 3p.

Rosen, M. R., Turner, J. V., Coshell, L., Gailitis, V., 1995, The effects of water temperature, stritification, and biological activity on the stable isotopic composition and timing of carbonate precipitation in a hypersaline lake, Geochimica et Cosmochimica Acta, v. 59, no. 5, p. 979-990.

Shaffron, M., and others, 1990, Water Quality, p. 147-165, in The Murray, edited by N. Mckay and D. Eastburn: Murray-Darling Basin Commission, Canberra.

Sharp. Z., 2005, Chapter 7: Carbon –Biogenic Carbonates: on-line text at http://epswww.unm.edu/facstaff/zsharp/505/carbonates%202.pdf, accessed 23 July 2005.

Shepherd, M. J., and Eliot, I. G., 1995, Major phases of coastal erosion ca. 6700-6000 and ca. 3000-2000 BP between Cervanted and Dongara, Western Australia: Quaternary International, v. 26, p. 125-130.

Sonneman, J. A., Sincock, A., Fluin, J., Reid, M., Newall, P., Tibby, J., and Gell, P., 2000, An illustrated guide to common stream diatom species from temperate Australia, Cooperative Research Centre for Freshwater Ecology Identification Guide No. 33, presented at the second Australian Algal Workshop, Adelaide University, Land and Water Resources Research & Development Corporation, 168 p.

Spencer, R.J., and 11 others, 1984, Great Salt Lake, and precursors, Utah: the last 30,000 years: Contributions to Mineralogy and Petrology: v. 86, p. 321-334.

Spencer, R.J., and 11 others, 1984, Great Salt Lake, and precursors, Utah: the last 30,000 years: Contributions to Mineralogy and Petrology: v. 86, p. 321-334.

Stein, M., Starinsky, A., Katz, A., Goldstein S. L., Machlus, M., and Schramm, A., 1997, Strontium isotopic, chemical, and sedimentological evidence for the evolution of Lake Lisan and the Dead Sea, Geochimica et Cosmochimica Acta: v. 61, no. 18, p. 3975-3992.

Talbot, M.R., 1990, A review of the palaeohydrological interpretation of carbon and oxygen isotopic ratios in primary lacustrine carbonates, Chemical Geology, Isotope Geosciences Section: v. 80, p. 261-279.

Taylor, R.E., 1987, Radiocarbon Dating: An Archaeological Perspective, Orlando, FL: Academic Press.

Taylor-George, S., Palmer, F.E., Staley, J.T., Borns, D.J., Curtiss, D.J., and Adams, J.B., 1983, Fungi and bacteria involved in desert varnish formation, Microbial Ecology: v. 9, no. 3, p. 227-245.

Tucker, M.E. and Wright, V. P., 1990, Carbonate Sedimentology, Blackwell Scientific Publications, London or Osney Mead, Oxford OX2 0 EL (editorial office) p. 482.

United States Department of Environmental Protection Agency, Drinking water standards, 2004, http://www.epa.gov/safewater/mcl.html, accessed 23 July 2005.

Wagner, G.A, 1998, Age Determination of Young Rocks and Artifacts: Physical and Chemical Clocks in Quaternary Geology and Archaeology, Springer, Berlin, 466 p.

Williams, W.D., and Mellor, M.W., 1991, Ecology of Coxiella (Mollusca, Gastropoda, Prosobranchia), a snail endemic to Australian salt lakes: Palaeogeography, Palaeoclimatology, Palaeoecology, v. 84, p. 339-355.

World Ocean Atlas, 2001, Ocean Climate Laboratory/National Oceanographic Data Center, http://www.nodc.noaa.gov, accessed 23 July 2005.

Yassini, I, and Kendrick G.W., 1988, Middle Holocene ostracodes, foraminifers and environments of beds at Point Waylen, Swan River Estuary, Southwestern Australia,, Alcheringa, v. 12, p. 107-121.

Zhang, J., P.D. Quay and D.O. Wilbur .1995. Carbon isotope fractionation during gas-water exchange and dissolution of CO_2. Geoch. Cosmo. Acta 59: p. 107-114.

Zheng, H., Powell, C.M., and Zhao, H., 2002, Eolian and lacustrine evidence of late Quaternary palaeoenvironmental changes in southwestern Australia, Global and Planetary Change: v. 35, p. 75-92.

Description of Core 1

Depth (cm)	Description	Fossils
Above 0	Loose organic material was cut off and lost from the top of the core. The remaining bits and pieces from the plug and the lid are purple-pink and contain lots of purple sulfur reducing bacteria.	
0-5.3	Dusky red ooze (DRO), grayish red purple (5R 3/4) Organic matter: 50% Sand: 50%, very fine (63-88 microns), structureless, well sorted Abrupt boundary	**Ostracodes, common**
5.3-6.0	Diffuse band of DRO with slightly higher very fine white carbonate grains Diffuse white layer Organic matter: 45% Sand: 55%, very fine (63-88 microns), structureless, well sorted Abrupt contacts	**Ostracodes, common**
6.0-7.1	DRO Abrupt contacts	**Ostracodes, common**
7.1-7.6	Diffuse band of DRO, Diffuse white layer Organic matter: 45% Sand: 55%, very fine (63-88 microns), structureless, well sorted Abrupt contacts	Ostracodes, common
7.6-9.7	DRO Abrupt contacts	Ostracodes, common
9.7-11	Diffuse band of DRO, Diffuse white layer Organic matter: 45% Sand: 55%, very fine (63-88 microns), structureless, well sorted Abrupt contacts	Ostracodes, common
11-12.1	DRO	Ostracodes, common
12.1-12.7	Diffuse band of DRO, Diffuse white layer Organic matter: 45% Sand: 55%, very fine (63-88 microns), structureless, well sorted	Ostracodes, common
12.7-13.8	DRO	Ostracodes, common
13.8-14.7	Diffuse band of DRO, Diffuse white layer Organic matter: 45% Sand: 55%, very fine (63-88 microns), structureless, well sorted	Ostracodes, common
14.7-15.8	DRO	Ostracodes, common

15.8-16.5	Diffuse band of DRO, Diffuse white layer Organic matter: 45% Sand: 55%, very fine (63-88 microns), structureless, well sorted	Ostracodes, common
16.5-19.6	DRO	Ostracodes, common
19.6-19.9	Diffuse band of DRO, Diffuse white layer Organic matter: 45% Sand: 55%, very fine (63-88 microns), structureless, well sorted	**Ostracodes, common**
19.9-22.0	DRO	Ostracodes, common
22.0-22.4	Diffuse band of DRO, Diffuse white layer Organic matter: 45% Sand: 55%, very fine (63-88 microns), structureless, well sorted	Ostracodes, common
22.4-25.8	Dark red brown ooze (DRB)	Ostracodes, common
25.8-30.3	DRO	**Ostracodes, common**
30.3-30.6	"Pinkish layer", moderate red 5R 5/4 Organic matter: 40% Sand: 60%, (63-250 microns) Top contact abrupt, Bottom contact gradual	Ostracodes, common
30.6-31.6	DRO	Ostracodes, common
31.6-32.2	Diffuse band of DRO, Diffuse white layer Organic matter: 45% Sand: 55%, very fine (63-88 microns), structureless, well sorted	Ostracodes, common
32.2-35.0	Diffuse band of DRO, Diffuse white layer Organic matter: 45% Sand: 55%, very fine (63-88 microns), structureless, well sorted	Ostracodes, common
35.0-36.0	Well defined white carbonate-rich sand layer Organic Matter: 35% Sand: 65%, fine to medium (63-250 microns)	Ostracodes, abundant
36.0-41.5	DRO	Ostracodes, common
41.5-43.0	Diffuse band of DRO, Diffuse white layer Organic matter: 45% Sand: 55%, very fine (63-88 microns), structureless, well sorted	Ostracodes, common
43.0-43.4	Well-defined white carbonate-rich sand layer Organic matter: 35% Sand: 65%, white, fine to medium (63-250 microns)	Ostracodes, abundant
43.4-44.8	DRO	Ostracodes, common

44.8-45.5	Diffuse band of DRO Diffuse white layer Organic matter: 45% Sand: 55%, very fine (63-125 microns), structureless, well sorted	Ostracodes, common
45.5-46.6	Very dark red (5R 2/6) ooze Organic matter: 80% Sand: 20%, white, very fine (63-125 microns) Top gradual contact, Bottom abrupt contact	Ostracodes, sparse
46.6-47.5	Diffuse band of DRO, "Pinkish layer", moderate red 5R 5/4, Diffuse white layer Organic matter: 45% Sand: 55%, very fine (63-88 microns), structureless, well sorted	Ostracodes, sparse
47.5-50.5	DRO	Ostracodes, sparse
50.5-51.0	Diffuse band of DRO. Diffuse white layer Organic matter: 45% Sand: 55%, very fine (63-88 microns), structureless, well sorted	Ostracodes, abundant
51.0-53.0	DRO	Ostracodes, common
53.0-54.7	Moderate brown 5YR 4/4 Organic matter: 60% Sand: 40%, white, very fine to fine (63-177 microns) Abrupt top contact, Gradual bottom contact	Ostracodes, sparse
54.7-56.0	DRO	Ostracodes, common
56.0-58.5	Moderate reddish brown 10R 3/4 Organic matter: 40% Sand: 60%, white, very fine to medium (63-250 microns) Gradual contacts	Ostracodes, sparse
58.5-60.5	Dusky brown 5YR 2/2 Organic matter: 90% Sand: 10%, white, fine (63-177 microns) Abrupt contacts	Ostracodes, rare
60.5-62.0	Grayish brown 5YR 3/2 Organic matter: 80% Sand: 20%, white, fine (63-177 microns) Gradual contacts	Ostracodes, sparse
62.0-62.4	Diffuse band of moderate reddish brown Organic matter: 70% Sand: 30%, component #1: white, fine (63-177 microns), 25%, component #2: orange coated	Ostracodes, rare

	grains (177-250 microns), 5% Abrupt bottom contact	
62.4-63.0	Dusky brown 5YR 2/2 Organic matter: 80% Sand: 20%, white, fine (63-177 microns) Abrupt contacts	Ostracodes, rare
63.0-63.5	Diffuse band of moderate reddish brown Organic matter: 70% Sand: 30%, component #1: white, fine (63-177 microns), 25%, component #2: orange coated grains (177-250 microns), 5% Abrupt bottom contact	Ostracodes, rare
63.5-64.2	Diffuse band of dusky brown 5YR 2/2 Organic matter: 90% Sand: 10%, white, fine (63-177 microns) Abrupt top contact, Gradual bottom contact	Ostracodes, rare
64.2-66.8	Dusky brown 5YR 2/2 Organic matter: 80% Sand: 20%, white, fine (63-177 microns) Gradual top contact, Abrupt bottom contact	Ostracodes, common
66.8-67.2	Dusky brown 5YR 2/2 Organic matter: 90% Sand: 10%, white, fine (63-177 microns) Gradual contacts	Ostracodes, sparse
67.2-67.6	White layer, Diffuse band of dusky brown 5YR 2/2 Organic matter: 40% Sand: 60%, white, fine to medium (63-250 microns), one white carbonate grain is 1.0 mm, no staining on grains Gradual top contact, Bottom abrupt contact	Ostracodes, common
67.6-69.1	Grayish brown 5YR 3/2 ooze Large black flecks up to 1.0 mm long, blade-shaped with wispy ends Organic matter: 90% Sand: 10%, white, fine (63-177 microns) Gradational bottom contact	Ostracodes, trace
69.1-69.8	White layer with grayish brown 5YR 3/2 ooze Organic matter: 30% Sand: 70%, white, fine to medium (63-250 microns) Gradational top contact, Abrupt bottom contact	Ostracodes, common

69.8-72.6	Grayish red 10R 4/2 Organic matter: 80% Sand: 20%, white, fine (63-177 microns) Abrupt top contact, Gradual bottom contact	Ostracodes, common
72.6-73.1	Grayish brown 5YR 3/2 ooze Organic matter: 80% Sand: 20%, white, fine (63-177 microns) Gradual top contact	Ostracodes, common
73.1-74.6	White sand with grayish brown 5YR 3/2 ooze Organic matter: 50% Sand: 50%, white, fine (63-177 microns) Gradual top contact, Abrupt bottom contact	Ostracodes, common
74.6-75.8	Grayish brown 5YR 3/2 ooze Organic matter: 80% Sand: 20%, component #1: white, fine (63-177 microns), 15%, component #2: orange grains, (63-125 microns), 5% Gradual contacts	Ostracodes, sparse
75.8-76.2	Grayish brown 5YR 3/2 ooze, Thin diffuse white band Organic matter: 80% Sand: 20%, white, fine to medium (63-250 microns) Gradual contacts	Ostracodes, rare
76.2-77.4	Light brown 5YR 5/6 ooze Organic matter: 80% Sand: 20%, component #1: white, fine (63-177 microns), 10%, component #2: orange stained grains, (63-125 microns), 10% Gradual contacts	Ostracodes, trace
77.4-78.1	Light brown 5YR 5/6 sandy ooze Organic matter: 50% Sand: 50%, component #1: white, fine to medium (63-250 microns), 40%, component #2: orange stained grains, (63-125 microns), 10% Gradual top contact, Abrupt bottom contact	Ostracodes, trace
78.1-79.2	Reddish brown ooze, carb sand grains not stained Light brownish gray 5YR 6/1 Organic matter: 80% Sand: 20%, white, fine to medium (63-250 microns) Abrupt top contact Gradual bottom contact	Ostracodes, rare

79.2-79.6	Thin diffuse white band Similar to above layer, but with sand grains up to 710 microns and well-rounded Gradual contacts	Ostracodes, sparse
79.6-80.2	Reddish brown ooze, carbonate sand grains not stained Light brownish gray 5YR 6/1 Organic matter: 80% Sand: 20%, white, fine to medium (63-250 microns) Gradual top contact, Abrupt bottom contact	Ostracodes, rare
80.2-80.5	White, carbonate-rich layer Organic matter: 30% Sand: 70%, white, fine to medium (63-250 microns) Abrupt contacts	Ostracodes, common
80.5-82.6	Brownish gray 5YR 4/1 Organic matter: 90% Sand: 10%, white, fine (63-125 microns) Abrupt contacts	Ostracodes, trace
82.6-83.2	White, carbonate-rich layer Organic matter: 20% Sand: 80%, white, fine to medium (63 to 250 microns) Abrupt contacts	Ostracodes, common
83.2-84.5	Light brownish gray 5YR 6/1 Organic matter: 80% Sand: 20%, component #1: white, fine (63-177 microns), 18%, component #2: orange-coated, fine (63-177 microns), 2% Abrupt contacts	Ostracodes, trace
84.5-85.0	White, carbonate-rich layer Organic matter: 20% Sand: 80%, component #1: white, fine to medium (63 to 250 microns), 75%, component #2: orange-coated, fine (63-177 microns), 5% Abrupt contacts	Ostracodes, sparse
85.0-86.6	Light brown 5YR 5/6 Organic matter: 60% Sand: 40%, well-rounded, component #1: white, fine (63-177 microns), component #2: orange-coated, fine to medium (63 to 350 microns), 35% Abrupt top contact, Gradual bottom contact	Ostracodes, trace
86.6-87.6	Pale yellowish brown 10YR 6/2 Mud: 95%	Ostracodes, trace

	Sand: 5%, white, larger grains towards the bottom, fine to medium (63-350 microns) Minor scattered black flecks Gradual top contact, Abrupt bottom contact	
87.6-90.0	Light brownish gray 5YR 6/1 Organic matter: 70% Sand: 30%, white, fine to medium (63-250 microns) Abrupt contacts	Ostracodes, sparse
90.0-91.3	Brownish gray 5YR 4/1 Organic matter: 80% Sand: 20%, white, fine to medium (63-250 microns) Abrupt contacts	Ostracodes, sparse
91.3-91.9	White, carbonate-rich layer Organic matter: 10% Sand: 90%, component #1: 50%, white, fine (63-125 microns), component #2: 40%, white, medium to coarse (250-710 microns) Abrupt contacts	Ostracodes, common
91.9-94.3	Light brownish gray 5YR 6/1 Organic matter: 60% Sand: 40%, white, fine to medium (63-250 microns) Abrupt contacts	Ostracodes, common
94.3-94.5	White diffuse band, carbonate-rich, White, carbonate-rich layer Organic matter: 10% Sand: 90%, component #1: 50%, white, fine (63-125 microns), component #2: 40%, white, medium to coarse (250-710 microns) Abrupt contacts	Ostracodes, common
94.5-95.0	Brownish gray 5YR 4/1 Organic matter: 60% Sand: 40%, white, fine (63-250 microns) Abrupt contacts	Ostracodes, sparse
95.0-95.5	Very grainy layer Dark yellowish orange 10YR 6/6 Organic matter: 40% Sand: 60%, white and brown stained, fine to medium (63-350 microns) Abrupt contacts	Ostracodes, common
95.5-96.2	Pale red purple 5RP 6/2 Organic matter: 80%	Ostracodes, sparse

	Sand: 20%, white, fine (63-177 microns) Abrupt contacts	
96.2-96.4	Diffuse white band Organic matter: 30% Sand: 70%, white and brown stained, fine to medium (63-350 microns) Abrupt contacts	Ostracodes, common
96.4-97.0	Pale red purple 5RP 6/2 Organic matter: 80% Sand: 20%, white, fine (63-177 microns) Abrupt contacts	Ostracodes, common
97.0-97.2	Diffuse white band Pale red purple 5RP 6/2 Organic matter: 80% Sand: 20%, white, fine to medium (63-250 microns) Abrupt top contact, Gradual bottom contact	Ostracodes, common
97.2-97.4	Diffuse band with brown-stained grains Pale red purple 5RP 6/2 Organic matter: 80% Sand: 20%, white, fine to medium (63-250 microns) Gradual contacts	Ostracodes, trace
97.4-99.6	Grayish red purple 5RP 6/2 Organic matter: 80% Sand: 20%, white, fine (63-177 microns) Gradual contacts	Ostracodes, trace
99.6-100.0	Diffuse white band Pale red purple 5RP 6/2 Mud: 80% Sand: 20%, white, fine to medium (63-250 microns), not rounded Gradual contacts	Ostracodes, rare
100.0-101.4	Brownish gray 5YR 4/1 Mud: 80% Sand: 20%, white, fine (63-177 microns) Gradual top contact, Abrupt bottom contact	Ostracodes, rare
101.4-102.0	Brownish gray 5YR 4/1 Organic matter: 70% Sand: 30%, white, fine to medium (63-250 microns), not rounded Abrupt top contact, Gradual bottom contact	Ostracodes, trace

102.0-102.2	Grayish black ooze Mud: 99% Sand: 1%, white, very fine to fine (63-177 microns) Gradual contacts	Ostracodes, trace
102.2-102.6	Diffuse white band, Grayish black ooze Organic matter: 60% Sand: 40%, white, fine to medium (63-250 microns) Gradual contacts	Ostracodes, sparse
102.6-102.8	Grayish black ooze Mud: 99% Sand: 1%, white, very fine to fine (63-177 microns) Gradual contacts	Ostracodes, trace
102.8-103.0	Diffuse white band, Grayish black ooze Mud: 70% Sand: 30%, white, fine to medium (63-250 microns) Gradual contacts	Ostracodes, trace
103.0-103.5	Grayish black ooze Mud: 99% Sand: 1%, white, very fine to fine (63-177 microns), not stained Gradual contacts	Ostracodes, trace
103.5-104.0	Grayish black ooze Mud: 99% Sand: 1%, white, very fine to medium (63-250 microns) Gradual contacts	Ostracodes, trace
104.0-105.4	Brownish gray 5YR 4/1 Organic matter: 80% Sand: 20%, white, fine (63-177 microns), rounded Grains in lenses Gradual top contact, Abrupt bottom contact	Ostracodes, trace
105.4-107.8	White band, sand-rich Organic matter: 15%, brownish gray 5YR 4/1 Sand: 85%, white, not rounded, not stained, fine to medium (63-250 microns) Gradual contacts	Ostracodes, trace Charophyte oogonia, sparse
107.8-108.5	White band, sand-rich Organic matter: 25%, brownish gray 5YR 4/1 Sand: 75%, white, not rounded, not stained, fine to medium (63-250 microns) Gradual contacts	Ostracodes, trace Charophyte oogonia, rare

108.5-109.0	White band, sand-rich Organic matter: 15%, brownish gray 5YR 4/1 Sand: 85%, white, not rounded, not stained, fine to medium (63-250 microns) Gradual contacts	Trace
109.0-110.3	White band, sand-rich Organic matter: 25%, brownish gray 5YR 4/1 Sand: 75%, white, not rounded, not stained, fine to medium (63-250 microns) Gradual top contact, Abrupt bottom contact	Trace
110.3-111.0	White band, sand-rich Organic matter: 5%, brownish gray 5YR 4/1 Sand: 95%, white, not rounded, not stained, fine to medium (63-250 microns) Abrupt contacts	Trace
111.0-112.1	White band, sand-rich Organic matter: 40%, brownish gray 5YR 4/1 Sand: 60%, white, not rounded, not stained, fine to medium (63-250 microns) Abrupt contacts	Trace
112.1-112.5	White sandy layer Organic matter: 15%, brownish gray 5YR 4/1 Sand: 85%, white, not rounded, not stained, fine to medium (63-250 microns) Abrupt contacts	Trace
112.5-114.5	Brownish gray 5YR 4/1 Organic matter: 90% Sand: 10%, white, not rounded, not stained, fine to medium (63-250 microns) Abrupt contacts	Trace
114.5-115.3	Alternating thin (~2-mm thick) white sandy layers Organic matter: 15-20%, brownish gray 5YR 4/1 Sand: 80-85%, white, not rounded, not stained, fine to medium (63-250 microns) Abrupt contacts	Trace
115.3-116.6	White sandy layer Organic matter: 10%, brownish gray 5YR 4/1 Sand: 90%, white, subrounded, not stained, fine to medium (63-250 microns) Abrupt contacts	Ostracodes, rare
116.6-117.1	Brownish gray 5YR 4/1 Organic matter: 80% Sand: 20%, white, not rounded, not stained, very fine (63-125 microns) Abrupt contacts	Ostracodes, trace

117.1-117.5	Light gray sandy layer Organic matter: 30% Sand: 70%, white, very fine (63-125 microns) Abrupt contacts	Ostracodes, common One translucent tube-like fossil???
117.5-118.0	Red-brown ooze Brownish gray 5YR 4/1 Organic matter: 80% Sand: 20%, white, scattered, fine (63-177 microns) Abrupt contacts	Ostracodes, trace
118.0-118.2	Thin white sandy layer Organic matter: 25% Sand: 75%, white, fine-grained (63-125 microns) Abrupt contacts	Ostracodes, rare
118.2-118.4	Red-brown ooze Brownish gray 5YR 4/1 Poorly defined layer Organic matter: 80% Sand: 20%, white, scattered, fine (63-125 microns) Abrupt contacts	Ostracodes, trace
118.4-118.6	Thin sandy layer Organic matter: 25% Sand: 75%, white, fine (63-177 microns) Abrupt upper contact, Gradual lower contact	Ostracodes, rare
118.6-119.5	Brown-red ooze Grayish red purple 5RP 4/2 Organic matter: 90% Sand: 10%, white, fine grained (63-177 microns) Gradual contacts	Ostracodes, trace
119.5-119.8	Grayish red purple 5RP 4/2 Organic matter: 65% Sand: 35%, white, scattered, fine to medium (63-350 microns) Gradual contacts	Ostracodes, sparse
119.8-120.4	Brown-red ooze Grayish red purple 5RP 4/2 Organic matter: 80%	Ostracodes, trace

	Sand: 20%, white, fine grained (63-177 microns) Gradual contacts	
120.4-121.6	Whitish sandy layer in brown red ooze, (Grayish red purple 5RP 4/2) Organic matter: 35% Sand: 65%, white, fine (63-177 microns) Gradual upper contact, Abrupt lower contact	Ostracodes, trace
121.6-121.8	White sandy layer Organic matter: 10% Sand: 90%, white, fine grained (63-177 microns) Abrupt contacts	Ostracodes, trace
121.8-122.1	Brownish blue ooze, Medium bluish gray 5B 5/1 Organic matter: 80% Sand: 20%, faint, white, fine grained (63-177 microns) Abrupt contacts	Ostracodes, trace
122.1-122.5	White sandy layer Organic matter: 10% Sand: 90%, white, fine grained (63-177 microns) Abrupt contacts	Ostracodes, trace
122.5-123.5	Brown-red ooze, Dark gray Organic matter: 70% Sand: 30%, white, fine (63-177 microns) Odd lenses of medium to coarse grained white grains (250-1000 microns). One is small, 3-mm long and 2-mm wide vertical pipe and others follow shallow scoop shape. Perhaps, burrows? Abrupt upper contact, Gradational lower contact	Ostracodes, trace
123.5-126.0	Grayish red purple 5RP 4/2 Organic matter: 25% Sand: 75%, white, fine to medium grained (63-250 microns) Gradational contacts	Ostracodes, sparse, articulated
126.0-126.4	Brownish gray 5YR 4/1 ooze Organic matter: 90% Sand: 10%, white, fine grained (63-177 microns) Gradational contacts	Ostracodes, trace
126.4-126.9	Grayish red purple 5RP 4/2 ooze Organic matter: 65% Sand: 35%, white, fine grained (63-177 microns) Gradational contacts	Ostracodes, rare

126.9-127.3	Medium dark gray ooze Organic matter: 80% Sand: 20%, white, fine grained (63-177 microns) Gradational contacts	Ostracodes, rare
127.3-127.5	Dark gray ooze Organic matter: 65% Sand: 35%, white, fine (63-177 microns) Gradational contacts	Ostracodes, trace
127.5-128.1	Brownish gray 5YR 4/1 ooze Organic matter: 80% Sand: 20%, white, fine grained (63-125 microns) Gradational contacts	Ostracodes, trace
128.1-128.5	Brownish gray 5YR 4/1 ooze Organic matter: 50% Sand: 50%, white, very fine grained (63-125 microns) Gradational contacts	Ostracodes, trace
128.5-129.0	Brownish gray 5YR 4/1 ooze Organic matter: 80% Sand: 20%, white, very fine (63-125 microns) Basal has little or no sand grains Gradational contacts	Ostracodes, trace
129.0-130.8	White sandy layer in a Brownish gray 5YR 4/1 ooze Organic matter: 25% Sand: 75%, white, very fine grained (63-177 microns) Gradational upper contact, Abrupt lower contact	Ostracodes, sparse Gastropod, one, small, highly-spiral, 1-mm long
130.8-131.0	medium light gray ooze Organic matter: 20% Sand: 80%, white, very fine grained (63-125 microns) Abrupt upper contact, Gradational lower contact	Ostracodes, sparse
131.0-131.6	Medium light gray ooze Organic matter: 80% Sand: 20%, white, scattered, fine grained (63-177 microns) Gradational contacts	Ostracodes, sparse
131.6-132.0	light gray ooze Organic matter: 80% Sand: 20%, white, scattered, fine grained (63-177 microns) Gradational contacts	Ostracodes, sparse

132.0-133.3	Grayish orange pink 5YR 7/2 ooze Organic matter: 95% Sand: 5%, white, very fine grained (63-88 microns) Gradational contacts	Ostracodes, trace
133.3-135.0	Light brownish gray 5YR 6/1 Organic matter: 40% Sand: 60%, white, scattered, fine to medium grained (63-250 microns) Gradational contacts	Ostracodes, trace
135.0-136.3	Pinkish gray 5YR 8/1 mud Mud: 15% , Sand: 85%, white, fine grained (63-125 microns) Gradational contacts	Ostracodes, sparse; Mytilocypris first appear
136.3-141.6	Very faintly laminated medium light gray sandy mud Mud: 15-20% , Sand: 80-85%, white, fine grained (63-177 microns) Gradational contacts	Ostracodes, sparse, Myt.
141.6-143.7	Olive gray 5Y 3/2 mud Mud: 20% Sand: 80%, white, fine grained (63-177 microns), Tiny black specks of Mn or Fe Gradational upper contact, Abrupt lower contact	Ostracodes, trace
143.7-145.5	White sandy layer in a matrix within an olive gray 5Y 3/2 mud Mud: 10-15% Sand: 85-90%, white, fine grained (63-177 microns) Abrupt contacts	Ostracodes, sparse, Myt.
145.5-147.5	Grayish red purple 5RP 4/2 Mud: 25%, Sand: 75%, white, fine grained (63-177 microns) Abrupt upper contact, Gradational lower contact	Ostracodes, trace
147.5-147.7	Very light gray Mud: 75% Sand: 25%, white, very fine grained (63-88 microns) Gradational contacts	Ostracodes, rare, Myt.
147.7-149.0	Olive gray 5Y 3/2 Mud: 10-15% Sand: 85%-90%, white, very fine grain (63-88 microns), no distinctive white grains Gradational contacts	Ostracodes, trace
149.0-151.0	Pinkish gray 5YR 8/1 Mud: 70% Sand: 30%, very fine grain (63-88 microns) This is the end of the core that was extruded from the ring.	Ostracodes, rare

Description of Core 2

Depth (cm)	Sediment Type	Organic Matter (%)	Mud (%)	Sand (%)	Description	Fossils	Thickness (cm)
Above 0	Dusky red sludge	45	5	50	Loose organic material was cut off and lost from the top of the core. The remaining bits and pieces from the plug and the lid are purple-pink and contain lots of purple sulfur reducing bacteria.	SAMPLED FOR DIATOMS AND AMS	
0-14.0	Dusky red sludge	45	5	50	grayish red purple (5R 3/4); sand is very fine (63-88 microns), structureless, well sorted, gradational boundaries	Ostracodes, common	14
14.0-14.4	White sand	25	5	70	Diffuse band of DRS with slightly higher very fine white carbonate grains; very fine (63-88 microns), structureless, well sorted		0.4
14.4-18.9	Dusky red sludge	45	5	50	grayish red purple (5R 3/4); sand is very fine (63-88 microns), structureless, well sorted, gradational boundaries	Ostracodes, common	4.5
18.9-19.2	White sand	35	5	60	Dusky red sandy sludge; very diffuse band of DRS; very fine sand (63-88 microns), white, carbonate, well sorted	Ostrocodes, common	0.3
19.2-21.0	Dusky red sludge	45	5	50	grayish red purple (5R 3/4); sand is very fine (63-88 microns), structureless, well sorted, gradational boundaries	Ostracodes, common	1.8
21.0-21.3	White sand	35	5	60	Dusky red sandy sludge; very diffuse band of DRS; very fine sand (63-88 microns), white, carbonate, well sorted	Ostracodes, common	0.3
21.3-22.2	Dusky red sludge	45	5	50	grayish red purple (5R 3/4); sand is very fine (63-88 microns), structureless, well sorted, gradational boundaries	Ostracodes, common	0.9
22.2-22.5	White sand	35	5	60	very diffuse band of DRS; very fine grained sand (63-88 microns), white, carbonate, well sorted	Ostracodes, common	0.3
22.5-23.7	Dusky red sludge	45	5	50	grayish red purple (5R 3/4); sand is very fine (63-88 microns), structureless, well sorted, gradational boundaries	Ostracodes, common	1.2
23.7-24.2	White sand	25	5	70	very diffuse band of DRS, very fine grained (63-177 microns), white, carbonate, well sorted	Ostracodes, common	0.5

24.2-25.3	Dusky red sludge	45	5	50	grayish red purple (5R 3/4); sand is very fine (63-88 microns), structureless, well sorted, gradational boundaries	Ostracodes, common	1.1
25.3-25.5	White sand	35	5	60	very diffuse band of DRS, very fine grained (63-177 microns), white, carbonate, well sorted	Ostracodes, common	0.2
25.5-26.6	Dusky red sludge	45	5	50	grayish red purple (5R 3/4); sand is very fine (63-88 microns), structureless, well sorted, gradational boundaries	Ostracodes, common	1.1
26.6-26.8	White sand	25	5	70	Dusky red sandy sludge; very diffuse band of DRS; very fine sand (63-88 microns), white, carbonate, well sorted	Ostracodes, common	0.2
26.8-27.1	Dusky red sludge	45	5	50	grayish red purple (5R 3/4); sand is very fine (63-88 microns), structureless, well sorted, gradational boundaries	Ostracodes, common	0.3
27.1-28.4	Yellowish orange sand	5	5	90	Orangy brown layer; Well-defined band of sandier DRS. Fresh purple red ooze (DRS), grayish red purple (5RP 4/2); very fine to fine (63-177 microns), 80%; fine to medium grained sand, subrounded to rounded, white, carbonate, 8%; medium grained (250-350 microns), well-rounded, carbonate sand, 2%; erosional bottom contact	Ostracodes, abundant	1.3
28.4-32.0	White sand	25	5	70	Sand is 70%, white, very fine to fine grained (63-177 microns), rare black flecks, gradational bottom contact	Ostracodes, abundant; at 31.1 c, diatom collected	3.6
32.0-36.2	White sand	10	5	85	Sand is 85%, very fine (63-88 microns), white, carb grains; rare black flecks, 0.25 mm	Ostracodes, abundant	4.2
36.2-38.5	White sand	25	5	70	Sand is 70%, very fine to fine (63-177 microns), white, carbonate	Ostracodes, common	2.3
38.5-42.8	White sand	15	5	80	Sand is 80%, very fine to fine (63-177 microns), white, carb grains; basal 1 cm is sandiest; rare black specks and rods	Ostracodes, common	4.3
42.8-44.0	Dusky red sludge	45	5	50	DRS	Ostracodes, common	1.2

44.0-45.0	Yellowish gray sludge	30	5	65	Slightly darker and browner DRS than above, gradational upper and lower contacts. A few grains are coated with Fe ox stain and organic matrix is orangier in color that up core; sand is 20% orange coated, very fine to fine (63-177 microns), carbonate grains; 30%, white, very fine to fine (63-177 microns), carbonate grains	Ostracodes, common	1
45.0-45.7	Yellowish orange sand	25	5	70	Gradational upper and lower contacts. A few grains are coated with Fe ox stain and organic matrix is orangier in color up core; sand is 30 % orange-coated, fine to medium grained (177-250 microns), subrounded to rounded; sand is 40%, white, fine to medium grained (177-250 microns), subrounded to rounded		0.7
45.7-48.1	Yellowish gray sludge	45	5	50	Gradational upper and lower contacts. A few grains are coated with Fe ox stain and organic matrix is orangier in color up core; sand is 20 % orange-coated, fine to medium grained (177-250 microns), subrounded to rounded; sand is 30%, white, very fine to fine grained (63-177 microns), subrounded to rounded	Ostracodes, common	2.4
48.1-52.1	Yellowish orange sand	25	5	70	Fresh dark yellowish orange (10YR, 6/6) (DYO); sand is 65% fine to medium grained (177-350 microns), subrounded to well-rounded, orange-coated sand; sand is 5% medium grained (250-350 microns), white; layer contains trace amount of glassy grains, which could be detrital quartz; a few black charred remains of vegetation; coarsening towards 50 cm from top to bottom	Ostracodes, common	4
52.1-58.1	Dusky red sludge	45	5	50	DRS	Ostracodes, sparse	6
58.1-62.0	White sand	20	5	70	sand is 70%, subrounded to well-rounded, white, 177-500 microns; trace amounts of clastic quartz silt; a few scattered charred remains of vegetation; poorly sorted; upper boundary is gradational with coarsening white grains; erosional bottom contact	Ostracodes, sparse	3.9
62.0-64.0	Dusky red sludge	45	5	50	64-64.3 cm: black layer of charred remains of vegetation; abrupt bottom contact marked by blackish red layer		2

64.0-64.5	White sand	15	5	80	Blackish red (5R, 2/2); sand is 80% fine to medium grained (125-350 microns), white, opaque, subangular to well-rounded; trace amounts of clastic quartz silt is present; erosional bottom contact		0.5
64.5-72.8	Yellowish orange sand	10	5	85	Sand is orange-coated, white, carb grains, fine to medium grained (125-250 microns); lower contact abrupt erosional bottom contact		8.3
72.8-75.4	White sand	25	5	70	Grayish red purple (5RP, 4/2); sand is 70%, fine grained (125-177 microns), white, subrounded to rounded; well-sorted; lower contact abrupt		2.6
75.4-77.1	White sand	35	5	60	White layer is pinkish grey (5YR, 8/1); sand is 60%, fine sand (88-177 microns), white, subrounded to well-rounded, well-sorted: a few black charred remains of vegetation are present; lower contact is abrupt		1.7
77.1-80.5	White sand	25	5	70	Grayish red purple (5RP, 4/2); sand is 65%, fine grained (88-177 microns), white, subangular to well-rounded; well-sorted; lower contact abrupt; there is a white layer of subrounded to well-rounded, fine grained (88-177 microns) at 77.6-78.3 cm; sand is 5%, white, medium grained (250-350 microns); subangular to well-rounded; trace amounts of clastic quartz silt is present; lower contact is abrupt	Ostracodes, rare	3.4
80.5-81.3	White sand	10	5	85	White layer (WL) of sand is pinkish grey (5YR, 8/1); organic matter is grayish red purple (5RP, 4/2); the sand is fine grained (88-177 microns), white, well-sorted; a few scattered charred remains of vegetation are present; lower contact is abrupt	Ostracodes, sparse	0.8
81.3-82.6	White sand	25	5	70	Grayish red purple (5RP, 4/2); sand is 70%, fine grained (125-177 microns), white, subrounded to rounded; well-sorted; lower contact abrupt		1.3
82.6-83.3	White sand	5	5	90	White layer (WL) of sand is pinkish grey (5YR, 8/1); organic matter is grayish red purple (5RP, 4/2); the sand is fine grained (88-177 microns), white, well-sorted; lower contact is abrupt		0.7

83.3-84.1	White sand	25	5	70	Grayish red purple (5RP, 4/2); sand is 70%, fine grained (125-177 microns), white, subrounded to rounded; well-sorted; lower contact abrupt	Ostracodes, rare	0.8
84.1-86.3	Purple organic-rich sand	80	5	15	Pale brown "purplish" (5YR, 5/2) organic material; sand is fine grained (88-177 microns), white, well-sorted; a few charred remains of vegetation are present; lower contact is abrupt; lower contact contains coarser grain (88-250 microns) white sand		2.2
86.3-89.0	Yellowish-orange organic-rich sand	45	5	50	Yellowish grey (5Y, 8/1) organic material; sand is 45%, white, fine grained (88-177 microns), subrounded to well-rounded; sand is 5%, white, medium grained (250-350 microns), subangular to well-rounded; abrupt erosional bottom		2.7
89.0-91.7	Purple organic-rich sand	85	5	10	Pale brown "purplish" (5YR, 5/2) organic organic material; sand is 10%, subrounded to well-rounded, fine to medium grained (88-350 microns); a few scattered remains of vegetation are present; gradational coarsening downwards towards bottom contact	Ostracodes, rare	2.7
91.7-92.7	Purple organic-rich sand	70	5	25	Pale brown "purplish" (5YR, 5/2) organic organic material; sand is 10%, subrounded to well-rounded, fine to medium grained (88-350 microns); a few scattered remains of vegetation are present; gradational coarsening downwards towards bottom contact	Ostracodes, abundant	1
92.7-93.4	Yellowish-orange organic-rich sand	70	5	25	Diffuse sandy layer, dark yellowish orange (10YR, 6/6); 2 sands are present; 20%, fine to medium grained white sand (88-250 microns); 10%, medium grained (250-350 microns), orange-coated; subrounded to well-rounded; gradational fining downwards towards bottom contact	ostracodes, white, translucent, common	0.7
93.4-94.4	White sand	25	5	80	pale brown "purplish" (5YR, 5/2); sand is white, very fine grained (63-88 microns), very well sorted; subrounded to well rounded; lower contact is abrupt with appearance of medium coarse grained orange coated sand	Ostracodes, white, translucent, sparse	1

94.4-95.5	Yellowish-orange sand	20	5	75	dark yellowish orange (10YR, 6/6); sand has 2 components; sand is 10% white, fine grained (88-177 microns), subrounded to well rounded; sand is orange coated, medium to coarse grained (200-500 microns); fining downwards; lower contact is abrupt with the appearance of abundant ostracodes	ostracodes, white translucent, common to abundant	1.1
95.5-96.7	White sand	25	5	70	pale brown "purplish" (5YR, 5/2); sand is white, very fine grained (63-88 microns), very well sorted; subrounded to well rounded; lower contact is abrupt with appearance of medium coarse grained orange coated sand	ostracodes, white, translucent, rare	1.2
96.7-97.2	White sand	25	5	70	pale brown "purplish" (5YR, 5/2); sand has 2 components; sand is 60% white, fine grained (63-177 microns), very well sorted; subrounded to well rounded; sand is 10% orange-coated, medium to coarse grained (200-500 microns), subrounded to well-rounded; lower contact is gradational with the appearace of more medium grained orange coated sand	ostracodes, white, translucent, rare	0.5
97.2-99.3	Yellowish-orange organic-rich sand	55	5	40	dark yellowish orange (10YR, 6/6); sand has 2 components; sand is 30% white, fine grained (88-177 microns), subrounded to well rounded; sand is 10% orange coated, medium to coarse grained (200-500 microns); fining downwards; lower contact is gradational with the appearance of more purplish organic material and less orange coated grains	ostracodes, white, translucent, sparse	2.1
99.3-100.8	Purple organic-rich sand	90	5	5	pale brown "purplish" (5YR, 5/2); sand is white, very fine grained (63-88 microns), very well sorted; subrounded to well rounded; lower contact is gradational with the appearace of more medium grained orange coated sand; lower contact is gradual	ostracodes, white, translucent, rare	1.5
100.8-101.7	White sand	30	5	65			0.9

101.7-102.1	White sand	25	5	70	very dusky purple organic material; sand has 2 components; sand is subrounded to rounded, mostly white grains with a few orange coated grains; sand is 60% white carbonate grains, fine-sized (63-250 microns), very well sorted, subrounded to well rounded; sand is 5% orange coated, fine-sized (63-250 microns), rounded to well rounded; fining downwards; lower contact is gradual		0.4
102.1-102.6	White sand	25	5	70	Very dusky purple (5RP, 2/2); sand is white, very fine grained (63-88 microns), well sorted, subrounded to well rounded; gradual bottom contact with the appearce of coarser white grains		0.5
102.6-103.4	Yellowish orange sand	5	5	90	pale yellowish orange (10YR, 8/6); sand has 2 components; sand is 80%, white, fine to medium grained (63-500 microns), well sorted, subrounded to well rounded; sand is 10%, orange coated, fine to medium grained (88-500 microns), well rounded; abupt lower contact		0.8
103.4-104.4	White sand	25	5	70	very dusky purple organic material; sand has 2 components; sand is 65%, white, very fine (63-88 microns); sand is 5%, orange coated, medium grained (250-350 microns), well rounded; gradational towards lower contact with the appearance of coarser white and orange grains		1
104.4-104.7	Yellowish orange sand	25	5	70	very dusky purple organic material (5RP, 2/2) with pale yellowish orange grains (10YR 8/6); sand has 2 components; sand is 50%, white, very well sorted, fine grained (63-177 microns); sand is 20%, orange coated, well sorted, fine to medium grained (88-500 microns), subrounded to well rounded; abrupt lower contact		0.3
104.7-106.1	White sand	30	5	60	gradual change from very dusky purple to grayish purple; sand is white, fine grained (63-88 microns), very well sorted; lower abrupt contact	AMS (105.2-106.3)	1.4

106.1-107.2	White sand	5	5	90	sand is very angular to subangular, fine to medium grained (63-500 microns), poorly sorted; lower abrupt contact	charophyte oogonia, common	1.1
107.2-108.0	White sand	35	5	60	grayish purple (5P, 4/2); sand is white, very fine grained (63-88 microns), well sorted, subrounded to rounded; gradual lower contact		0.8
108.0-108.8	White sand	10	5	85	grayish purple organic material; sand is 55%, white, well sorted, very fine-grained (63-88 microns); gradual lower contact		0.8
108.7-110.1	Purple organic-rich sand	85	5	10	grayish purple (5P, 4/2); sand is white, very fine to fine grained (63-177 microns), well sorted, subrounded to rounded; black charred remains of vegetation; coarsening downwards; gradual lower contact		1.4
110.1-111.7	Purple organic-rich sand	40	5	55	grayish purple (5P, 4/2) organic material; sand is white, fine grained (63-177 microns), well sorted; coarsening downwards; gradual lower contact	spiral blue shells, sparse, Dr. Pedone observed one oogonium	1.6
111.7-112.3	White sand	25	5	70	grayish purple (5P, 4/2) organic material; sand is white, well sorted, fine grained (63-177 microns); fining downwards, lower contact is gradual		0.6
112.3-112.6	White sand	25	5	70	grayish purple (5P, 4/2) organic material; sand is white, well sorted, fine grained (63-177 microns); fining downwards, lower contact is abrupt with the appearance of coarser white grains		0.3
112.6-112.8	White sand	5	5	90	very dusky purple (5P, 2/2) organic material; sand is white, well-sorted, very fine grained to fine grained (63-177 microns); abrupt lower contact		0.2
112.8-113.2	White sand	35	5	60	very dusky purple (5P, 2/2) organic material; sand is white, well-sorted, very fine grained to fine grained (63-177 microns); gradual lower contact		0.4
113.2-114.4	White sand	10	5	85	very dusky purple (5P, 2/2) organic material; sand is white, well-sorted, very fine grained to fine grained (63-177 microns); gradual lower contact		1.2

114.4-115.1	Purple organic-rich sand	90	5	5	very dusky purple (5P, 2/2) organic material; sand is white, well-sorted, very fine grained to fine grained (63-177 microns); gradual lower contact		0.7
115.1-115.7	White sand	25	5	70	very dusky purple (5P, 2/2) organic material; sand is white, well-sorted, fine grained to coarse grained (63-500 microns), subrounded to well rounded; coarsening downwards; gradual lower contact		0.6
115.7-116.2	White sand	5	5	90	very dusky purple (5P, 2/2) organic material; sand is white, well-sorted, very fine grained to fine to medium (63-350 microns); coarsening downwards; gradual lower contact		0.5
116.2-117.1	White sand	25	5	70	very dusky purple (5P, 2/2) organic material; sand is white, well-sorted, fine grained to coarse grained (63-500 microns), subrounded to well rounded; coarsening downwards; gradual lower contact		0.9
117.1-118	White sand	10	5	85	very dusky purple (5P, 2/2) organic material; sand is white, well-sorted, very fine grained to fine to medium (63-350 microns); abrupt lower contact		0.9
118-118.4	White sand	25	5	70	very dusky purple (5P, 2/2) organic material; sand is white, well-sorted, fine grained to coarse grained (63-250 microns), subrounded to well rounded; coarsening downwards; abrupt lower contact with the appearance of orange sandy layer		0.4
118.4-119	Yellowish orange sand	25	5	70	dark yellowish orange (10YR, 6/6); sand has 2 components; sand is 30%, white, well sorted, fine to medium grained (63-250 microns), very angular to subrounded; sand is 40%, orange coated, well sorted, fine to medium grained (125-500 microns); trace amounts of silt size clastic quartz are present; abrupt lower contact	Ostracodes, rare	0.6
119-120.1	White sand	35	5	60	very dusky purple (5P 2/2); sand is white, well sorted, fine grained (63-250 microns); lower contact is gradual and diffuse	ostracodes, sparse, AMS (119.2-119.5)	1.1

120.1-120.6	White sand	25	5	70	very dusky purple (5P, 2/2); sand is white, well sorted, fine grained (63-250 microns); coarsening downwards; gradual lower contact	ostracodes, common	0.5
120.6-121.5	Red sand	25	5	70	red-brown organic material; sand is 70% grains, NFV, fairly abrupt contact, red-brown coated; lower contact is abrupt; **Rare ostracodes in interval between 120.6 and 123.8.**	Ostracodes, rare	0.9
121.5-121.6	Red sand	15	5	80	very dusky purple (5RP 2/2) organic material; sand is for the most part white, with sand grains coated with organic dusky purple material, very fine-grained (63-88 microns) sand; abrupt lower contact		0.1
121.6-121.9	Red sand	25	5	70	very dusky purple (5P 2/2) organic material; sand is for the most part white, with sand grains coated with organic dusky purple material, very fine-grained (63-88 microns) sand; abrupt lower contact	Ostracodes, sparse	0.3
121.9-122.3	White sand	5	5	90	very dusky purple (5P 2/2) organic material; sand is white, very fine-grained (63-88 microns); abrupt lower contact		0.4
122.3-122.5	Red sand	25	5	70	very dusky purple (5P 2/2) organic material; sand is for the most part white, with sand grains coated with organic dusky purple material, very fine-grained (63-88 microns) sand; abrupt lower contact		0.2
122.5-122.8	White sand	5	5	90	very dusky purple (5P 2/2) organic material; sand is white, very fine-grained (88-177 microns); abrupt lower contact		0.3
122.8-122.9	Red sand	25	5	70	very dusky purple (5P 2/2) organic material; sand is for the most part white, with sand grains coated with organic dusky purple material, very fine-grained (63-88 microns) sand; abrupt lower contact		0.1
122.9-123.2	White sand	5	5	90	very dusky purple (5P 2/2) organic material; sand is white, very fine-grained (88-177 microns); abrupt lower contact		0.3

123.2-123.3	Red sand	5	5	90	very dusky purple (5P 2/2) organic material; sand is for the most part white, with sand grains coated with organic dusky purple material, very fine-grained (63-88 microns) sand; abrupt lower contact		0.1
123.3-123.4	White sand	5	5	90	very dusky purple (5P 2/2) organic material; sand is white, very fine-grained (88-177 microns); abrupt lower contact		0.1
123.4-123.5	Red sand	25	5	70	very dusky purple (5P 2/2) organic material; sand is for the most part white, with sand grains coated with organic dusky purple material, very fine-grained (63-88 microns) sand; abrupt lower contact		0.1
123.5-123.8	White sand	25	5	70	Concave layer; Base is sand, trough is filled by slightly less sandy ooze, but more sand than interlaminated material in above sequences, 90% grayish purple 5P 4/2, 10% grayish orange 10YR 7/4, abrupt lower contact	Ostracodes, common	0.3
123.8-124	White sand	35	5	60	very dusky purple (5P, 2/2); sand is white, very fine grained (88-177 microns); abrupt lower contact	Ostracodes, common	0.2
124-126	White sand	25	5	70	10% grayish purple 5P 4/2, 90% grayish orange 10YR 7/4; sand is white, very fine to fine grained (88-177 microns), well sorted, subrounded to rounded; gradual lower contact	Ostracodes, sparse	2
126-127.0	White sand	25	5	70	very dusky purple (5RP, 2/2) organic material; sand is white, very fine grained (63-177 microns); gradual lower contact	Ostracodes, common;	1
127.0-129	White sand	25	5	70	very dusky purple (5P, 2/2) organic material; sand is white, very fine grained (63-177 microns); gradual lower contact	Ostracodes, common;	2
129-131.4	Purple organic-rich sand	60	5	35	very dusky purple (5RP, 2/2) organic material; sand is white, very fine grained (63-177 microns); gradual lower contact	Ostracodes, common	2.4
131.4-133.3	Purple organic-rich sand	45	5	50	very dusky purple (5P, 2/2) organic material; sand is white, very fine grained (63-88 microns); gradual lower contact	Ostracodes, common	1.9

133.3-135	Purple organic-rich sand	45	5	50	very dusky purple (5P, 2/2) with some pale yellowish brown (10YR, 6/2) organic material; sand is white, very fine grained (63-88 microns); gradual lower contact		1.7
135-143.1	Yellowish-orange organic-rich sand	65	5	30	pale yellowish brown (10YR, 6/2) organic material; sand is white, very fine grained (63-88 microns); gradual lower contact	Ostracodes, common	8.1
143.1-143.2	Purple organic-rich sand	45	5	50	brownish gray (5YR, 4/1) organic material; sand is white, very fine grained (63-88 microns); abrupt lower contact		0.1
143.2-144.7	Red sand	35	5	60	light brownish gray (5YR, 6/1) organic material; sand is white with very dusky purple coating, very fine grained (63-88 microns); gradual lower contact	Ostracodes, common; SAMPLED FOR AMS	1.5
144.7-145.3	Red sand	10	5	85	grayish orange (10YR, 7/4) organic material; sand is white with very dusky purple coating, very fine grained (63-88 microns); gradual lower contact		0.6
145.3-150.3	Red sand	5	5	90	Pale yellowish brown (10YR, 6/2) organic material; sand is white with very dusky purple coating, very fine grained (63-88 microns); gradual lower contact; The irregular, streaky lamination is visible by color changes that vary from medium brown, light brown, and pinkish brown. Some of the boundaries are shallow, concave downward and some shallow convex upward.	Ostracodes, some articulated	5
150.3-150.7	Reddish-brown organic-rich sand	40	5	55	Pale yellowish brown (10YR 6/2) organic material; sand is white with very dusky purple coating, very fine grained (63-88 microns); gradual lower contact; projected base of trough is 151.4		0.4
150.7-152.0	Reddish-brown organic-rich sand	90	5	5	Light brown (pale yellowish brown 10YR 6/2) with flat base and concave top; minor very fine sand		1.3

152.0-152.1	Reddish-brown organic-rich sand	90	5	5	Lenticular streak of brown ooze (pale yellowish brown 10YR 6/2) that goes only 25% across the core		0.1
152.1-152.5	Red sand	20	5	75	pale yellowish brown (10YR 6/2); sand is very fine sand (63-88 microns), white, subrounded to rounded, well sorted; gradual lower contact		0.4
152.5-153.5	Reddish-brown organic-rich sand	90	5	5	Trough-shaped light brown-red organic; minor vf sand; abrupt lower contact		1
153.5-154.4	Pink organic-rich sand	90	5	5	silty with minor vf sand, abrupt upper and lower. Irregular thickness because of overlying trough, but also base slopes slightly to side opposite tape, where layer is 2 cm thick		0.9
154.2-155.2	Reddish-brown organic-rich sand	70	5	25	Wavy layer of light brown mud (5YR, 8/1); minor vf sand, abrupt lower contact		1
155.2-156.9	Pink organic-rich sand	90	5	5	pink organic material (5YR, 8/1); abrupt lower contact; Irregular thickness, wavy. Min thickness 0.8 cm		1.7
156.9-158.1	Reddish-brown organic-rich sand	90	5	5	Light brown organic material, silty with minor vf sand, abrupt upper and lower. The left side of the core is disrupted by core cutting. Not sure if layer is continuouos across; abrupt lower contact		1.2
158.1-159.4	Reddish-brown organic-rich sand	90	5	5	Variegated band, with medium brown 2-mm thick top and base and interior that varies from pink to red-brown. The left side has streaks that pinch out to the right that are pink. silty with minor vf sand, abrupt lower contact		1.3

159.4-159.5	Reddish-brown organic-rich sand	90	5	5	Red-brown ooze, silty with minor vf sand, NVF, abrupt upper and lower.		0.1
159.5-161.0	Red sand	20	5	75	5YR 8/1; sand is white with very dusky purple organic coating, very fine (63-88 microns); abrupt upper and lower. The center of this layer is cut out by a trough of laminated sed that is brown-red-pink at base (0.5 cm), light brown in center (0.2 cm) and brown-red-pink on top (0.8).		1.5
161.0-161.1	Reddish-brown organic-rich sand	90	5	5	light brown ooze, silty with minor vf sand, abrupt lower and upper.		0.1
161.1-162.2	Red sand	25	5	70	red-pink organic material (5YR, 8/1); sand is white, very fine (63-88 microns), white		1.1
162.2-162.5	Reddish-brown organic-rich sand	90	5	5	light brown ooze, silty with minor vf sand, abrupt lower and upper.		0.3
162.5-163.7	Red sand	25	5	70	Red-pink (5YR, 8/1) organic material; sand is 70%, white with stains of red-pink organic material, very fine (63-88 microns)		1.2
163.7-164.0	Reddish-brown organic-rich sand	95	5?	0	Convex upward medium brown ooze.	Sampled for AMS	0.3
164.0-165.0	Red sand	25	5	70	Red-pink (5YR, 8/1) organic material; sand is 70%, white with stains of red-pink organic material, very fine (63-88 microns); abrupt upper and lower. The center of this layer is cut out by a trough of laminated sed that is slightly sandy brown-red-pink ooze at base (0.4 cm), and dark red-pink dense ooze on top (0.5)		1

165.0-165.1	Pink organic-rich sand	90	5	5	light brown ooze, dense; minor vf sand, abrupt lower and upper.		0.1
165.1-165.3	Pink organic-rich sand	90	5	5	Red-pink (5YR, 8/1) organic material; trough-shaped, max thickness 0.7 cm, width thinner than other trough beds		0.2
165.3-166.1	Pink organic layer	90	5	5	Pink ooze (5YR, 8/1), trough-shaped, parallel to above layer		0.8
166.1-167.0	Red-brownish organic layer	90	5	5	light brown organic material; minor vf sand, abrupt lower and upper contacts		0.9
167.0-167.8	Red sand	25	5	70	Red-pink (5YR, 8/1) organic material; sand is 70%, white with stains of red-pink organic material, very fine (63-88 microns); Sandy brown layer, pinches out against micro-column of pink		0.8
167.8-168.5	Red sand	25	5	70	Red-pink (5YR, 8/1) organic material; sand is 70%, white with stains of red-pink organic material, very fine (63-88 microns); develops into micro-column near center,with max thickness of 2.3 cm; it also has a slightly concave base that truncates the thin layer below		0.7
168.5-169.2	Pink organic-rich sand	90	5	5	Pink brown organic material (5YR, 8/1), truncated in middle by overlying layer, wavy base because of underlying convex up layer		0.7
169.2-170.8	Red sand	10	5	85	Red-pink (5YR, 8/1) organic material; sand is white with stains of red-pink organic material, very fine (63-88 microns); Nearly flat base, but small upward bulge. Max thickness 1.4 cm.	Ostracodes, rare	1.6
170.4-171.4	Red sand	25	5	70	Red-pink (5YR, 8/1) organic material; sand is 70%, white with stains of red-pink organic material, very fine (63-88 microns)		1

171.4-172.4	Reddish-brown organic-rich sand	90	5	5	light brown organic material; minor vf sand, abrupt lower and upper contacts	Ostracodes, rare	1
172.4-172.6	White sand	25	5	70	Light brown sand, silt and very fine sand, scoop-shaped, lines the bottom of a deep trough that goes across the core (base in parentheses); sand is white, very fine (63-88 microns), whiteThe trough is filled by horizontally laminated sed: 0.7 cm dense pink brown ooze, overlain by 0.3 cm light brown sand, overlain by 0.3 cm dense pink brown ooze. All with abrupt boundaries.	Ostracodes, rare	0.2
172.6-174.4	Reddish-brown organic-rich sand	90	5	5	light brown organic material; minor vf sand, abrupt lower and upper contacts; Flat base, middle truncated by overlying.		1.8
174.4-174.8	Reddish-brown organic-rich sand	90	5	5	light brown organic material; minor vf sand, abrupt lower and upper contacts		0.4
174.8-175.1	Reddish-brown organic-rich sand	70	5	25	Very light brown organic material; flat; abrupt contacts		0.3
175.1-176.5	Reddish-brown organic-rich sand	90	5	5	light brown organic material; minor vf sand, abrupt lower and upper contacts; trough shaped; rare broken ostracodes along lower contact	Ostracodes, rare	1.4
176.5-177.6	Reddish-brown organic-rich sand	90	5	5	Medium brown dense organic material, slightly scoop shaped, center eroded by overlying layer; abrupt contacts		1.1

177.6-179.0	Pink organic-rich sand	75	5	20	Pinch-and-swell layer over bulge of lower layer. Min thickness of 1.0 cm. Variegated medium and light brown ooze, slightly sandy; Sand: 20%, white, silt and very fine (63-88 microns), white; abrupt lower contact		1.4
179.0-179.2	Reddish-brown organic-rich sand	45	5	50	Lenticular layer, with max thickness of 1.5 cm. (bulges up and down in center) Variated very light and light brown dense ooze; gradual lower contact	Ostracodes, rare; SAMPLED FOR DIATOMS. Very organic-rich from diatom processing.	0.2
179.2-180.0	Reddish-brown organic-rich sand	70	5	25	Scoop-shaped dark brown dense ooze, truncates layer below in center. No sand, NVF. Grad upper, abrupt lower. Very organic-rich from diatom processing.	SAMPLED FOR DIATOMS AND AMS.	0.8
180.0-180.4	Reddish-brown organic-rich sand	75	5	20	Very slightly concave, partly truncated by overlying layer; sand is white, silt and very fine (63-88 microns), white; abrupt contacts	Ostracodes, rare	0.4
180.4-181.2 (181.5)	Reddish-brown organic-rich sand	65	5	30	Wedge-shaped light brown ooze, about 2 cm long; sand is white, silt and very fine (63-88 microns); abrupt contacts		0.8
181.2-182.3 (182.5)	Red sand	20	5	75	pink brown; sand is white with stains of pinkish brown, silt and very fine (63-88 microns); abrupt contacts	Either ostracode or tiny flat spiraled gastropod?	1.1
182.3-182.7	Reddish-brown organic-rich sand	45	5	50	Multiple lenses of dark brown ooze lenses fill in bumpy, underlying topography; sand is white, silt and very fine (63-88 microns), white; abrupt contacts	Ostracodes, rare	0.4
182.7-183.4 (184.4)	Reddish-brown organic-rich sand	70	5	25	Medium red brown organic material; gradual with overlying, irregular contact. Flat base; abrupt lower contact		0.7

183.4-183.7 (183.8)	Red sand	25	5	70	Sandy medium dark red brown ooze, irregular, convex, bumpy top, possibly micro-columns. Max thickness of 2.1 cm; sand is white with dark red brown stains,very fine (63-88 microns), gradual lower contact	Ostracodes, rare	0.3
183.7-185.9	Red sand	25	5	70	Sandy dark brown organic material; sand is very fine sand (63-88 microns); abrupt lower contact		2.2
185.9-186.7	Reddish-brown organic-rich sand	90	5	5	medium red brown organic material; gradual with overlying, irregular contact. Flat base; base is bottom of core	SAMPLED FOR DIATOMS AND AMS	0.8

APPENDIX B

Images of Core 1 taken four days after core was opened.
The measuring tape is in centimeters.

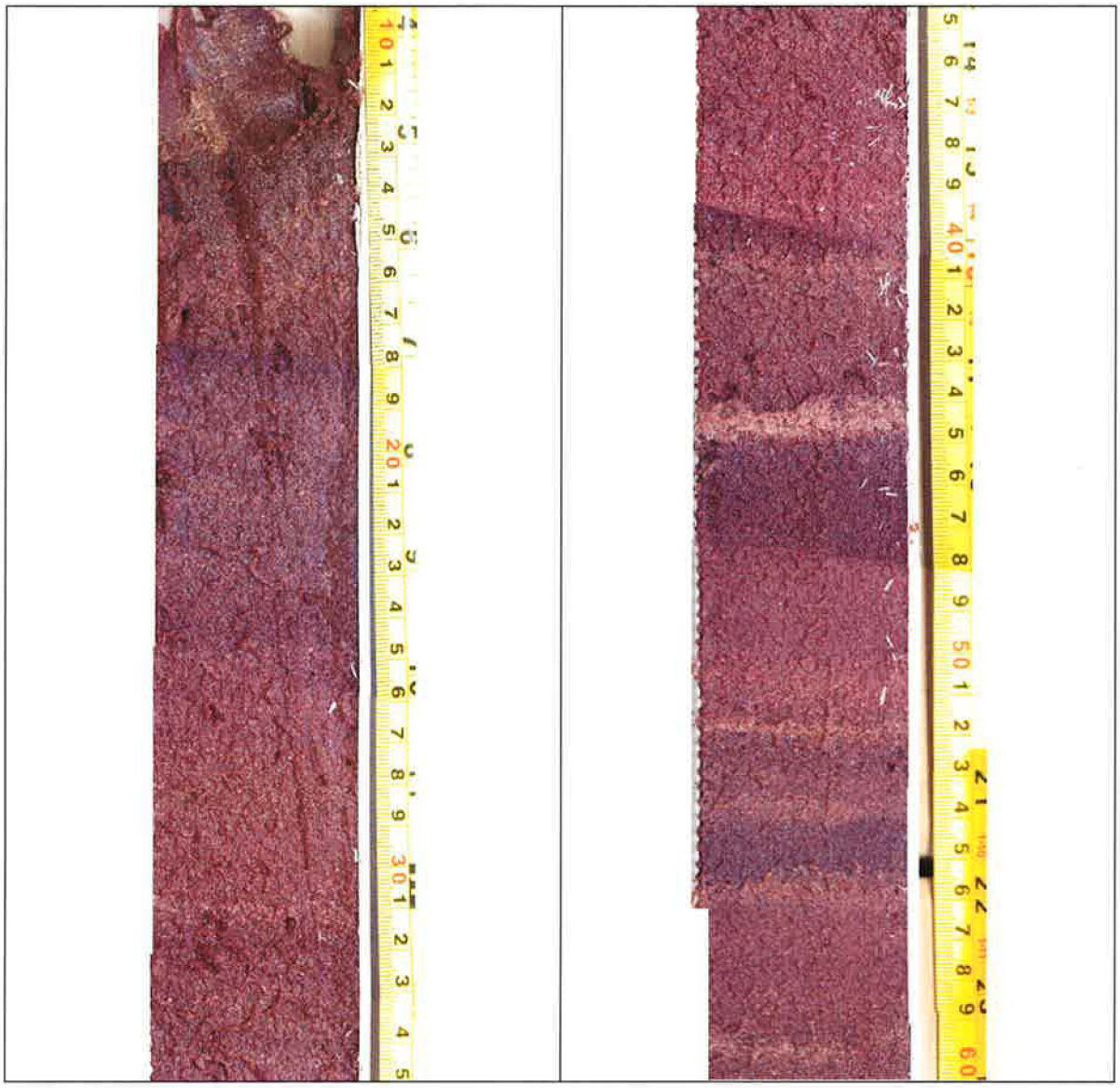

Images of core 1, continued

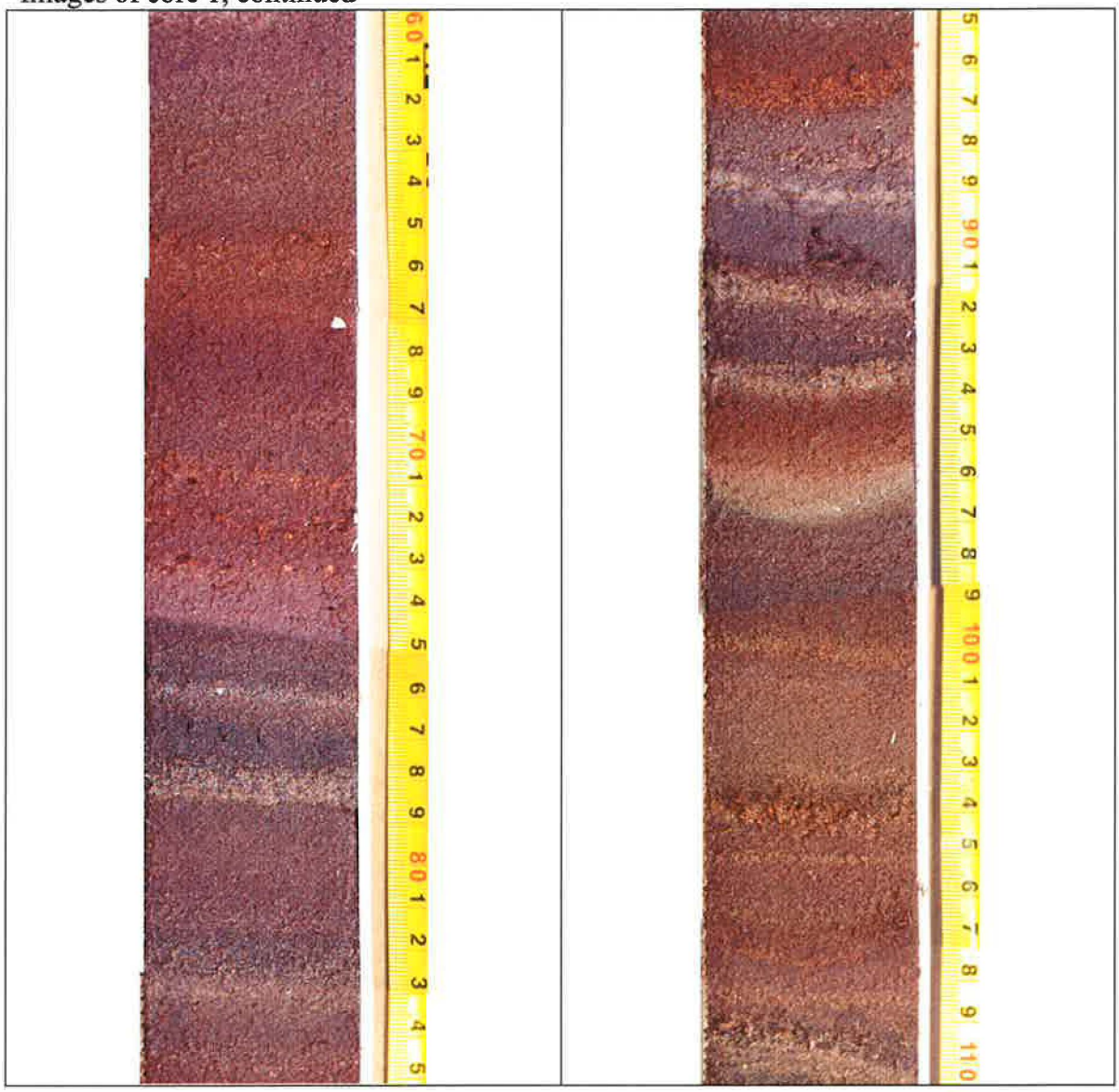

Images of core 1, continued

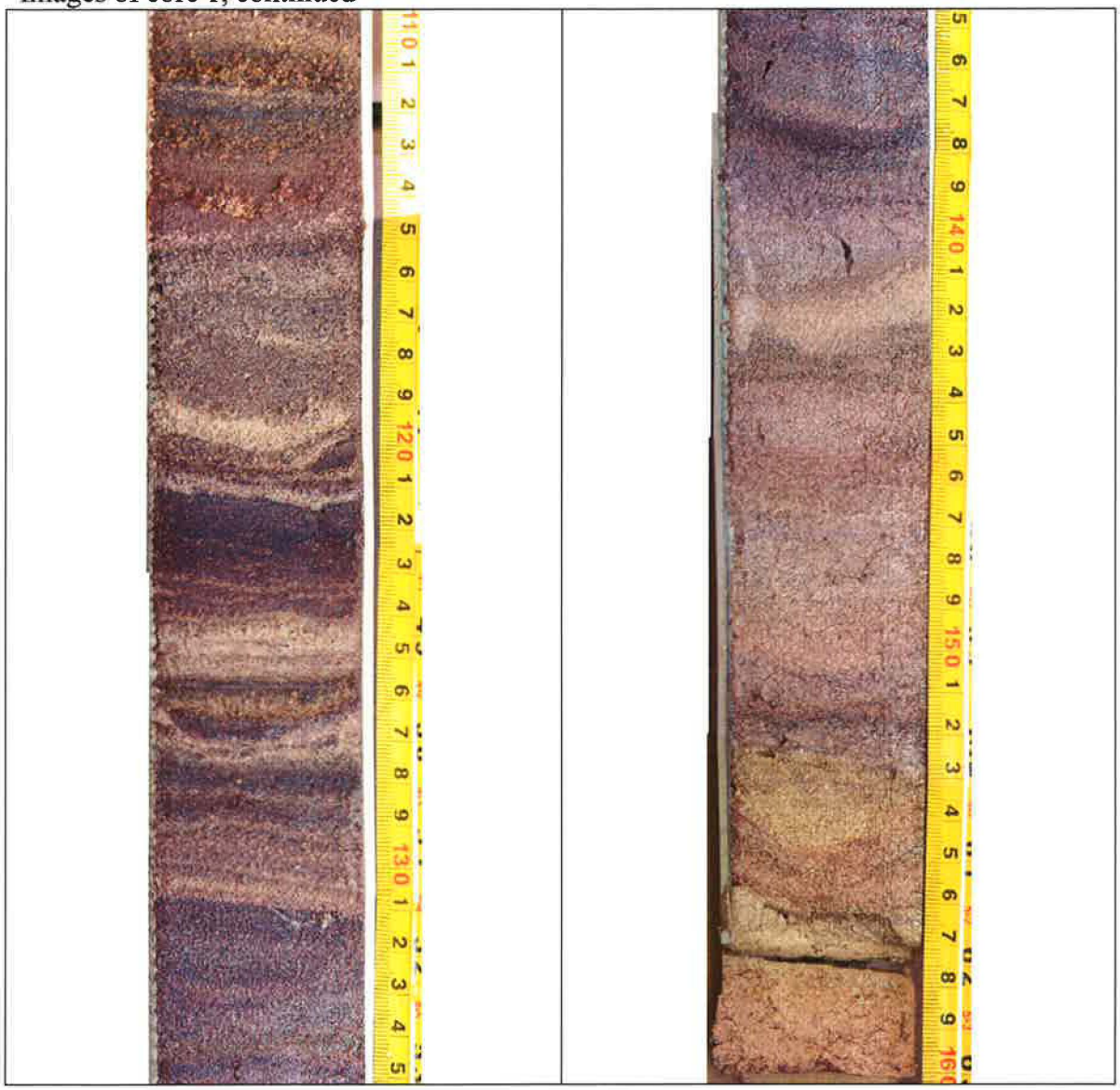

Images of Core 2 taken four days after core was opened.
The measuring tape is in centimeters.

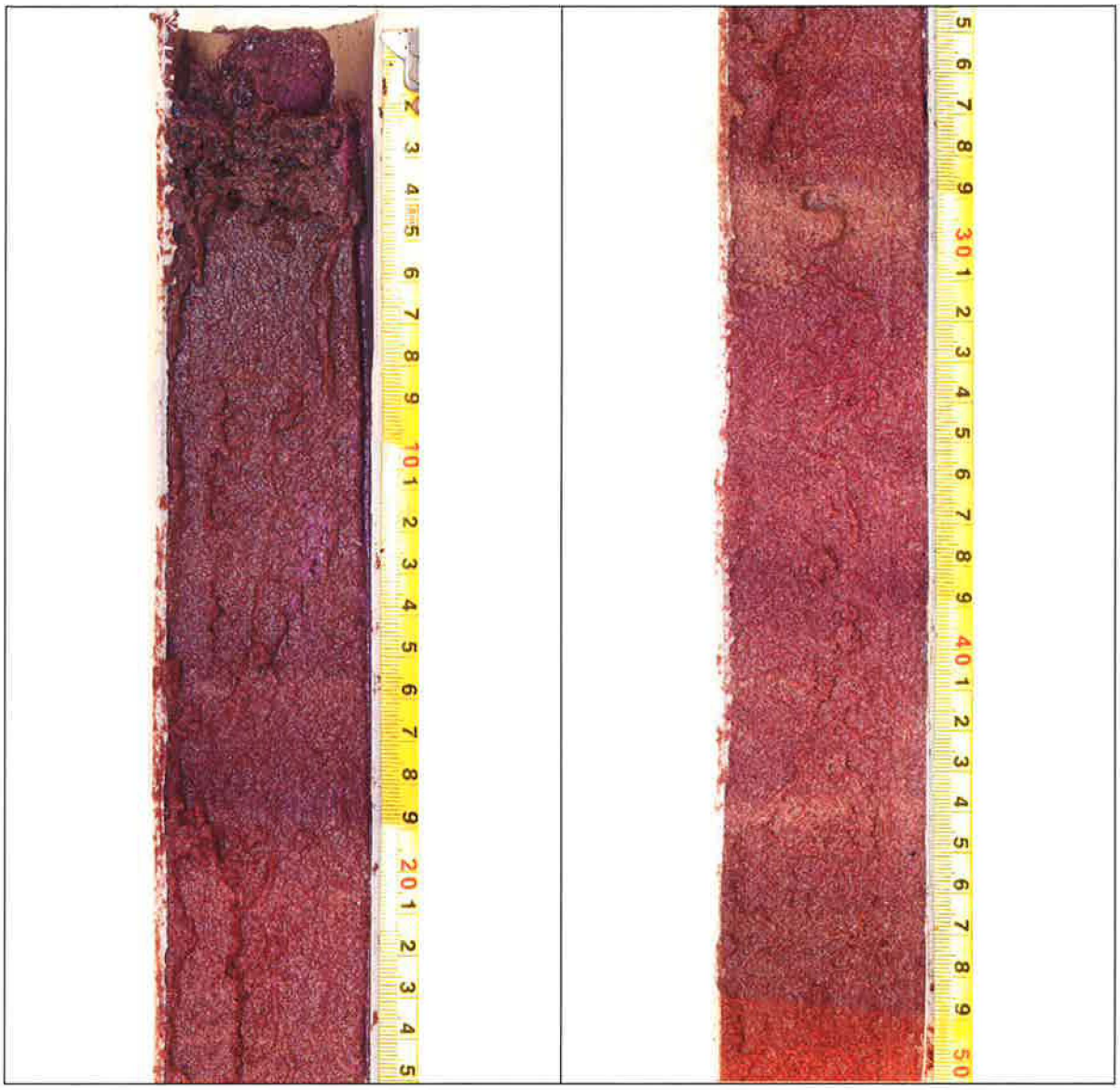

Images of core 2, continued

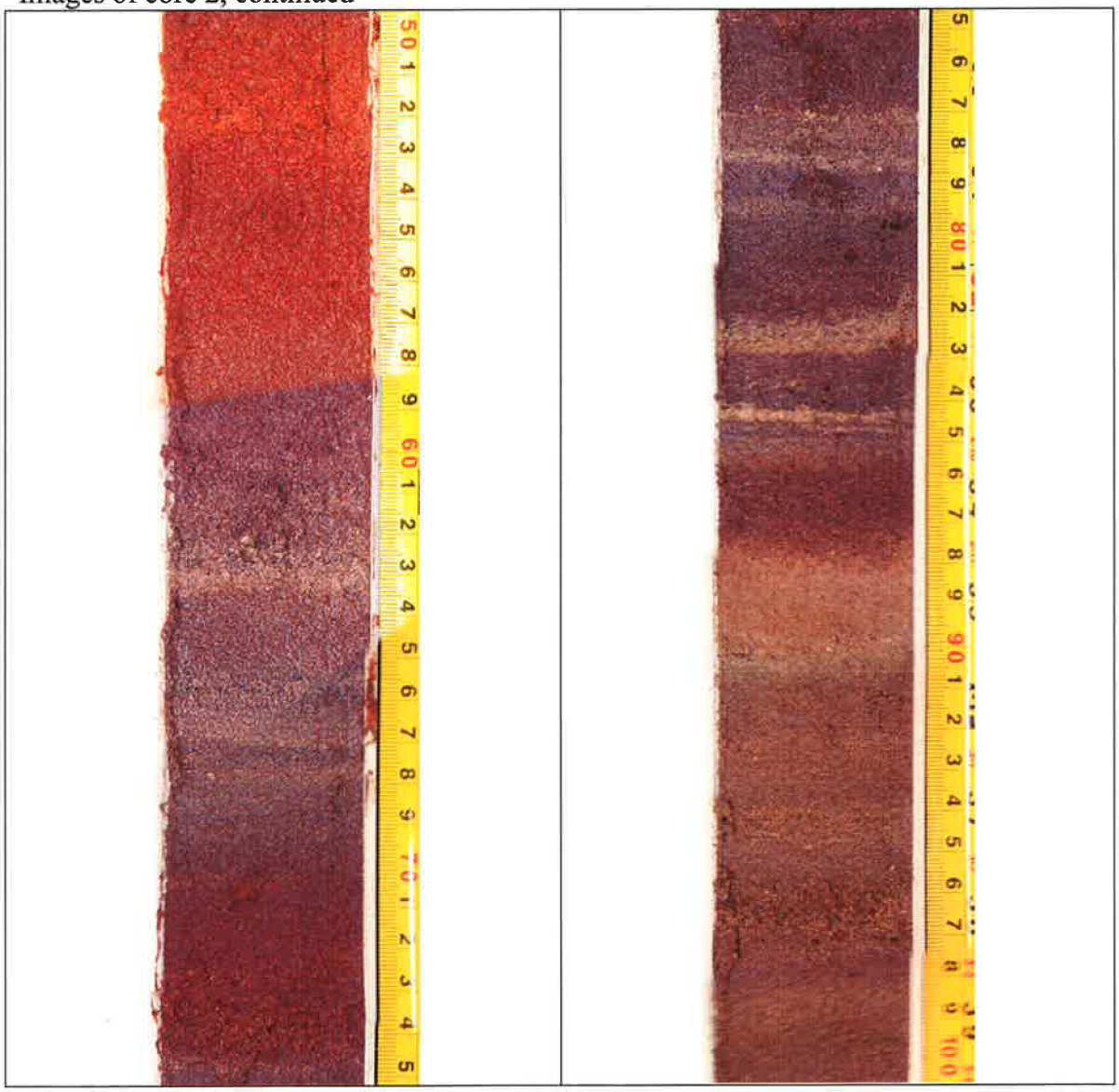

Images of core 2, continued

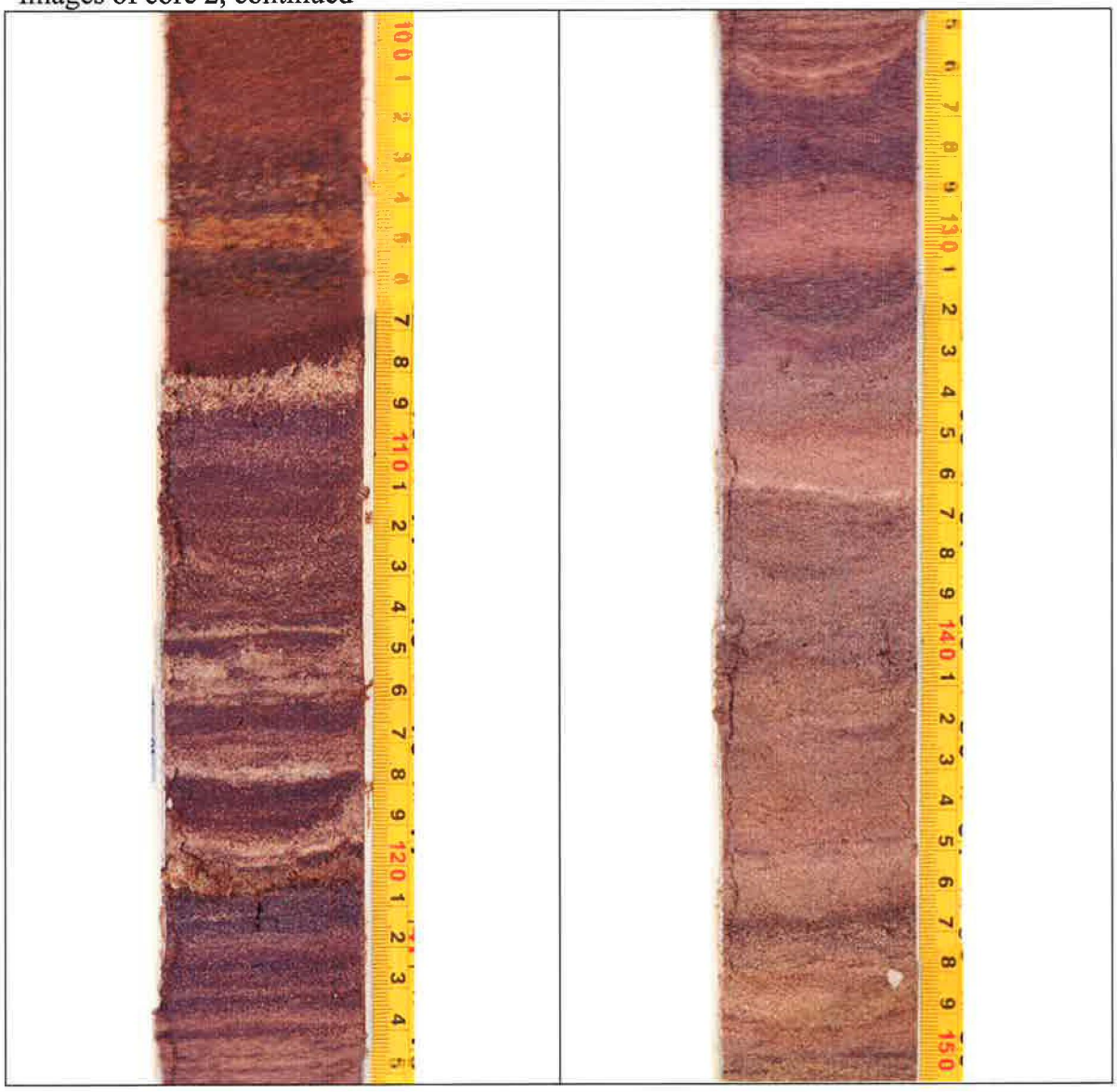

Images of core 2, continued

APPENDIX C

Observations from Smear Slides using Transmitted-, Polarized-, and Reflected-light Microscopy

CORE 1

Depth (cm)	Description	Fossils
0	Organic and mud: brownish reddish Sand: light pink to light orange carb grains; Silt aggregates bound by organics	Ostracodes: Cyprideis australiensis Diatoms: Navicula (only one found)
4	Organic and mud: brownish reddish Sand: light pink to light orange carb grains; Silt aggregates bound by organics	Ostracodes: Cyprideis australiensis Diatoms – common, two species; Navicula, rare
4.5	Organic and mud: brownish reddish Sand: light pink to light orange carb grains; Silt aggregates bound by organics	Ostracodes: Cyprideis australiensis Diatoms – abundant, various species, climax of abundance
5	Organic and mud: brownish reddish Sand: light pink to light orange carb grains; Silt aggregates bound by organics	Ostracodes: Cyprideis australiensis Diatoms: Navicula (only one found)
10	Organic and mud: brownish reddish Sand: light pink to light orange carb grains; Silt aggregates bound by organics	Ostracodes: Cyprideis australiensis Diatoms: Navicula (only two found)
35	Organic and mud: brownish reddish, very little Sand: light pink to light orange carb grains; Silt aggregates bound by organics Endogenic carbonate growing around organics	Ostracodes: Cyprideis australiensis
56.5	Organic and mud: brownish reddish Sand: light pink to light orange carb grains; Silt aggregates bound by organics Endogenic carbonate growing around organics	Ostracodes: Cyprideis australiensis
67	Organic and mud: brownish reddish, very little Sand: light pink to light orange carb grains; Silt aggregates bound by organics Endogenic carbonate growing around organics	No ostracodes
68.5	Organic and mud: brownish reddish Sand: white carb grains; Silt aggregates bound by organics	Ostracodes: Cyprideis australiensis
79	Organic and mud: brownish reddish, very little Sand: light pink to light orange carb grains; Silt aggregates bound by organics Endogenic carbonate growing around organics	Ostracodes: Cyprideis australiensis
82.5	Organic and mud: brownish reddish Sand: white carb grains; Silt aggregates bound by organics Endogenic carbonate growing around organics	Ostracodes: Cyprideis australiensis
84.5	Organic and mud: brownish reddish, very little Sand: pink, white, orange carb grains; Silt aggregates bound by organics Endogenic carbonate growing around organics	Ostracodes: Cyprideis australiensis

85.5	Organic and mud: brownish reddish, very little Sand: pink, white, orange carb grains; Silt aggregates bound by organics Endogenic carbonate growing around organics One charred fragment of vegetation	Ostracodes: Cyprideis australiensis
87	Organic and mud: brownish reddish, orange Sand: pink, white, orange carb grains; Silt aggregates bound by organics Endogenic carbonate growing around organics	Ostracodes: Cyprideis australiensis, fragmented Shell fragment of mollusk with fungal borings Sponge spicule
91	Organic and mud: brownish reddish, orange Sand: pink and white carb grains; Silt aggregates bound by organics Endogenic carbonate growing around organics	No ostracodes
95	Organic and mud: brownish reddish, orange Sand: pink and white carb grains; Silt aggregates bound by organics Endogenic carbonate growing around organics	Ostracodes: Cyprideis australiensis
102	Organic and mud: brownish reddish Sand: white carb grains; Silt aggregates bound by organics Endogenic carbonate growing around organics	No ostracodes
105.5	Organic and mud: brownish reddish Sand: white carb grains; Silt aggregates bound by organics Endogenic carbonate growing around organics	No ostracodes
106	Organic and mud: transparent, white, brownish Sand: white carb grains; Silt aggregates bound by organics Endogenic carbonate growing around organics	No ostracodes
106.5	Organic and mud: transparent, white, brownish Sand: white carb grains; Silt aggregates bound by organics Endogenic carbonate growing around organics	No ostracodes
107	Organic and mud: transparent, white, brownish Sand: white carb grains; Silt aggregates bound by organics Endogenic carbonate growing around organics	Charophyte oogonia (1)
110.5	Organic and mud: pinkish brown, very little Sand: white carb grains; Silt aggregates bound by organics Endogenic carbonate growing around organics	Sponge spicules
117.2	Organic and mud: pinkish brown, very little Sand: white carb grains; Silt aggregates bound by organics Endogenic carbonate growing around organics	No ostracodes
132.5	Organic and mud: reddish brown, mostly Sand: white carb grains; Silt aggregates bound by organics Endogenic carbonate growing around organics	Sponge spicule

CORE 2

Depth (cm)	Sediment Type	Organic (%)	Mud (%)	Sand (%)	Description	Fossils
0	Dusky red sludge	75	5	20	Organic and mud: brownish orange blobs, could also contain Fe-O; sand is light pink to light orange carb grains; most are aggregates bound by organics; some occur in circles stuck together	Ostracodes - articulated
2.5	Dusky red sludge	65	5	30	Organic and mud: brownish red blobs; sand is light pink to light orange carb grains; most are aggregates bound by organics	Ostracodes – fragments; Diatoms – abundant, various species
3.5	Dusky red sludge	30	5	65	Organic and mud: brownish red blobs; sand is white, light pink, most are bound up in organics; subangular to well-rounded, most are bounded up in organics	Ostracodes – articulated; Diatoms – abundant, various species
4	Dusky red sludge	70	5	25	Organic and mud: brownish red blobs; sand is white, light pink, carb grains	Ostracodes – articulated; Diatoms – abundant, various species
5	Dusky red sludge	80	5	15	Organic and mud: brownish orange blobs, could also contain Fe-O; Sand grains are aggregates bounded together by organics	Ostracodes – articulated; Diatoms – abundant, various species, climax of abundance
5.5	Dusky red sludge	70	5	25	Organic and mud: brownish red blobs; sand is white, light pink, carb grains	Diatoms - sparse
6.5	Dusky red sludge	60	5	35	Organic and mud: brownish red blobs; sand: white, light pink, carb grains	Diatoms – rare
7.5	Dusky red sludge	60	5	35	Organic and mud: brownish red blobs; sand is white, light pink, carb grains	Diatoms – rare
8.5	Dusky red sludge	60	5	35	Organic and mud: brownish red blobs; Sand: white, light pink, carb grains	Diatoms – rare
9.5	Dusky red sludge	60	10	30	Organic and mud: brownish red blobs; Sand: white, light pink, carb grains	Ostracodes – articulated; No diatoms
10	Dusky red sludge	25	5	70	Organic and mud: light brown to pink blobs; Sand is pink to light orange, angular, aggregates bounded by organics; Some black charred vegetation	Ostracodes – articulated

15	Dusky red sludge	70	5	25	Organic and mud: light brown to pink blobs; Sand: pink, anhedral, carb grains, aggregates bounded by organics	Ostracodes – articulated
20	Dusky red sludge	80	5	15	Organic and mud: light brown, dark brownish red; sand is fine, pink, subangular to well-rounded	Ostracodes – articulated
27	Dusky red sludge	25	5	70	Organic and mud: light brown, dark brownish red; Sand: medium, pink, subangular to very well-rounded independent grains, some bounded by organics	Ostracodes – articulated
32	Dusky red sludge	60	5	35	Organic and mud: light brown to reddish brown; sand: very fine, pink, subangular to subrounded, some bounded by organics	Ostracodes – articulated
35	Dusky red sludge	60	5	35	Organic and mud: dark reddish brown; Sand: vf, subangular to subrounded, pink, some bounded by organics	Ostracodes – articulated, well-defined boundaries
40	Dusky red sludge	60	5	35	Organic and mud: more bright red; sand is vf, pink, subangular to subrounded, some bounded by organics	Ostracodes – articulated
45	Yellowish gray sludge	30	5	65	Organic and mud: light brown and red; Silt: clastics, transparent, trace amounts; Sand: fine to medium grained, subangular to subrounded, pink, some bounded by organics; Some black charred pieces of vegetation	Ostracodes – articulated for the most part, some fragments
50	Yellowish orange sand	10	5	85	Organic and mud: reddish, trace amounts; Sand: medium, orange, some contain organic on the edges of grains; strands of organics present	
55	Dusky red sludge	40	5	55	Organic and mud: light brown, red; Sand: fine to medium, subangular to well-rounded, orange, some coated with light brown, some bounded with light brown and red organics	Ostracodes – articulated
60	Dusky red sludge	50	5	45	Organic and mud: reddish brown blobs; Sand: vf to fine grained, pink, subrounded to well rounded, bounded by	

					organic; Charcoal	
64	Dusky red sludge	50	5	45	Organic and mud: reddish brown fragments; Sand: pink, bounded by organics	Ostracodes – articulated; Fragment of jacks found on 80cm slide
70	Yellowish orange sand	10	5	85	Organic and mud: brownish red; sand: orange coated, medium, independent for the most part, some bounded by organics; Charcoal piece	Ostracodes - fragments
75	Purple muddy sand	60	5	35	Organic and mud: reddish brown; Sand: vf to fine, yellow, subangular to rounded, some bounded by organics	Ostracodes - fragments
80	Purple muddy sand	80	5	15	Organic and mud: reddish brown; Sand: component #1: transparent, clastic, vf-f,; component #2: vf, subangular to well-rounded, yellow to orange coated, some bounded by organics	Sponge spicule
81	White sand	10	5	85	Same as 80 cm	Bivalve mollusk shell fragment; Sponge spicules
85	Purple muddy sand	80	5	15	Organic and mud: reddish brown Silt: component #1: pink, some bound by organics; component #2: transparent, very angular to subrounded	Ostracodes – articulated
90	Purple muddy sand	90	5	5	Organic and mud: light reddish brown; Sand: pink, white, light orange, vf, pink, white, subrounded to well-rounded some bound by organics; silt is transparent, clastic, trace	Ostracodes – fragmented; Shell fragment from a mollusk with fungal borings
95	Yellowish orange mud	40	5	55	Organic: reddish brown; Sand: fine to medium, yellowish pink, subangular to well-rounded, some are bound by organics; silt is transparent, clastic, trace	Ostracodes – fragmented and articulated
100	Purple muddy sand	90	5	5	Organic: reddish brown; sand: light yellow and light pink, fine to medium, subangular to well-rounded; ; silt is transparent, clastic, trace	Ostracodes – fragmented and articulated Small coiled "shell"
105	Purple muddy sand	90	5	5	Organic: reddish brown; Silt: transparent, clastic, trace; Sand: subangular to well-rounded, pinkish orange, fine	Ostracodes: fragmented

106.5 (labeled as 107b)	White sand	5	5	90	----------	Charophyte oogonia: 800 microns in length and 500 microns in width
107	White sand	5	5	90	Organic: reddish brown; Silt: trace amounts, clastic, transparent; Sand: subrounded, carb grains, brownish	Charophyte oogonia
110	Purple muddy sand	85	5	10	Organic: reddish brown; Silt: clastic, transparent, trace; Sand: white to pink, subrounded to well rounded, fine to medium, some are bounded by organics	
114	White sand	10	5	85	Organic: dark reddish brown; Silt: clastic, trace, most are bound up in the organics; Sand: white, pinkish white, subangular to subrounded, fine to medium	Fragments of shells
115	Purple muddy sand	90	5	5	Organic: reddish brown, sparse; Silt: trace, clastic, transparent; Sand: subrounded to well rounded, light pink, fine to medium, some are bounded by organics	
118	White sand	10	5	85	Organic: reddish brown, sparse; Silt: trace, clastic, transparent; Sand: subrounded to well rounded, light pink, fine to medium, some are bounded by organics	Ostracodes – articulated
120	Purple muddy sand	70	5	25	Organic: brownish red, sparse; Sand: f to medium, pinkish orange, subrounded to well-rounded; silt is transparent, clastic, trace	Ostracodes – articulated and fragmented
125	White sand/PMS???	10	5	85	Organic: brownish red, sparse; Sand: f to medium, pinkish orange, subrounded to well-rounded; silt is transparent, clastic, trace	Ostracodes – articulated and fragments
130	Purple muddy sand	40	5	55	Organic: yellowish brown to reddish brown; Silt: trace, transparent, clastics; Sand: fine to medium; component #1: transparent; component #2: light yellow to pink, subangular to subrounded, carb grains	Fossil fragment with organic streaks

135	Purple muddy sand	60	5	35	Organic: yellowish brown; Silt: trace, transparent, clastics; Sand: light pink, carb grains, subangular to well-rounded	Fossil angular fragment, thin shelled invertebrate
140	Yellowish orange organic-rich sand	60	10	30	Organic: yellowish brown; Silt: trace, transparent, clastics; Sand is most bounded by organics; component #1: vf, transparent, clastic; component #2: vf-fine, light yellow to pink, subangular to subrounded	Ostracodes: articulated and fragmented
145	Red sand	10	5	85	Organic: yellow; Silt: transparent, clastics; sand: vf, pink, light yellow, most bounded by organics	
150	Red sand	5	5	90	Organic: yellow and transparent; Sand: vf, subrounded to well-rounded, yellow to light pink	
155	Reddish-brown organic-rich sand	70	5	25	Organic: light brown and white; Silt: trace, clastic, most are bounded by organics; Sand: vf-fine, light pink, subangular to subrounded	
160	Red sand	10	5	85	Organic: light and white; Silt: transparent, bounded by organics, trace; Sand: vf-fine, light pink, some are bounded by organics	Diatoms: sparse, whole and fragments
165	Red sand	10	5	85	Organic: reddish brown; Silt: clastic, trace, bounded by organics; Sand: vf-fine, light pink, subrounded, bounded by organics	
170	Red sand	10	5	85	Organic: reddish brown and white; Silt: bounded by organics, trace, clastic; Sand: bounded by organics, vf-fine, light pink, subangular to subrounded	Diatoms: rare, whole and fragments
175	Brownish-red mud	70	5	25	Organic: light brown, yellow, white, and transparent; Silt: transparent, clastics	
179	Pink mud	80	5	15	Organic: yellow, white, transparent	Ostracodes: fragment, rare; Diatoms: fragment, rare, 15 μm width, 50 μm length, Anomoeoneis

180	Red-brownish mud	70	5	25	Organic and mud: yellowish brown, white; Silt: trace, clastic; mud: #1: 15-45 micron diameter endogenic transparent carbonates; component #2: transparent clastics, trace	Ostracodes: fragment, rare; Mollusk: fragment, rare
180.5	Red-brownish mud	70	5	25	Organic: yellow, white; mud: 20 micron diameter endogenic yellow carbonates	Ostracodes: fragment, rare
181	Red-brownish mud	70	5	25	Organic: yellow, white; mud: 10-30 micron diameter endogenic yellow carbonates	Diatoms: whole, rare, Anomoeoneis; Fragment of something: brown n transmitted light, white in reflected light
183	Red-brownish mud	70	5	25	Organic: brownish red, yellow; Silt: trace, bound by organics, clastics, transparent	

Appendix D -- Bleach-Treated Samples

sediment type	depth	% wt loss	mode	phi of mode
dusky-red sludge	18.0-18.5	87.69	uni	3
yellowish-orange sand	27.0-27.5	31.48	uni	2
white sand	30-31	63.68	uni	3
white sand	40-41	60.84	uni	3
white sand	42-42.5	34.72	uni	3
yellowish-gray sludge	47.0-47.5	60.43	uni	3
yellowish-orange sand	50.0-50.5	27.11	uni	2
dusky-red sludge	52.5-53.0	65.70	uni	3
dusky-red sludge	55.0-55.5	67.82	uni	3
dusky-red sludge	56.5-57.0	78.19	uni	3
white sand	59.0-59.5	78.70	uni	3
white sand	61.0-61.5	64.23	uni	3
white sand	64.0-64.5	79.07	uni	4
yellowish-orange sand	70.0-70.5	65.52	uni	3
yellowish-orange sand	72.0-72.5	47.84	uni	1
white sand	74.0-74.5	84.58	uni	3
white sand	76.0-76.5	72.75	uni	3
white sand	79.0-79.5	84.33	uni	3
white sand	80.0-80.5	50.33	uni	3
white sand	81.5-82.0	74.57	uni	3
purple organic-rich sand	85.2-85.5	75.43	uni	3
yellowish-orange organic-rich sand	86.3-86.8	75.26	bi	2,4
yellowish-orange organic-rich sand	87.0-87.5	75.94	uni	3
yellowish-orange sand	95.0-95.5	32.00	uni	1
white sand	105.2-106	80.34	uni	3
white sand	106.3-107	38.94	uni	2
white sand	108.0-108.5	48.52	uni	3
white sand	119.5-120.1	74.39	uni	3
white sand	127.0-127.5	65.29	uni	3
white sand	127.5-128.0	63.26	uni	3
purple organic-rich sand	129-129.5	58.22	uni	3
yellowish-orange organic-rich sand	139-139.5	62.20	uni	3
red sand	144-145	58.12	uni	4
red sand	159.5-160.0	3.10	uni	4
red-brownish organic-rich sand	163.7-164	96.61	bi	2,4
red-brownish organic-rich sand	179-179.2	88.06	bi	2,4
red-brownish organic-rich sand	182.4-182.9	87.68	bi	3-4,5

APPENDIX E

Cyprideis australiensis

Date	Sample (cm)	$\delta^{13}C$	$\delta^{18}O$
2/5/2005	5	-5.905	2.147
6/20/2005	5	-5.572	2.029
6/20/2005	5	-5.549	1.992
12/3/2004	27	-4.671	1.313
2/5/2005	27	-1.2	2.772
3/15/2005	30	-4.719	1.245
3/15/2005	30	-4.832	1.88
3/15/2005	40	-5.436	1.797
3/15/2005	40	-5.776	1.522
3/15/2005	42	-4.857	1.706
3/15/2005	42	-5.472	1.428
2/5/2005	47	-5.998	1.484
12/3/2004	50	-7.721	0.727
2/5/2005	50	-6.142	1.35
11/23/2004	50	-9.261	0.652
6/20/2005	52.5	-6.561	1.445
6/20/2005	52.5	-6.23	1.157
2/5/2005	53	-7.808	1.489
3/15/2005	55	-6.472	1.789
6/16/2005	55	-4.43	1.989
6/16/2005	55	-3.23	2.207
3/15/2005	57	-4.684	1.915
3/15/2005	57	-4.71	1.744
6/16/2005	57	-4.996	1.908
3/15/2005	59	-4.883	1.498
3/15/2005	59	-4.571	1.217
6/16/2005	59	-5.113	1.575
3/15/2005	61	-5.369	1.61
6/16/2005	61	-5.562	2.124
6/16/2005	61	-4.579	1.693
3/15/2005	63	-5.691	1.325
6/20/2005	63	-4.728	1.032
6/20/2005	63	-5.623	1.342
3/15/2005	64	-5.06	1.172
6/20/2005	64	-4.612	2.119
3/15/2005	70	-3.463	1.941
4/14/2005	70	-6.076	1.477
6/20/2005	70	-4.534	1.71
3/15/2005	72	-4.765	1.715
6/20/2005	72	-5.112	1.408
6/20/2005	72	-5.116	1.154
3/15/2005	76	-5.658	1.461
6/20/2005	76	-5.332	0.857
3/15/2005	79	-5.771	2.062

4/14/2005	79	-7.408	0.993
6/20/2005	79	-7.205	1.289
6/20/2005	79	-6.049	1.691
3/15/2005	80	-6.5	1.392
6/20/2005	80	-7.199	1.015
6/16/2005	80	-5.561	1.166
3/15/2005	82	-7.507	0.621
4/14/2005	82	-6.621	1.347
6/20/2005	82	-6.435	0.974
11/23/2004	85	-8.627	-0.179
5/6/2005	95	-5.417	1.287
5/6/2005	95	-3.688	1.329
6/16/2005	95	-4.337	1.296
6/16/2005	95	-5.339	1.904
12/3/2004	106	-6.171	2.344
11/23/2004	106	-7.011	1.661
12/3/2004	107	-4.783	0.799
11/23/2004	107	-5.999	1.208
12/3/2004	108	-5.684	1.318
11/23/2004	108	-5.615	1.473
3/15/2005	120	-5.481	1.314
4/14/2005	120	-4.208	1.306
3/15/2005	127	-2.903	1.236
4/14/2005	127	-4.318	1.063
6/20/2005	127	-3.675	1.112
3/15/2005	128	-4.232	0.983
3/15/2005	128	-3.576	0.704
4/14/2005	128	-4.179	0.924
12/3/2004	129	-5.063	0.504
11/23/2004	129	-4.981	0.632
5/6/2005	135	-2.098	1.767
3/15/2005	139	-3.543	1.192
3/15/2005	139	-0.307	0.285
12/3/2004	144	-6.892	-0.479
11/23/2004	144	-5.441	0.653
3/15/2005	150	-4.71	-0.357
4/14/2005	160	-3.029	0.833
6/16/2005	170	-3.36	1.278
6/20/2005	182.4	-5.522	1.886

Mytilocypris ambiguosa

Date	Sample (cm)	$\delta^{13}C$	$\delta^{18}O$
3/15/2005	128	2.251	2.239
6/20/2005	129	2.382	2.769
11/23/2004	129	0.832	2.686
12/3/2004	129	0.77	2.607
3/15/2005	139	1.774	1.871
6/20/2005	139	2.243	2.585

6/20/2005	139	1.611	1.257
6/20/2005	139	1.578	1.289
3/15/2005	160	1.956	2.656
3/15/2005	160	1.198	1.958
4/14/2005	160	2.966	2.511
12/3/2004	164	3.506	1.772
4/14/2005	170	4.267	3.349
6/16/2005	170	2.436	2.693
6/16/2005	170	-1.132	1.763
6/20/2005	170	5.476	3.288
2/5/2005	179	3.651	3.585
4/14/2005	182	4.238	3.26
6/16/2005	182	-0.094	0.751
6/16/2005	182	5.467	3.303
6/16/2005	182	3.725	3.012

Micrite

Date	**Sample (cm)**	**$\delta^{13}C$**	**$\delta^{18}O$**
3/11/2005	5	0.743	0.114
3/29/2005	5	-0.58	1.251
3/29/2005	42	-0.048	2.38
3/11/2005	47	-1.165	3.388
3/29/2005	47	-1.206	3.196
4/15/2005	47	-1.201	3.152
11/23/2004	47	-1.446	2.418
12/3/2004	50	-2.42	-0.845
11/23/2004	50	-2.571	0.675
11/23/2004	50	-2.283	1.668
12/3/2004	53	-1.306	2.089
3/11/2005	53	-1.067	2.688
4/15/2005	53	-1.134	1.861
12/3/2004	53	-1.09	2.188
11/23/2004	53	-1.216	4.468
11/23/2004	53	-1.094	2.075
3/11/2005	57	0.112	1.259
3/29/2005	59	0.657	2.411
4/15/2005	59	0.683	1.889
3/11/2005	61	0.721	2
4/15/2005	61	0.373	2.141
3/11/2005	63	0.36	2.129
3/29/2005	63	0.196	2.177
4/15/2005	63	0.163	1.905
3/11/2005	64	0.594	1.86
4/15/2005	64	0.513	2.059
3/11/2005	70	1	2.097
3/29/2005	70	-0.783	2.254
3/11/2005	72	-0.1	1.308
3/29/2005	72	-1.27	1.935

3/29/2005	74	-0.093	2.148
3/11/2005	76	0.315	1.684
3/29/2005	76	0.543	1.994
3/11/2005	79	-0.426	0.835
3/29/2005	79	-0.555	0.56
3/11/2005	80	-2.91	1.499
3/29/2005	85.5	-2.134	0.688
12/3/2004	86.8	-2.723	0.723
3/29/2005	86.8	-2.287	0.961
12/3/2004	86.8	-2.445	0.766
11/23/2004	86.8	-2.63	1.296
11/23/2004	86.8	-2.862	0.898
12/3/2004	87	0.056	1.494
12/3/2004	87	-0.217	1.443
3/11/2005	87	0.118	1.768
3/29/2005	87	0.635	1.687
11/23/2004	87	-0.048	1.378
11/23/2004	87	-0.423	1.533
3/11/2005	106	0.413	1.671
3/11/2005	107	1.145	2.091
11/23/2004	107	1.447	1.285
11/23/2004	107	1.342	1.155
3/29/2005	108	1.067	1.451
12/3/2004	108	0.661	0.959
12/3/2004	108	0.988	1.065
11/23/2004	108	-0.154	-0.173
11/23/2004	108	0.482	0.725
3/11/2005	120	0.243	1.511
3/29/2005	120	0.35	0.964
3/11/2005	127	2.285	1.409
3/11/2005	128	1.307	1.034
3/11/2005	129	-2.825	1.247
3/11/2005	139	2.486	1.014
3/29/2005	144	-0.018	0.523
3/11/2005	150	2.131	0.948
3/11/2005	160	3.899	1.648
3/29/2005	164	3.987	1.269
3/29/2005	179	2.827	0.916
12/3/2004	179	2.805	1.008
12/3/2004	179	2.776	0.832
11/23/2004	179	2.924	0.892
11/23/2004	179	2.196	0.795
3/11/2005	182	4.824	1.694
3/29/2005	182	5.578	1.42